Density Functional Theories and the Structure of Fluids near

Walls

Andreas T. Augousti

Physics Laboratory, University of Kent, Canterbury

June 6, 1985

For Mum, Dad and Michele

CONTENTS

Acknowledgements

DENSITY FUNCTIONAL THEORIES AND THE STRUCTURE OF FLUID
NEAR WALLS

submitted by A.T.Augousti
for the degree of
Doctor of Philosophy

ABSTRACT

The structure of fluids near walls is examined using density functional
techniques. A brief introduction to the subject is given, followed by a
mathematical derivation of some important basic results. A linear
(Chap.3) and non-linear (Chap.4) density functional approximation for the
thermodynamic potential is used to treat a model fluid comprised of hard
spheres with embedded point ions or dipoles confined between two hard
infinite planar walls. Results are obtained and compared for the charge
and polarisation densities. Both theories produce oscillatory charge and
polarisation density profiles, in agreement with results at a single wall
from other workers. These results differ qualitatively with those given
by earlier, continuum theories of the electrical double layer such as
Debye-Huckel and Poisson-Boltzmann.

A modified functional is introduced (Chap.5), and is used to treat a
simple fluid of hard spheres. A single variable parameter of the theory
is chosen to ensure thermodynamic consistency, and results for the number
density are obtained. These results are in excellent agreement with
results from Monte Carlo computer experiments, even up to unrealistically
high fluid densities. The modified functional is further applied to a
hard sphere fluid with attractive long-range interactions. This leads to
wetting of the walls by vapour, a result also observed previously at a
single wall.

Finally,. a perturbation treatment is applied to experimental scattering
data to give a potential of mean force for an aqueous dispersion of
polystyrene spheres.

1. INTRODUCTION

1.1. Background

The static structural properties of a fluid near a wall have recently become a field of intense interest. These properties form the basis for phenomena such as electrical double-layers, wetting of a solid surface by liquid or gas, and the effective interaction of solute particles, as well as for others. Thus a knowledge of the distribution of a fluid near a wall allows one to predict its behaviour in a number of circumstances, in addition to providing an explanation for experimental results.

The structure of a fluid near a wall is of direct consequence in the field of colloid science. For sufficiently large colloid particles, the boundary between particle and fluid may be taken to be planar to a good approximation. Thus the pressure obtained from calculations involving two walls may be used to infer a colloidal interparticle potential.

1.2. DLVO Theory

The earliest attempts at providing such a potential came from the work of Derjaguin, Landau, Verwey and Overbeek, and is referred to as DLVO theory. The essence of the theory was to represent the interparticle force between the colloid particles as the superposition of repulsive forces arising from colloidal double-layer interactions, and the van der Waals forces of attraction, a phenomenon due to the fluctuations of the colloidal charge distributions. The resulting superposition gives a potential of the form shown in Fig. 1.1

The theory met with considerable success, not the least of which was its theoretical justification for the empirical Schulze-Hardy rule, viz.

$$critical\ coagulation\ concentration = 8.65 \times \frac{10^{-39}}{z^6 A^2} \tag{1.1}$$

where z was the valency of the electrolyte, and A, the Hamaker constant, a measure of

the strength of the van der Waals forces. However this apparent success may have been more than slightly coincidental, particularly when one closely examines the assumptions which serve as the basis of the theory. The solvent was treated as a continuum, with the dielectric constant of the fluid taken as constant throughout. This may be so at some distance from the particle, but the solvent structure near it, and hence the dielectric constant, is undoubtedly different from that in the bulk. As this must significantly affect the form of the double-layer, the corresponding modification of the repulsive forces is not negligible. Secondly, no allowance was made for redistribution of material on the surface of the particle due to the influence of other particles, a condition that is almost certainly not true when the particles are densely packed, or close to flocculation or coagulation.

Furthermore, the practice of assuming the validity of DLVO theory and then using the Schulze-Hardy rule to calculate the value of A, the Hamaker constant, from the experimental data, hardly constituted a rigorous test of the theory.

1.3. Stern layer modification

An attempt at improving the theory to allow for the effects of structure in the interfacial region, without having to specify this structure, was made by Stern. He postulated a layer adjacent to to the surface of the particle whose dielectric constant and thickness could be chosen at will. This was to take into account the phenomenon of " charge crowding ". The charge adsorbed on the surface of the colloid could not increase indefinitely. Stern was able to derive the equation

$$\frac{\psi_0 - \psi_\delta}{\delta} = \frac{4\pi}{\epsilon_s} \frac{\sigma_{s_0} K n_0}{1 + K n_0} \tag{2.1}$$

where ψ_0 is the potential at the colloid surface, ψ_δ is the potential at a distance δ from the surface, and δ is the width of the Stern layer. K is a Boltzmann factor and σ_{s_0} is the surface charge density at saturation. This was a useful equation, as it became evident that as the concentration, n_0, increases, the potential in the Stern layer

increases up to a constant value when the surface is saturated.

Note that: (i) One can consider the modification of Stern layer theory to the analysis of double-layers as effectively positioning a new wall at $x - \delta$ with surface potential ψ_δ rather than ψ_0, with an internal dielectric constant ϵ_s. However ϵ_s and δ were hard to measure, and were generally chosen to fit the data; (ii) As the concentration increases, increasing amounts of the drop in potential occur across the Stern layer; (iii) ψ_δ is only much smaller than ψ_0 in dilute solutions if ψ_0 is relatively large. So Debye-Hückel theory, which assumes low surface potential, is then useful in replacing the more exact Gouy-Chapman theory; (iv) ψ_δ varies only slightly as ψ_0 changes. It is, however, very sensitive to the concentration, until ψ_0 is relatively large.

This modification of electrical double-layer theory by Stern brought DLVO theory more in line with experimental results, yet the modification was an *ad hoc* one, and no fundamental proof of the existence of the layer was given.

1.4. Experimental Evidence for DLVO theory

There are two main techniques for obtaining information regarding the interparticle potential:-

(1) Studies of the kinetics of slow coagulation

(2) Equilibrium measurement of the force of interaction directly

1.4.1. Studies of the Kinetics of Slow Coagulation

These measurements are related to $V_{\max}$, the height of the potential barrier in the potential-distance curve.

Ottewill and Shaw [1] did *not* find good agreement with the theory, although they claimed the zeta potential (the potential at the boundary of the Stern layer and the fluid) varied. Still, they may only have detected the flocculation which occurs in the second minimum of potential, so that even for allowing for variation of ψ_d, the wall

potential, the experiment may not have been a valid test of DLVO theory.

Matthews and Rhodes [2] found tentative confirmation of the prediction of increase in stability for increase in size, working with a monodisperse system , and particles in the range $0.74 < d < 1.4$ μm (d is the diameter). However in this experiment $\kappa a \approx 1$, whereas it should have been $<<1$ (κ is the inverse Debye length, a is particle size). For the condition $\kappa a <<1$ to be satisfied requires that the concentration be $<10^{-3}M$. Once again doubt is cast on the experiment, as aggregation may have been due to a deep secondary minimum.

Joseph-Petit *et al* [3], working with monodisperse selenium hydroxide, with $45 < d < 135$ nm, found the stability increased up to 50nm, and then decreased. DLVO theory, including the Vold effect and viscous interactions fit the data only up to 50nm. From there, it was shown quite well, quantitatively, that secondary minimum flocculation was taking place.

The conclusion is that DLVO theory is not accurately tested with respect to aggregation kinetics of a dispersion. Is is necessary to work with a monodisperse system with well-characterised surfaces, and particles small enough to preclude secondary minimum flocculation at a given concentration. The results seem to be in reasonable accord with theory, although there are peculiarities, such as the dependence of A, the Hamaker constant, on electrolyte concentration.

Even so, studies of coagulation kinetics are not particularly useful, as they measure W, the stability ratio, which is an integral over the separation of two particles of a function related to the potential. It is therefore relatively insensitive to spatial variation. It does not allow one to say whether the repulsive and attractive potentials are incorrectly calculated, or that DLVO theory is fundamentally wrong, and that other forces are important.

1.4.2. Equilibrium Studies of the Force of Interaction

Norrish [4], using the clay mineral montmorillonite found the force-distance curve close to the theoretical when pressure was applied, but when removed, the equilibrium spacing was smaller than predicted. The failure was argued to be due the fact that the system was not identical to the model e.g. improperly aligned particles, heterogeneous charge distribution on the surfaces etc.

Work on soap films was carried out independently by Derjaguin, Scheludko, Sonntag and others. Scheludko worked on plane-parallel systems, applicable to foams, finding quantitative and semi-quantitative evidence for dispersion and DLVO forces. Sonntag's work leaned more towards emulsions, and there, too, agreement was good when suction pressure was applied, but the equilibrium thickness was too small at low salt content, and too high at high salt content. This was not entirely explicable in terms of dependence of A on concentration. Also, agreement was not good for separations $<$ 10^{-9} m. Corrections, too, were required , and these were mostly system-specific.

More recently [5-9], very precise measurements have been carried out by Israelachvili and coworkers. The system was composed of a pair of crossed, molecularly smooth mica cylinders an an electrolyte solution. The separation could be varied between 20Å to infinity. For a 1:1 electrolyte, the forces measured were in excellent agreement, even up to concentrations of 10^{-1}M. For R<20Å different effects became apparent. There were also discrepancies for asymmetric electrolytes, and Poisson-Boltzmann theory, which describes how the potential and charge distributions vary across the double-layer, was found to be not very good.

In order to obtain measurable effects for R>20Å, a solvent with a larger diameter was needed. Octalmethylcyclotetrasiloxane $((CH_3)_2SiO)_4$ was chosen. It is an inert organic liquid, non-polar, and almost spherically symmetric (a slightly oblate spheroid, in fact). It has a diameter of very nearly 1nm. Oscillations in force were detected at up to 10 molecular diameters, comparable, and for very small separations (<3nm), much

greater then van der Waals forces. For R>3nm, the average periodicity was 1.05 ± .05nm, which is almost exactly a molecular diameter. For R<3nm, the average periodicity was . 8 ± .1nm which suggests that the molecules are then lining up with their shorter axes perpendicular to the wall.

Similar experiments were performed for cyclohexane, but for that system, only six oscillations were measurable, with periodicity again similar to the size of the molecular diameter. The reason for fewer oscillations may be due to the the greater distance of the temperature from the melting point. (Both experiments were performed at 22°C -m.p. of cyclohexane is 6.6°C, m.p. of octamethylcyclotetrasiloxane is 17.5°C).

Further results, such as the dependence of the force on temperature and other factors are eagerly awaited awaited.

1.4.3. Conclusion

DLVO theory applies best to aggregation in systems where V_{max} occurs at large separation relative to the molecular diameter. As this is normally $\approx \frac{1}{\kappa}$, this implies low concentrations are necessary. At high ionic concentrations($\approx 10^{-2}M$), corrections due to viscous interactions, entropic effects etc. become important. They are always important in coalescence, and DLVO theory is not adequate to describe this. It may also be stated with confidence that DLVO theory fails at very small separations, where the continuum approximation breaks down, and forces due to structure become appreciable.

1.5. Theories based on Integral Equations

The next logical step was to introduce a formalism that was capable of accounting for the discrete nature of the electrolyte and, if possible, the solvent, albeit on on an averaged basis of some kind. The methods of statistical mechanics were capable of just such a representation. A brief outline of the basic principles and results of the

statistical mechanical representation of fluids is given in the next chapter.

There are two closely related formulations of the problem:- the integral equation method, and application of a variational principle to a functional form. The former consists of formulating integral equations for chosen functions directly by consideration of the interactions of the particles. This is achieved by writing down a formally exact but insoluble equation (such as the Born-Green-Yvon equation or the Ornstein-Zernike equation), and supplementing this with an additional approximate equation, called a closure relation, involving the same quantities as the first, and usually of integral form too.

The latter involves approximating the free energy of the system by a functional expansion of a function of position, usually the density or external potential, and then by using a variational principle for the free energy, obtaining an equation to be solved for the appropriate function. This procedure, too, normally requires a supplementary equation and often the same equations as the ones used in the first method are chosen.

The results of this more recent work differ qualitatively with that of the older DLVO theory. They reveal that at small separations of the particle surfaces, the interparticle potential oscillates strongly as a function of the separation, and can be large compared with the van der Waals potential, as well as having several local minima. This is in good agreement with the results of Israelachvili *et al* as discussed in the previous section.

The implications for the stability of colloids are great. Loose, and even fairly tight aggregations of particles are now more likely to be considered flocculation, occuring in the second minimum or even higher minima, rather than coagulation, which should occur only in the first, and generally deepest, minimum.

Another bonus of the newer methods is the calculation of adsorption of material on the surface directly. It is a simple matter to calculate this either numerically or analytically from the density profile derived from the solution of the integral

equations. It is then possible to investigate how this adsorption excess depends on various parameters: electrolyte concentration, charge and potential on the wall representing the the colloid particle surface, proximity of the other wall, and bulk dielectric constant, to name but a few. It is also possible to establish how this adsorption excess affects the pressure between the walls, or equivalently, the interparticle force.

1.6. Overview of the thesis

These latest treatments described above have been applied to a variety of systems with differing degrees of success as tested against results provided by experiments or the increasingly important computer simulations. The strength and weaknesses of particular treatments have been uncovered, and these will be touched on later.

The main aim of this work is to extend the present formalism, in particular that of the functional approach, and to apply it to more complex systems than have hitherto been dealt with. There is in addition some work presented which deals with the structure of a fluid near a wall from the point of view of perturbation theory.

Chapter 2 gives a brief outline of the results given by the application of statistical mechanical principles to liquid theory. The distribution functions and the correlation functions used to describe the structure of a liquid are introduced here, and the meaning of these functions is explained.

A density functional formalism is applied to a model consisting of equally sized hard spheres with point charges and dipoles embedded in them, confined between two hard planar infinite walls, in Chapter 3. Results for the charge and polarisation profiles are obtained, and these are compared with earlier continuum theories such as Debye-Huckel. The pressure between the walls due to electrostatic effects is calculated in two ways, and these are shown to be equivalent. The results are found to be different from those of the older continuum theories, and agree with those obtained by

other workers dealing with a single wall.

In Chapter 4 the formalism is extended by treating the entropy of the fluid exactly, instead of using the linearised approximation of Chap. 2. In this case, the equation involving the number density does not decouple from the remainder, and must be solved simultaneously with the equations governing the charge and polarisation profiles. The same quantities as in the previous chapter are calculated and a comparison is made. The most striking difference is the large increase in the value of the charge and polarisation profiles at the wall.

Chapter 5 introduces a functional for the free energy which is exact for direct correlation functions that are expandable functionals of the number density. The exact (but unknown) functional is replaced by a tractable approximation, and applied to a fluid of hard spheres confined between hard planar walls and excellent agreement is found between the theory and results obtained from computer simulation. The theory is also applied to a fluid of Lennard-Jones-type particles, and wetting of the wall by vapour is observed.

Up to this point the thesis deals with the pressure between two walls confining a fluid directly, by calculation of the variation of the free energy of the system with respect to variation of the separation of the walls. Insofar as this represents the interparticle potential for colloid particles in solution, this method is acceptable. However, one may approach the problem from the point of view of a related quantity, the structure factor. From a knowledge of a potential of mean force, the structure factor may be calculated under a given approximation. When this is compared with experimental measurements, the difference in the two structure factors may be used within a perturbation theory to establish a new potential of mean force. This is done in Chapter 6, with two reference potentials of mean force, a shouldered hard-sphere potential and a " soft core " potential, for a system of polystyrene spheres in solution.

Finally, in Chapter 7, the results of previous chapters are discussed in a broader context, and possible future developments are explored.

The thesis closes with a series of appendices introducing functional techniques, relating the theory in Chapter 3 to Debye-Huckel theory, and showing that the two methods used in that chapter to calculate the electrostatic pressure are equivalent.
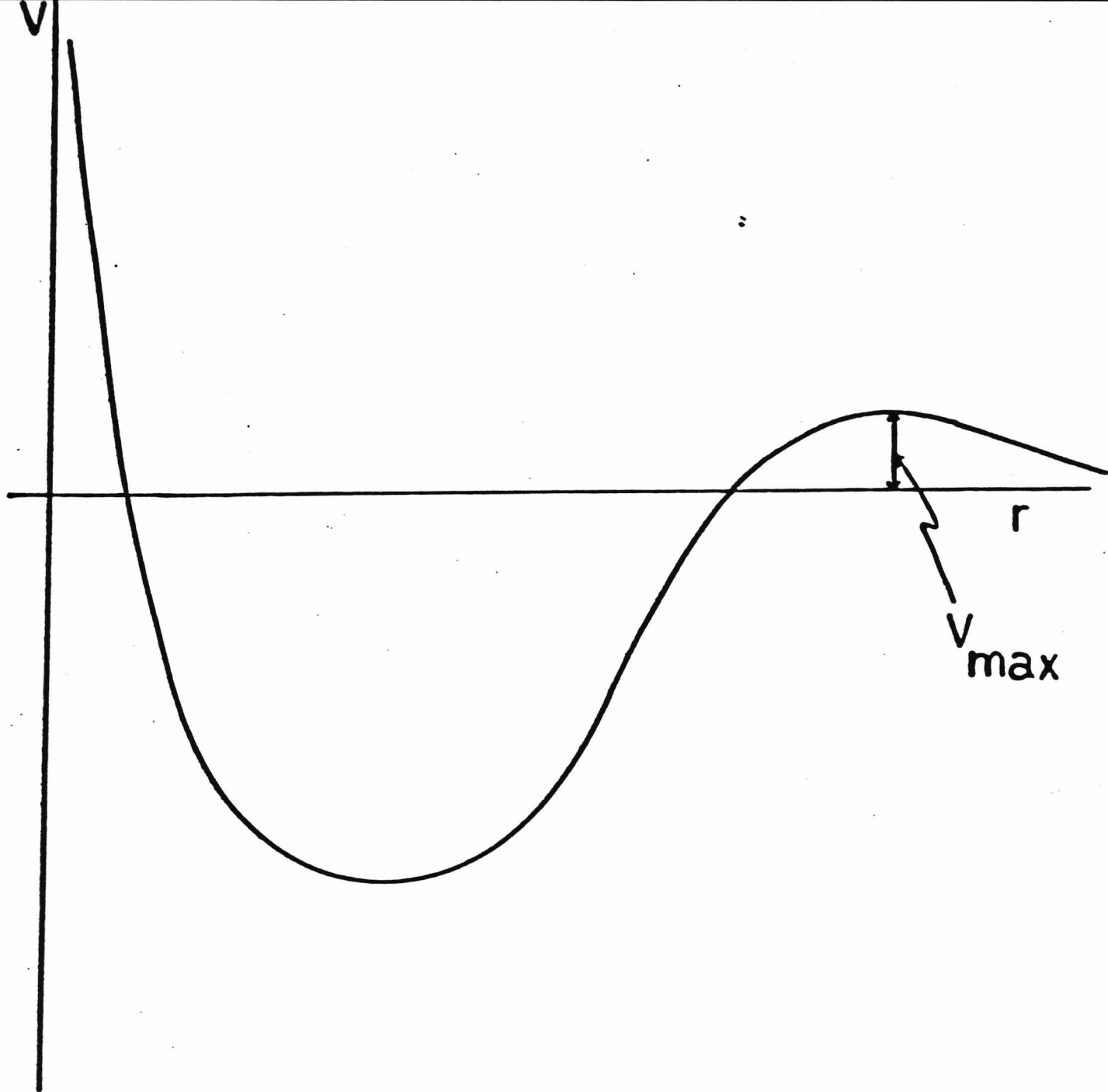
Fig 1.1: Sketch showing the intercolloidal potential $V(r)$ according to DLVO theory.

2. STATISTICAL MECHANICAL BACKGROUND

The starting point for a statistical mechanical consideration of a fluid comprised of N particles in a volume V is the probability distribution function. This gives the probability of finding molecule 1 in the region dr_1, molecule 2 in dr_2, etc. as

$$P^{(N)}(\mathbf{r})d^N\mathbf{r} \equiv P^{(N)}(\mathbf{r}_1, \cdots, \mathbf{r}_N)d\mathbf{r}_1 \cdots d\mathbf{r}_N$$
$$= \frac{e^{-\beta\Phi_N}d\mathbf{r}_1 \cdots d\mathbf{r}_N}{Z_N} \tag{2.1}$$

where Z_N is the configuration integral

$$Z_N = \int \cdots \int P^{(N)}(\mathbf{r}_1 \cdots \mathbf{r}_N)d\mathbf{r}_1 \cdots d\mathbf{r}_N \tag{2.2}$$

and $\beta = 1/k_B T$, k_B being Boltzmann's constant.

We shall only consider molecules interacting via pair potentials $v(\mathbf{r})$. If the system is in an external field $U(\mathbf{r})$ which couples to the density, the potential energy may then be written as

$$\Phi_N = \sum_{i>j=1}^{N} v(\mathbf{r}_i - \mathbf{r}_j) + \sum_{i=1}^{n} U(\mathbf{r}_i) \tag{2.3}$$

The distribution functions follow from these equations immediately. The probability distribution function of a molecule in $d\mathbf{r}_1$ at $\mathbf{r}_1$, ... , and any molecule in $d\mathbf{r}_n$ at $\mathbf{r}_n$ irrespective of the position of the remaining $N-n$ molecules is

$$P^{(N)}(\mathbf{r}_1, \cdots, \mathbf{r}_n) = \frac{N!}{(N-n)!}\int \cdots \int P^{(N)}(\mathbf{r}_1, \cdots, \cdots, \mathbf{r}_N)d\mathbf{r}_{n+1} \cdots d\mathbf{r}_N \tag{2.4}$$

The most important distribution and correlation functions are the one- and two-particle functions which can be measured experimentally. Note that for a homogeneous system $P^{(1)}(\mathbf{r}) = N/V$, *i.e.* the bulk density.

The set of equations termed the Born-Green-Yvon (BGY) equations that relate the distribution functions, $P^{(n)}$, to themselves, follow from eqn (2.4). Thus consider

$$P^{(1)}(\mathbf{r}_1) = \int \cdots \int e^{-\beta\left[\sum v(\mathbf{r}_1 - \mathbf{r}_j) + U(\mathbf{r}_1) + \sum v(\mathbf{r}_i - \mathbf{r}_j) + \sum U(\mathbf{r}_i)\right]} \times \frac{d\mathbf{r}_2 \cdots d\mathbf{r}_N}{Z_N} \tag{2.5}$$

where in the exponent the co-ordinates of particle 1 have been separated explicitly. Now differentiating $P^{(1)}$ w.r.t. $\mathbf{r}_1$, one obtains

$$\nabla P^{(1)}(\mathbf{r})=-\beta P^{(1)}(\mathbf{r})\nabla U(\mathbf{r})-\beta\int d\mathbf{r}_1\nabla v(\mathbf{r}-\mathbf{r}_1)P^{(2)}(\mathbf{r},\mathbf{r}_1) \tag{2.6}$$

This equation forms the first in a hierarchy of N equations that relate the large number of correlation functions, $P^{(n)}$. The usual method of reducing these equations to a tractable form is by making an approximation which neglects correlations above a certain order thereby reducing the set to a smaller number. When applied to an inhomogeneous fluid it is usual to truncate at the first equation, which may then be written

$$\nabla P^{(1)}(\mathbf{r})=-\beta P^{(1)}(\mathbf{r})\nabla U(\mathbf{r})-\beta\int d\mathbf{r}_1\nabla v(\mathbf{r}-\mathbf{r}_1)P^{(1)}(\mathbf{r})P^{(1)}(\mathbf{r}_1)g(\mathbf{r},\mathbf{r}_1) \tag{2.7}$$

and replace the inhomogeneous pair distribution function $g(\mathbf{r},\mathbf{r}_1)$ by the function appropriate for a bulk homogeneous fluid. The BGY hierarchy will not be discussed further in this thesis, but it is included for completion, as it formed the basis of the earliest studies of dense fluids.

A newer class of integral equations based on the consideration of the so-called direct correlation function $c(r,r')$ were later formulated. The physical significance of this function is somewhat obscure, although it is approximately equal to minus the reduced two-body potential for dilute fluids. Its relationship to the distributions functions already mentioned will now be discussed.

First recall the definition of the Helmholtz free energy F

$$e^{-\beta(F-F_0)}=\frac{Z_N}{V^N} \tag{2.8}$$

where F_0 is the free energy of a non-interacting ideal system. Now

$$e^{-\beta F}=C\int d\mathbf{r}_1\cdots d\mathbf{r}_N\int d\mathbf{p}_1\cdots d\mathbf{p}_N e^{-\beta\sum_i\frac{p_i^2}{2m}-\beta\sum_i U(\mathbf{r}_i)-\beta v(\mathbf{r}_1,\cdots,\mathbf{r}_n)} \tag{2.9}$$

for a fluid in an external potential $U(\mathbf{r})$, and C is a normalisation constant. Integrating over the momenta gives

$$e^{-\beta F} = C' \beta^{-3N/2} \int dr_1 \cdots dr_N e^{-\beta \sum_i U(r_i) - \beta v(r_1, \ldots, r_a)} \tag{2.10}$$

where C' is a new normalisation constant. Thus F is now a functional of $U(r)$

$$i.e. \quad F \equiv F[U]$$

Taking the functional derivative of F w.r.t. $U(r)$ gives

$$\frac{\delta F}{\delta U(r)} = <\sum_i \delta(r - r_i)> = \rho(r) \tag{2.11}$$

$\sum_i \delta(r - r_i)$ is a density function $\hat{\rho}(r, r_i)$ and

$$<\sum_i \delta(r - r_i)> = \rho(r)$$

is the mean density at r

Also

$$<\cdots> = \int \cdots \frac{P^{(N)}(r) d^N r}{Z_N} \tag{2.12}$$

From Eqn 2.11 From eqn (2.11) $U(r)$ and $\rho(r)$ are therefore conjugate thermodynamic variables

Upon functionally differentiating eqn (2.11) w.r.t. $U(r')$, one obtains the the density fluctuation function

$$\frac{\delta^2(F - F_0)}{\delta U(r) \delta U(r')} = \frac{\delta \rho(r)}{\delta U(r')} = -\beta <\hat{\rho}(r', r_i) \hat{\rho}(r, r_i)> + \beta \rho(r) \rho(r')$$

$$= -\beta \rho(r)[\delta(r - r') + \rho(r') h(r - r')] \tag{2.13}$$

where $h(r, r')$ is termed the total pair correlation function. For a homogeneous system

$$h(r, r') = g(r, r') - 1$$

Now form the thermodynamic potential

$$\Omega[\rho] = -\int dr \rho(r) U(r) + (F - F_0) \tag{2.14}$$

It follows that

$$\frac{\delta \Omega}{\delta \rho(r)} = -U(r) \tag{2.15}$$

Thus $\rho(\mathbf{r})$ is the natural variable for Ω which one would expect since Ω is related to $(F - F_0)$ via the Legendre transform in eqn (2.14). For a non-interacting system

$$\rho(\mathbf{r})=\rho_0 e^{-\beta U(\mathbf{r})} \qquad i.e. \qquad U(\mathbf{r})=\frac{-1}{\beta}\ln\left(\frac{\rho(\mathbf{r})}{\rho_0}\right) \tag{2.16}$$

where ρ_0 is the density of the ideal uniform system for which $U(\mathbf{r})=0$. For an interacting system we can introduce an effective ' direct ' one-particle potential $c(\mathbf{r})$ and formally write

$$\rho(\mathbf{r})=\rho_0 e^{-\beta(U(\mathbf{r})+c(\mathbf{r}))}$$

i.e.

$$U(\mathbf{r})+c(\mathbf{r})=\frac{-1}{\beta}\ln\left(\frac{\rho(\mathbf{r})}{\rho_0}\right) \tag{2.17}$$

where ρ_0 is now the uniform density when $U(\mathbf{r})$ is zero. Noting that $c(\mathbf{r})$ is a functional of $\rho(\mathbf{r})$ one can immediately obtain from (2.15) and (2.17)

$$\frac{\delta^2\Omega}{\delta\rho(\mathbf{r})\delta\rho(\mathbf{r}')}=-\frac{\delta U(\mathbf{r})}{\delta\rho(\mathbf{r}')}=\frac{\delta(\mathbf{r}-\mathbf{r}')}{\beta\rho(\mathbf{r}')}-\frac{c(\mathbf{r},\mathbf{r}')}{\beta} \tag{2.18}$$

and the direct correlation function

$$c(\mathbf{r},\mathbf{r}')=-\frac{\beta\delta c(\mathbf{r})}{\delta\rho(\mathbf{r}')} \tag{2.19}$$

has been introduced. Using the identity

$$\int\frac{\delta U(\mathbf{r})}{\delta\rho(\mathbf{r}'')}\frac{\delta\rho(\mathbf{r}'')}{\delta U(\mathbf{r}')}d\mathbf{r}''=\delta(\mathbf{r}-\mathbf{r}') \tag{2.20}$$

in conjunction with eqns (2.13) and (2.18), one obtains the Ornstein-Zernike equation for inhomogeneous systems

$$h(\mathbf{r},\mathbf{r}')=c(\mathbf{r},\mathbf{r}')+\int d\mathbf{r}'' h(\mathbf{r},\mathbf{r}'')\rho(\mathbf{r}'')c(\mathbf{r}'',\mathbf{r}') \tag{2.21}$$

which is the basis for any approach based on the use of ' direct ' correlation functions.

This equation has to be supplemented by a second relation between these correlation functions which is usually obtained by summing appropriate subsets of diagrams obtained from perturbation theory or by an equivalent functional expansion.

This second relation is called a closure relation and the most commonly used ones are the Percus-Yevick approximation (PY) and the hyper-netted chain approximation (HNC). The PY closure relation is

$$g(1,2)=e^{[\beta v(1,2)]}[g(1,2)-c(1,2)] \tag{2.22}$$

and that of the HNC approximation is

$$\ln g(1,2)=-\beta v(1,2)+h(1,2)-c(1,2) \tag{2.23}$$

In the weak interaction limit (e.g. a dilute fluid), the difference $h(1,2) - c(1,2)$ is small and eqn (2.23) can be rewritten as

$$g(1,2)=e^{-\beta v(1,2)}e^{[h(1,2)-c(1,2)]} \tag{2.24}$$
$$=e^{-\beta v(1,2)}[1+h(1,2)-c(1,2)]$$
$$=e^{-\beta v(1,2)}[g(1,2)-c(1,2)] \tag{2.25}$$

In this limit the PY and HNC approximations agree.

In practice, it seems that for uniform fluids the PY approximation yields good results for short-range intermolecular potentials, while the HNC approximation provides good results when the interaction is long range. A modification of the PY approximation which appears to work well when the potential has a sharp short-range part such as a repulsive core surrounded by long-range interaction is the mean spherical approximation (MSA). This assumes eqn (2.22) for $|r_1-r_2|<a$ where a is the range of the short-range part (e.g. the radius of the core for hard spheres) and

$$c(1,2)=-\beta v(1,2) \tag{2.26}$$

otherwise. Equation (2.26) is asymptotically correct as

$$\left|r_1-r_2\right|\to\infty$$

These approximations have been used in the study of liquids bounded by one or two walls by taking the equations in the appropriate limit. For example, in the case of one wall, the equations are first generalised to the case of a liquid which is a mixture of two molecular species of different sizes and densities. One then allows the radius of one species to tend to infinity appropriately while its density tends to zero. If the large

species is spherically symmetric, the pair distribution function between molecules of the two species $g_{12}(1,2)$ can be written as a function of $(R+x)$ where R is the radius of the large species and x is the shortest distance of the centre of the smaller species from the surface of the larger. In the limit $R \rightarrow \infty$,

$$g_{12}(1,2) \rightarrow \frac{\rho(x)}{\rho_0} \qquad (2.27)$$

where $\rho(x)$ is the mean density of the smaller species at x and ρ_0 is its bulk density[14]

.

In the case of two walls, the starting point is a mixture of three molecular species. The radii of two of the species are then allowed to tend to infinity while their densities tend to zero. In this way the correlation $h(x)$ between the walls is obtained and from this correlation a potential of mean force can be constructed. A weakness of the method in this case is that it omits direct three-particle correlations between the two walls and the fluid and these are likely to be important.

Another class of approximations that have been much used for fluid problems is based on the use of the energy density-functional, $\Omega[\rho]$. This is the approach favoured in succeeding chapters of this thesis. The first workers to use this approach assumed that the density varied slowly in space compared with the correlation function[15]. It is then possible to expand $\Omega[\rho]$ in terms of the derivatives of ρ. Thus

$$\Omega[\rho] = \int F[\rho(\mathbf{r})] + F_\mu[\rho]\nabla_\mu\rho(\mathbf{r}) + F_{\mu\nu}[\rho]\nabla_\mu\nabla_\nu\rho(\mathbf{r}) \\ + F'_{\mu\nu}[\rho]\nabla_\mu\rho(\mathbf{r})\nabla_\nu\rho(\mathbf{r})\,d\mathbf{r} \qquad (2.28)$$

where $F, F_\mu, F_\nu, F'_{\mu\nu}$ are functions (not functionals) of the density $\rho(\mathbf{r})$. To use the approximation one needs to know these functions or to make further assumptions about them.

An alternative use of the energy density-functional, $\Omega[\rho]$, is to make some assumption about its form. Two fruitful approximations begin from the formal relation between $\Omega[\rho]$ and the direct correlation function $c(1,2;\rho)$ (eqn (2.18)) which is in

general a functional of the density $\rho(r)$ in an inhomogeneous system as well as of the two molecular co-ordinates '1' and '2'. This equation is really the definition of the direct correlation function and so does not contain any new information. However, one can make intuitively promising approximations for this correlation function and so obtain useful approximations for Ω.

Equation (2.18) can be integrated formally in a number of different ways. The method used here is that used by Saam and Ebner [16]. Suppose that we choose a reference state of uniform density ρ_0 and that we know or have an approximation for the direct correlation function along the path on which

$$\rho_\alpha(1) \equiv \rho_0 + \alpha[\rho(1) - \rho_0] \tag{2.29}$$

where $\rho(r)$ is the final density. Then

$$\Omega[\rho] - \dot{\Omega}[\rho_0] = \beta \int d1 U(1)[\rho(1) - \rho_0] + \int d1 \left\{ \rho(1)\ln\left(\frac{\rho(1)}{\rho_0}\right) - [\rho(1) - \rho_0] \right\}$$

$$- \int d1 d2 C(1,2)[\rho(1) - \rho_0][\rho(2) - \rho_0] \tag{2.30}$$

where

$$C(1,2) = \int_0^1 d\alpha \int_0^\alpha d\alpha' C(1,2;\alpha') \tag{2.31}$$

$C(1,2;\alpha)$ is the direct correlation function when the density is $\rho_\alpha(1)$ and U is the external potential. If the fluid undergoes no phase transition along the path, $C(1,2;\alpha)$ is unique and the result (2.30) is independent of the path.

Ebner et al (1980) have used the thermodynamic potential (2.30) with $C(1,2;\alpha)$ chosen to have a form for a uniform fluid with density

$$\frac{1}{2}[\rho_\alpha(1) + \rho_\alpha(2)]$$

This is not as simple as it may seem because the correlation function has to be found

for all pairs of points along the path $\rho(1)$, the end of the path. Ebner *et al* developed special numerical techniques to complete the calculation.

Grimson *et al* (1980)[17] in their studies of a fluid between two walls used as an approximation to $C(1,2;\alpha)$ the bulk direct correlation function $C(1,2;0)$. With this approximation,

$$C(1,2)=C(1,2;0) \tag{2.32}$$

This is a rather drastic approximation although it is exact for small departures from the bulk density. In fact, it is related to the use of the Ornstein-Zernike (OZ) equation with the HNC closure. For suppose we determine the density by using eqn (2.32) and by making (2.30) stationary w.r.t variations in ρ. Then the equation to determine ρ is

$$\beta U(1)+\ln\left(\frac{\rho(1)}{\rho_0}\right)-\int d2 C(1,2)[\rho(2)-\rho_0]=0 \tag{2.33}$$

Now suppose that $U(1)$ is the interparticle potential $V(1)$ due to a definite molecule of the fluid at the origin. Then

$$\rho(1)=\rho_0 g(1) \tag{2.34}$$

and

$$\rho(2)-\rho_0=\rho_0 h(2) \tag{2.35}$$

Thus eqn (2.33) becomes in this case

$$\ln g(1)=-\beta V(1)+\rho_0\int d2 C(1,2)h(2)$$
$$=-\beta V(1)+h(1)-c(1) \tag{2.36}$$

where the OZ equation was used in the last step. Equation (2.36) agrees with the HNC approximation, eqn (2.23). Grimson *et al* also used eqn (2.23) in the form obtained by linearising eqn (2.28) about the solution with $C(1,2)$ equal to zero. This form is similarly related to the PY closure. Again for a fluid bounded by a single wall this approximation is equivalent to that obtained by using the OZ equation plus HNC closure if one takes the limit of a binary mixture discussed earlier. The spirit of this

approximation is similar to that of the truncation of the BGY equations. However, in this approximation the direct correlation function is replaced by its bulk value while in the BGY approximation the pair distribution function is replaced by its bulk value. It is not obvious *a priori* which is the better starting point.

3. LINEAR FUNCTIONAL APPROXIMATION FOR THE FREE ENERGY OF AN IONIC-DIPOLAR SYSTEM

3.1. Introduction

The structure of a fluid near a wall is a desirable thing to know. If one allows the wall to represent a colloid particle, and the fluid to represent a solvent, then from a knowledge of the fluid structure one can determine, under certain approximations, a great deal of information about the behaviour of a system. Perhaps the most valuable results which can be obtained concerns the pressure between two walls, or alternatively, the intercolloidal potential.

Early workers on charged systems included the effects of the solvent via a monolayer at the wall-fluid interface [43-46]. The ultimate aim was to model an aqueous solvent, and although the attempts to model a bulk system over all phases were poor, some good results were obtained in the liquid phase [47-49]. The most succesful civilised model used is Hard Sphere Ion-Dipole Mixture (HSIDM) [61] model described later in this chapter. It yields analytical results under the MSA [50,51,53] and numerical results using HNC theory [52]. However, the usefulness of the HSIDM model is limited, and theories using more complex, anisotropic short-range potentials have emerged [54-58]. Most previous workers [18-20] have dealt exclusively with fluids bounded by a single wall. Now whilst the information from such work is undoubtedly useful, particularly in testing the accuracy of rival approximations, one cannot use such models to represent real colloid systems, since colloid particles are not found in isolation.

Some work has already been done on fluids bounded by two walls [17,21,22]. This chapter extends that work to deal with a fluid of greater complexity, a so-called 'civilised' model. In this model, the fluid is comprised of two species of hard spheres with equal and opposite point charges respectively embedded at their centre, representing the electrolyte as before. Now, however, the continuous background

dielectric medium is replaced by a third species of neutral hard spheres, equal in size to the electrolyte hard spheres, but with point dipoles embedded at their centre. The strength of the dipoles can be chosen to yield any given bulk dielectric constant. The density of dipoles, much higher than that of the electrolyte, is chosen to be like that of real liquids. This fluid is confined between two hard charged walls with a fixed surface potential, and results for the charge and polarisation density profiles at fixed wall separations, as well as the pressure between the walls as a function of their separation, are obtained.

The relation between the pressure and the contact values of the variables for charged systems can be obtained from exact sum rules [40-43]. It can also be obtained for purely polar and electrolyte/solvent systems [59,60]. The forms obtained in this chapter differ from the exact forms due to the linear nature of the theory. In the next chapter, the non-linear theory presented gives the correct sum rules.

The method employed here is the same as in earlier work of this kind. A density-functional is used to represent the free energy of the fluid, assuming only small perturbations of the density from its value in the bulk. This free energy is minimised with respect to variations in the density profile, and the resulting equation, which is satisfied uniquely by the equilibrium density profile, is solved. In point of fact, the free energy was not minimised directly with respect to the individual species densities (although, in principle, it could have been). It was instead found that the free energy could be represented in terms of the charge density, proportional to the difference of the two electrolyte species, the polarisation density, proportional to the angular-dependent dipole density, and the total density, which was just the sum of all the species densities. The advantage of this representation is that it produces a decoupling of the total density from the charge and polarisation densities, and further, one solves for the charge and polarisation directly. Also, angular-dependence is eliminated from the equations. The equation involving total density alone is not treated here, as this

has been fully solved elsewhere [17], and the pressure due to this component is simply additive.

The theory can be considered a generalisation both of Debye-Hückel (DH) theory, allowing for ions and dipoles of finite sizes, and the work of other authors [18-20] who deal with a single wall. The former connection is made in Appendix C.

The results for the charge density and the pressure obtained from this theory are therefore compared with those arising from DH theory with the inclusion of a Stern layer of unit dielectric constant at the walls. The best agreement was found for fluids with low dielectric constant. For high fluid dielectric constants, the deviations from uniformity are so great as to affect the colloidal stability, and this topic is discussed at the end of the chapter.

Now for a high value of the bulk dielectric constant, the electrostatic interaction of the two walls is greatly reduced. This modification is made evident in one of the derivations of the pressure, as the pressure is given by the difference of two large quantities. Since this procedure is sensitive to the values of these large quantities, any error in either one is greatly multiplied when their difference is taken, and large errors for the pressure ensue. Accordingly, an alternative form for the pressure is derived, one which is less sensitive to errors in the calculation. The equivalence of these two forms is established in Appendix B.

3.2. Theory

3.2.1. The Thermodynamic Potential

Since the model represents an electrolyte in a solvent, it is comprised of three species, two with equal and opposite point charges at their centre, and one with a point dipole. Now the dipole potential is not spherically symmetric, as are the potentials involved (Coulomb, hard-sphere), and hence the orientation, Ω, of the dipoles must be specified, as well as their position, r. The number density of species λ ($\lambda = 1,2,3$)

will then be dependent on both position and orientation,

$$\rho_\lambda(\mathbf{r},\Omega) \equiv \rho_\lambda(\mathbf{x}) \tag{3.1}$$

Although the ion densities do not depend on orientation, it is useful in the formalism to treat them as if they did.

In the uniform fluid, the orientation of the dipoles is random. This is another way of saying that the number densities are independent of orientation. Similarly, the number densities are also independent of position. Then

$$\rho_\lambda(\mathbf{r},\Omega) = \frac{\rho_{0\lambda}}{4\pi}$$

where $\rho_{0\lambda}$ is the number density of species λ. Perturbations in the densities caused by external fields can therefore be written as

$$\delta\rho_\lambda(\mathbf{x}) = \rho_\lambda(\mathbf{x}) - \frac{\rho_{0\lambda}}{4\pi}$$

Now the equilibrium bulk density is such as to make the free energy a minimum. So for small perturbations in the density caused by an external field, the free energy will not change to first order. In fact, only second-order terms are important, and one may therefore express the new free energy as a quadratic functional of $\delta\rho_\lambda(\mathbf{x})$. More specifically

$$\Omega(\delta\rho_\lambda) = \Omega(0) + \frac{1}{2}\sum_{\lambda\nu}\int d\mathbf{x}\,d\mathbf{x}'\,\delta\rho_\lambda(\mathbf{x})K_{\lambda\nu}(\mathbf{x},\mathbf{x}')\delta\rho_\nu(\mathbf{x}') \tag{3.2}$$

where the integration over $\mathbf{x}$ indicates an integral over all space and orientations. The significance of the function $K(\mathbf{x},\mathbf{x}')$ is discussed more fully in Chapter 5, section 2. It is the functional version of the first coefficient in a Taylor series. Strictly speaking, it should therefore be independent of the variable of expansion; in this case, the density. However, the function $K_{\lambda\nu}(\mathbf{x},\mathbf{x}')$ must also satisfy a condition which follows from the general theory of fluids, obtained by functionally differentiating the free energy twice with respect to the density

$$K_{\lambda\nu}(\mathbf{x},\mathbf{x}') = \frac{1}{\beta}\left\{\frac{4\pi\delta_{\lambda\nu}\delta(\mathbf{x},\mathbf{x}')}{(\rho_{0\lambda}\rho_{0\nu})^{1/2}} - c_{\lambda\nu}(\mathbf{x},\mathbf{x}')\right\} \tag{3.3}$$

In general, the direct correlation function of a fluid is known to vary with the density. So the function $K_{\lambda\nu}(x,x')$ is not, therefore, density independent.

Now the perturbations are caused by an external field, $\phi_\lambda(x)$. This will couple to the density components, giving rise to a term which must be included in the free energy,

$$\sum_\lambda \int \phi_\lambda(x)\rho_\lambda(x)dx \tag{3.4}$$

where $\beta=1/kT$ (k is Boltzmann's constant and T is the temperature, $\delta_{\lambda\nu}$ is the Kronecker delta, $\delta(x,x')$ is the Dirac delta function and $c_{\lambda\nu}(x,x')$ are the bulk direct correlation functions for the fluid mixture. With these modifications, the free energy will now have the form

$$
\begin{aligned}
\Delta\Omega[\delta\rho_\lambda(x)] &= \Omega[\delta\rho_\lambda(x)] - \Omega(0) \\
&= \frac{1}{2\beta}\sum_{\lambda\nu}\int dxdx'\delta\rho_\lambda(x)\left\{\frac{4\pi\delta_{\lambda\nu}\delta(x,x')}{(\rho_{0\lambda}\rho_{0\nu})^{1/2}} - c_{\lambda\nu}(x,x')\right\}\delta\rho_\nu(x') \\
&\quad + \sum_\lambda\int dx\phi_\lambda(x)\rho_\lambda(x).
\end{aligned}
\tag{3.5}
$$

The real direct correlation functions for such a system are unknown, but analytic forms may be obtained through an approximation scheme. In this case the mean spherical was chosen, as this approximation has been solved by various workers [23]. Under this approximation, the direct correlation function is simply proportional to the particle interaction potential beyond a given radius. For the system described above, the orientation dependence of these potentials is no greater than that given by first-order spherical harmonic functions. Thus for an electric external field, the induced densities can be expanded in terms of Legendre polynomials to first-order only,

$$\rho_\lambda(x) = \frac{\rho_\lambda(r)}{4\pi} + \mu_\lambda \cdot A_\lambda(r) \tag{3.6}$$

Higher order terms would vanish when convolved with the first-order (and zeroth order) terms arising from the direct correlation functions, since the Legendre functions form an orthogonal basis set.

One may now define the local polarisation, which depends on the orientation of all the dipoles at a given position, as

$$P_\lambda(r) = \int d\Omega \mu_\lambda \rho_\lambda(x) \tag{3.7}$$

If one substitutes eqn (3.6) for $\rho_\lambda(x)$ in eqn (3.7) and integrates over orientation, remembering that

$$\int \mu_\alpha d\Omega = 0$$

and

$$\int \mu_\alpha^2 d\Omega = \frac{4\pi\mu^2}{3}$$

where $\alpha = x, y, z$, then one obtains the relation between $A_\lambda(r)$ and the polarisation $P_\lambda(r)$,

$$A_\lambda(r) = \frac{3P_\lambda(r)}{4\pi\mu_\lambda^2} \tag{3.8}$$

Therefore

$$\sum_{\lambda\nu} \int 4\pi\delta_{\lambda\nu} \frac{\delta(x,x')}{(\rho_{0\lambda}\rho_{0\nu})^{1/2}} \delta\rho_\lambda(x)\delta\rho_\nu(x')dxdx'$$

$$= 4\pi \sum_\lambda \int \frac{\delta\rho_\lambda^2(x)}{\rho_{0\lambda}} dx = \sum_\lambda \frac{4\pi}{\rho_{0\lambda}} \int drd\Omega \left\{ \frac{\delta\rho_\lambda^2(r)}{(4\pi)^2} + \frac{9[\mu_\lambda \cdot P_\lambda(r)]^2}{(4\pi\mu_\lambda^2)^2} \right\}$$

$$= \sum_\lambda \int dr \frac{1}{\rho_{0\lambda}} \left\{ \delta\rho_\lambda^2(r) + \frac{3P_\lambda^2(r)}{\mu_\lambda^2} \right\}. \tag{3.9}$$

The cross-term arising from the square of the form given in eqn (3.6) for the density is not included, as this vanishes when the integration over orientation is performed. So the free energy now becomes

$$\Delta\Omega[\delta\rho_\lambda(r)] = \frac{1}{2\beta} \sum_\lambda \int \frac{dr}{\rho_{0\lambda}} \left\{ \delta\rho_\lambda^2(r) + \frac{3P_\lambda^2(r)}{\mu_\lambda^2} \right\}$$

$$- \frac{1}{2\beta} \sum_{\lambda\nu} \int dxdx' \delta\rho_\lambda(x)c_{\lambda\nu}(x,x')\delta\rho_\nu(x') + \sum_\lambda \int dx\phi_\lambda(x)\rho_\lambda(x). \tag{3.10}$$

In order to put this in a more useful form, we now introduce the total number density, $\rho(\mathbf{r})$, the charge density, $q(\mathbf{r})$, and a quantity, $n(\mathbf{r})$, defined by

$$\rho(\mathbf{r})=\sum_\lambda \rho_\lambda(\mathbf{r}), \quad q(\mathbf{r})=\sum_\lambda e_\lambda \rho_\lambda(\mathbf{r}), \quad n(\mathbf{r})=\rho(\mathbf{r})-\rho_3(\mathbf{r}) \tag{3.11}$$

where for the civilised model we have

$$\lambda=1,2,3; \quad e_\lambda=1,-1,0; \quad \mu_\lambda=0,0,\mu; \quad P_\lambda=0,0,P$$

and

$$\rho_0=\sum_i \rho_{0i}, \quad n_0=\rho_{01}+\rho_{02}. \tag{3.12}$$

After a little algebraic manipulation, eqn (3.10) may now be written in terms of these more useful quantities as

$$\Delta\Omega[\delta\rho_\lambda(\mathbf{r})]=\frac{1}{2\beta}\left\{\frac{1}{\rho_0}\int d\mathbf{r}\delta\rho^2(\mathbf{r})+\frac{1}{n_0}\int d\mathbf{r}q^2(\mathbf{r})+\frac{n_0\rho_{03}}{\rho_0}\int d\mathbf{r}u^2(\mathbf{r})\right.$$
$$\left.+\frac{3}{\rho_{03}\mu^2}\int d\mathbf{r}P^2(\mathbf{r})\right\}-\frac{1}{2\beta}\sum_{\lambda\nu}\int d\mathbf{x}d\mathbf{x}'\delta\rho_\lambda(\mathbf{x})c_{\lambda\nu}(\mathbf{x},\mathbf{x}')\delta\rho_\nu(\mathbf{x}')$$
$$+\sum_\lambda \int d\mathbf{x}\phi_\lambda(\mathbf{x})\rho_\lambda(\mathbf{x}) \tag{3.13}$$

where

$$u(\mathbf{r})=\frac{\delta n(\mathbf{r})}{n_0}-\frac{\delta\rho_3(\mathbf{r})}{\rho_{03}}. \tag{3.14}$$

The model being dealt with is that of a non-polar 1:1 electrolyte with a neutral third component. For simplicity equal radii components are chosen. Now since this is a linear theory, the perturbations from the equilibrium density are proportional to the equilibrium density. It is then a simple matter to show that

$$u(\mathbf{r})\equiv 0 \tag{3.15}$$

and this quantity no longer appears in the succeeding equations of this chapter.

Here we adopt (with some minor alterations) the notation of Chan et al., [23]. This suggests the following form for the bulk direct correlation functions

$$c_{\lambda\nu}(\mathbf{x},\mathbf{x}')=c_{\lambda\nu}{}^{HS}(r^0)+e_\lambda e_\nu c^c(r^0)+e_\lambda c^E(r^0)E_\nu-e_\nu c^E(r^0)E_\lambda$$

$$+c^{\Delta}(\mathbf{r}^0)\Delta_{\lambda\nu}+c^D(\mathbf{r}^0)D_{\lambda\nu} \tag{3.16}$$

where

$$E_{\lambda}=\hat{\boldsymbol{\mu}}(\omega_{\lambda})\cdot\hat{\mathbf{r}}^0, \qquad \Delta_{\lambda\nu}=\hat{\boldsymbol{\mu}}(\omega_{\lambda})\cdot\hat{\boldsymbol{\mu}}(\omega_{\nu}),$$

$$D_{\lambda\nu}=\hat{\boldsymbol{\mu}}(\omega_{\lambda})\cdot(3\hat{\mathbf{r}}\hat{\mathbf{r}}-I)\cdot\hat{\boldsymbol{\mu}}(\omega_{\nu}), \qquad \mathbf{r}^0=\mathbf{r}-\mathbf{r}' \tag{3.17}$$

and where c^{HS} are the bulk hard-sphere correlation functions, c^c are ion-ion correlation functions, c^E are ion-dipole correlation functions and c^{Δ} and c^D are dipole- dipole correlation functions. All the functions $c(\mathbf{r})$ are symmetric under a change of sign of their argument except for $c^E(\mathbf{r})$ which is antisymmetric. This follows intuitively if one considers what happens to the interaction potential, proportional to the direct correlation function beyond the hard-sphere radius in the MSA, when the positions of two interacting particles are exchanged, preserving the orientation of each one. This corresponds to reversing the sign of the argument of the direct correlation functions. Within the hard-sphere core there seems to be no reason why the functions should not maintain their symmetry or antisymmetry, and there are probably good physical reasons why this should be so.

Now the only external fields acting on the fluid are those due to the impenetrability of the walls and the charges thereon. In that case, the external fields can be represented by

$$\phi_{\lambda}(\mathbf{x})=\frac{1}{4\pi}\phi_{\lambda}(\mathbf{r})=\frac{1}{4\pi}[\phi^s(\mathbf{r})+ee_{\lambda}v(\mathbf{r})]. \tag{3.18}$$

where the first term represents the short-range impenetrability, and the second term represents the long-range Coulombic interaction.

With this modification the integrals over orientation can all be performed explicitly. This removes orientation dependence from the integrals, and the thermodynamic potential (or, equivalently, free energy) therefore becomes

$$2\beta\Delta\Omega(\delta\rho_{\lambda})=2\beta\Delta\Omega(\rho,q,\mathbf{P})$$

$$=\int d\mathbf{r}\left\{\frac{\delta\rho^2(\mathbf{r})}{\rho_0}+\frac{q^2(\mathbf{r})}{n_0}+\frac{3\mathbf{P}^2(\mathbf{r})}{\rho_{03}\mu^2}\right\}$$

$$-\int \mathbf{dr dr}' \left[\delta\rho(\mathbf{r})c^{HS}(\mathbf{r}^0)\delta\rho(\mathbf{r}')+q(\mathbf{r})c^c(\mathbf{r}^0)q(\mathbf{r}')\right.$$

$$+\mathbf{P}(\mathbf{r})\cdot\frac{c^\Delta(\mathbf{r}^0)}{\mu^2}\mathbf{P}(\mathbf{r}')$$

$$+\left(3[\mathbf{P}(\mathbf{r})\cdot\hat{\mathbf{r}}^0][\mathbf{P}(\mathbf{r}')\cdot\hat{\mathbf{r}}^0]-\mathbf{P}(\mathbf{r})\cdot\mathbf{P}(\mathbf{r}')\right)\frac{c^D(\mathbf{r}^0)}{\mu^2}$$

$$\left.+2\mathbf{P}(\mathbf{r})\cdot\hat{\mathbf{r}}^0 q(\mathbf{r}')c^E(\mathbf{r}^0)\frac{}{\mu}\ \right]+2\beta\int \mathbf{dr}[\phi^s(\mathbf{r})\rho(\mathbf{r})+ev(\mathbf{r})q(\mathbf{r})]. \qquad (3.19)$$

If we now specialise to a system in which the liquid is confined between two parallel hard walls with uniform surface charge, then all the densities will depend only on the direction perpendicular to these walls, x say. Furthermore, the electric field will everywhere point in this direction and so will the polarisation. Then one can integrate over the two transverse co-ordinates y and z where possible, and subsequently divide the equation by $\int dydz$ throughout. Then the thermodynamic potential per unit area can be written as

$$2\beta\Delta\Omega(q,\rho,P)=\frac{1}{\rho_0}\int\delta\rho^2(x)dx+\frac{1}{n_{0)}}\int q^2(x)dx+\frac{3}{\rho_{03}\mu^2}\int P^2(x)dx$$

$$-\int dxdx'\,[\delta\rho(x)C^{HS}(x^0)\delta\rho(x')+q(x)C^c(x^0)q(x')$$

$$+\frac{P(x)P(x')}{\mu^2}C^\Delta(x^0)$$

$$+P(x)P(x')\frac{2C^D(x^0)}{\mu^2}+\frac{2P(x)}{\mu}q(x')C^E(x^0)]$$

$$+2\beta\int dx\,[\phi^s(x)\rho(x)+ev(x)q(x)] \qquad (3.20)$$

where

$$C^{c,\Delta,HS}(x)=2\pi\int_x^\infty drr c^{c,\Delta,HS}(r)$$

$$C^E(x)=2\pi\int_x^\infty drx c^E(r)$$

$$C^D(x)=2\pi\int_x^\infty drr\frac{1}{2}(3x^2-1)c^D(r) \qquad (3.21)$$

Now the equilibrium distributions $\rho(x),q(x)$, and $P(x)$ make the free energy a

minimum. Hence they can be found by differentiating the free energy with respect to each of these quantities, and setting the result equal to zero. This provides us with three integral equations, the solutions of which are the equilibrium distributions.

$$\frac{q(x)}{n_0}-\int dx'\left[q(x')C^c(x^0)-\frac{P(x')}{\mu}C^E(x^0)\right]+\beta ev(x)=0 \qquad (3.22)$$

$$\frac{3P(x)}{\rho_{03}\mu^2}-\int dx'\left[\frac{P(x')}{\mu^2}[C^\Delta(x^0)+2C^D(x^0)]+q(x')\frac{C^E(x^0)}{\mu}\right]=0 \qquad (3.23)$$

The equation involving the total density has not been included, as this is identical to the one obtained elsewhere [17], and has been fully solved there. Note that the equations involving the charge and polarisation density profiles, $q(x)$ and $P(x)$ respectively, are coupled.

One may make one further simplification to the form for the free energy. The term $\phi^s(x)$, representing the impenetrability of the walls, can be dropped as its sole effect on the fluid can incorporated in a modification of the range of integration. At present, the range of integration extends over all space. However, since the walls exclude the fluid from occupying the same position, the term $\phi^s(x)$ may be neglected if one simultaneously alters the integration limits to extend only over the range in which the fluid exists, namely $0<x<h$. So,

$$2\beta\Delta\Omega=\int_0^h dx\left[\frac{q^2(x)}{n_0}+\frac{3P^2(x)}{\rho_{03}\mu^2}+\frac{\delta\rho^2(x)}{\rho_0}\right]$$
$$-\int_0^h\int_0^h dxdx'\,[\delta\rho(x)C^{HS}(x^0)\delta\rho(x')+q(x)C^c(x^0)q(x')$$
$$+\frac{P(x)P(x')}{\mu^2}2C^D(x^0)+\frac{P(x)P(x')}{\mu^2}C^\Delta(x^0)$$
$$+\frac{2P(x)q(x')}{\mu}C^E(x^0)]+2\beta\int_0^h dx\,[\phi^s(x)\rho(x)+ev(x)q(x)]. \qquad (3.24)$$

3.2.2. The pressure

One can see from fundamental arguments that for an incremental change in the separation of the walls, h, the free energy per unit area will change by an amount

proportional to the pressure. Hence the pressure may be obtained by differentiating the free energy with respect to the separation, h. By considering the sign of the change in the free energy, one can see that the pressure is, in fact, the negative differential of the free energy. So

$$-2\beta\frac{\partial\Delta\Omega}{\partial h}=-\left\{\frac{q^2(h)}{n_0}+\frac{3P^2(h)}{\rho_{03}\mu^2}+\frac{\delta\rho^2(h)}{\rho_0}\right.$$

$$-2\int_0^h dx'\left[\delta\rho(h)C^{HS}(h-x')\delta\rho(x')+q(h)C^c(h-x')q(x')\right.$$

$$+\frac{P(h)P(x')}{\mu^2}C^\Delta(h-x')+\frac{P(h)P(x')}{\mu^2}2C^D(h-x')$$

$$+\frac{P(h)}{\mu}q(x')C^E(h-x')-\frac{P(x')}{\mu}q(h)C^E(h-x')\ \Bigg]$$

$$\left.+2\beta\frac{\partial}{\partial h}\int_0^h dx\,[ev(x)q(x)]\ \right\} \tag{3.25}$$

Most of the terms on the righthand side of eqn (3.25) can be eliminated by use of the three equations for the equilibrium distributions, with the value of x chosen as h. Then the total pressure is seen to be a simple additive function of terms coming from each of the macroscopic variables, $i.e$

$$-\frac{\partial\Delta\Omega}{\partial h}=\frac{\rho^2(h)}{2\beta\rho_0}+p_q$$

where p_q is the electrostatic component of the pressure between the walls,

$$p_q=\frac{1}{2\beta}\left[\frac{q^2(h)}{n_0}+\frac{3P^2(h)}{\rho_{03}\mu^2}\right]-\frac{Q^2(h)}{2\epsilon_0} \tag{3.26}$$

and $Q(h)$ is the surface charge density on a single wall on which the potential is fixed at V_0 and can be obtained from the electroneutrality condition, $viz.$

$$\int_0^h eq(x)\,dx+2Q(h)=0 \tag{3.27}$$

The term in the pressure due to the total density has been dealt with elsewhere [17], and since it is simply additive, will not therefore be discussed further here.

The electrostatic pressure, p_q, can also be derived in a way which is not explicitly dependent upon the discrete nature of the fluid. For this grand canonical system it can be shown [22] that the pressure is given by

$$p_q(h) = -\left(\frac{\partial F}{\partial h}\right)_{V_i} \tag{3.28}$$

where

$$F = \Omega - \sum_i V_i Q_i \tag{3.29}$$

$$V_i = \frac{\partial \Omega}{\partial Q_i}, \qquad d\Omega = \sum_i V_i dQ_i \tag{3.30}$$

and where V_i and Q_i are the potential and charge per unit area at the i' th wall, $i = 1,2$. If one slowly increases the charges on each wall from 0 to Q_i by adding increments of charge $q_i d\lambda$, then, from eqn (3.30)

$$d\Omega = \sum_i V_i(\lambda) Q_i d\lambda \tag{3.31}$$

where $V_i(\lambda)$ is the potential on the i' th surface when the charges are λQ_i. Integrating this equation gives

$$\Omega(Q) = \sum_i Q_i \int_0^1 V_i(\lambda) d\lambda \tag{3.32}$$

Since in this approximation the equations are linear, $V_i(\lambda)$ is proportional to λ, and

$$V_i(\lambda) = \lambda V_i$$
$$\Omega(Q) = \frac{1}{2}\sum_i Q_i V_i \tag{3.33}$$
$$F(Q) = -\frac{1}{2}\sum_i Q_i V_i$$

The system under consideration is one in which the walls are identical. By symmetry, therefore, the charge and potential on each wall is the same. The free energy then simplifies to

$$F = -QV_0$$
$$p_q(h) = V_0\left(\frac{\partial Q}{\partial h}\right)_V. \tag{3.34}$$

This is the alternative formula for calculating $p_q(h)$. It is not obvious that eqn (3.34) will lead to the same values for the pressure as eqn (3.26). It is therefore shown in Appendix C that the two formulae are equivalent. One can see that the resultant electrostatic component of the pressure between the walls, $f_q(h)$, is simply the difference of the pressures acting on either side of one wall. Now fluid is presumed to exist at infinity (see ref 21, fig 1) -- this is the limit of a wall with finite width immersed in fluid, with the wall width allowed to tend to infinity. Since no other wall exists beyond the far side of the wall as the limit is taken, the pressure at the far side corresponds to that for a single wall, namely $p_q(\infty)$. Therefore

$$f_q(h)=p_q(h)-p_q(\infty)$$

3.3. Calculation of the Correlation Functions

As mentioned earlier, the functions $c_{\lambda\nu}(x,x')$ are the bulk direct correlation functions. These are not known exactly for this fluid, but analytical functions for them may be obtained using certain approximations. In this case the mean spherical approximation (MSA) was used, in conjunction with the Ornstein-Zernike relations for this fluid mixture. The bulk direct correlation functions can be obtained from these. A further simplification is the use of these bulk direct correlation functions in place of the (unknown) inhomogeneous ones, a step taken by many workers [e.g.18-23].

The MSA for this system has been solved by Carnie and Chan [18], and their results are used here. They utilised a method due to Baxter based on the Wiener-Hopf procedure, which relates the direct correlation functions to auxiliary $Q_{\alpha\beta}(t)$ through the equations

$$C_{\alpha\beta}(x)=Q_{\alpha\beta}(x)-\sum_\gamma\int_0^\infty dt Q_{\alpha\beta}(t)Q_{\alpha\beta}(x+t) \tag{3.35}$$

where

$$\begin{aligned}
C_{11}(x)&=C^c(x)\\
C_{12}(x)&=C_{21}(-x)=C^E(x)
\end{aligned} \tag{3.36}$$

$$C_{22}(x)=C^{\Delta}(x)+2C^{D}(x)=C^{+}(x).$$

The functions $Q_{\alpha\beta}(t)$ are listed below.

$$Q_{11}(r)=-A_{11} \quad r>R$$
$$=(\rho_1 A_{11}H_{11}-\rho_2 H_{21}M_{12}^0)(r-R)-A_{11} \quad 0<r<R$$
$$Q_{21}(r)=-A_{21} \quad r>R$$
$$=(\rho_1 A_{21}H_{11}+H_{21}a_2)(r-R)-A_{21} \quad 0<r<R$$
$$Q_{12}(r)=0 \quad r>R$$
$$=-\frac{1}{2}\left(\rho_1 A_{21}H_{21}+\frac{24\xi}{R^3}M_{12}^0\right)(r^2-R^2)$$
$$+\left[-H_{21}(a_1-\rho_1 A_{11}R)+\frac{24\xi}{R^3}(RM_{12}^0-M_{12}^1)\right](r-R) \quad 0<r<R$$
$$Q_{22}(r)=0 \quad r>R$$
$$=\frac{1}{2}\left[\frac{24\xi}{\rho_2 R^3}a_2-\rho_1 A_{21}H_{21}\right](r^2-R^2)$$
$$+\left[\rho_1 H_{21}M_{21}^0+\rho_1 A_{21}H_{21}R_{12}-\frac{24\xi}{\rho_2 R^3}(Ra_2-s)\right](r-R) \quad 0<r<R$$

The simple form of the functions is due to a symmetry of the fluid, namely the equal size of the ions and the dipoles. This furthermore simplifies the ranges over which the functions exist.

The constants are the solutions of the following eleven simultaneous non-linear equations.

$$4\pi\beta e^2=\rho_1 A_{11}^2+\rho_2 A_{21}^2$$
$$4\pi\beta e\,\mu=A_{21}a_2-\rho_1 A_{11}M_{12}^0$$
$$4\pi\beta\rho_2\mu^2=a_2^2+\rho_1\rho_2 M_{12}^{(0)2}-q(-\xi)$$
$$1-a_1=-\rho_1 A_{11}R+\tfrac{1}{2}\rho_1 R^2[\rho_2 H_{21}M_{12}^0-\rho_1 A_{11}H_{11}]$$
$$H_{21}s=-\tfrac{1}{2}A_{21}+\rho_1 H_{11}M_{21}^0$$
$$M_{21}^0=-A_{21}R-\tfrac{1}{2}R^2(\rho_1 A_{21}H_{11}+H_{21}a_2)$$
$$H_{11}a_1=-\tfrac{1}{2}A_{11}+\rho_2 H_{21}M_{12}^1$$
$$M_{12}^0=\frac{\tfrac{1}{2}R^2 H_{21}}{(1-2\xi)^2}\left\{a_1-\frac{1}{3}\rho_1 A_{11}R(1+\xi)\right\}$$
$$M_{12}^1=-\frac{\tfrac{1}{2}R^2 H_{21}}{(1-2\xi)^2}[\frac{1}{3}a_1(\xi-2)+\frac{\rho_1 A_{11}R}{4}]$$

$$a_2 = [q(2\xi)]^{1/2} + \frac{\frac{1}{2}\rho_1\rho_2 R^2 H_{21}}{(1-2\xi)^2} \left\{ M_{21}^0 + \frac{1}{3} A_{21} R (1+xi) \right\}$$

$$\frac{s}{R} = \frac{1+\xi}{(1-2\xi)^2} + \frac{\frac{1}{2}\rho_1\rho_2 R^2 H_{21}}{(1-2\xi)^2}$$

$$\times \left\{ \left(\frac{2-\xi}{1} \right) M_{21}^0 + \frac{1}{4} A_{21} R \right\}$$

and $q(x)$ is defined as

$$q(x) = \frac{(1+2x)^2}{(1-x)^4}$$

These must, in general, be solved numerically on a computer, although analytic low ion density solutions are available [18]. These were used as the initial input, and an iterative solution for higher densities was obtained. Convergence is slow but can be obtained.

3.4. Results and Discussion

3.4.1. Computation

The analytically intractable equations for the charge and polarisation densities were also solved by computer, following previous work of this kind [17,21,22]. The region in which the fluid exists was divided into discrete intervals. The integrals were thereby converted to sums by use of Simpson's Rule. This gave a matrix equation which was then solved by inversion. For a mesh size of 0.125R, the estimated error was <1% in the charge and polarisation density at a dielectric constant of 78, although a comparable accuracy could be maintained with larger mesh sizes as the dielectric constant decreased.

However, as simple error theory reveals, the corresponding accuracy of the pressure as given by eqn (3.26) is much less. Inspection of this equation shows that the difference of the term due to the polarisation density at the wall and the term due

to the charge on the wall is required. Now these terms are found to be nearly equal, and both are considerably larger than the term due to the fluid charge density (by a factor of $\approx$ 10 for $\epsilon_r = 78$ and a separation of 20R). In fact, the difference between these terms is approximately equal to the wall charge term divided by the dielectric constant, the result one obtains from macroscopic theory. Small errors in the value of either of these terms result in very large errors in their difference, even to the point of giving the wrong sign for it. As the separation increases, the polarisation and wall-charge terms both increase considerably, and consequently the contribution of their difference to the pressure increases in importance both relatively and absolutely, and errors acceptable for these terms individually become unacceptable for the pressure.

By contrast, eqn (3.34) provides us with the pressure with an accuracy comparable to that of the wall-charge term. Since this is estimated to be <1% with the moderate mesh size of 0.25R, this equation for the pressure was chosen in preference to the less accurate form (3.26).

3.4.2. The Charge and Polarisation profiles

The results for the charge and polarisation profiles are displayed in Figs 3.1(a) and 3.1(b). The ion concentration is 0.0051 mol dm^{-3}, the bulk dielectric constant of the pure dipolar component is 78, and the results are plotted for separations of the walls of 2R, 5R, and 10R. Naturally, only half of the profile is shown in each case, since the profiles are symmetric about the mid-point for the charge density, and antisymmetric for the polarisation density. From the graphs one can see that the value of both the charge and polarisation densities at the wall are very dependent on the wall separation at small wall separations. Furthermore, structural effects are quite evident within three or four molecular diameters of the wall, particularly for the polarisation density. This is more remarkable when one considers the low ion density involved.

The comparison between this 'civilised' model and macroscopic theory is made in Fig 3.2, where the charge profile of the present theory is plotted with one obtained

from Debye-Hückel (DH) theory, assuming a Stern layer of one molecular radius thickness, and with a dielectric constant of unity. Three values for the bulk dielectric constant of the fluid were chosen; 78, 7.8 and 3. The macroscopic theory cannot, of course, reproduce the structural effects, but it also differs from the present theory in giving a different value of the charge density at the wall. As already mentioned, the effects of structure are very pronounced in the polarisation profile, making it very different from the monotonic form predicted by macroscopic theory. The perturbation on the charge profile, therefore, is considerable, and is probably sufficient to explain the difference between the two theories. Furthermore, upon analysis of the equations given by Carnie and Chan [18] for a single wall (the limit of infinite separation in this case) , one can obtain a correction to Debye-Huckel theory, in the limit of low densities, of the order of

$$\frac{\epsilon_r - 1}{4q_+^{1/4}} \kappa R$$

where κ^{-1} is the Debye length and q_+ is determined from

$$q_+ \left[1 - \frac{1}{\epsilon_r} \right] = \frac{\beta \rho_{03} \mu^2}{3\epsilon_0} \tag{3.37}$$

The Debye length and the dipole density are kept fixed, and in order to vary the dielectric constant, the strength of the dipoles is changed. One can see from this that the deviation of DH theory grows as the dielectric constant increases, and this is, in fact, what occurs (see Fig 3.2). Unfortunately, the choice of dielectric constant of the Stern layer is not constrained by any stringent conditions, and so the absolute value of the charge density as given by macroscopic theory is not known.

For reasons discussed earlier, eqn (3.34) was chosen to calculate the electrostatic component of the pressure. In order to use this equation, the total charge per unit area on each wall, Q, needed to be evaluated at all values of the wall separation. Because the electroneutrality condition was incorporated in the formalism at the start,

the charge per unit area on the wall is simply equal and opposite to half of the total area under the charge profile. This quantity is therefore plotted against wall separation in Fig 3.3, with a Debye length of 10R, and dielectric constants of 78, 7.8 and 3. The graph shows that the dependence is monotonic, and the larger the dielectric constant is, the faster $Q(h)$ approaches its asymptotic value $Q(\infty)$. The former feature is useful in that the derivative of Q with respect to h, the quantity directly required for the pressure, can be calculated accurately since the graph is smooth and monotonic, and the gradient does not change rapidly anywhere.

3.4.3. Force and Colloidal Stability

The results for the calculation of the pressure by eqn (3.34) are displayed in Figs 3.4(a)-(c). The pressure is shown as a function of wall separation for the three values of the bulk dielectric constant used throughout, and the macroscopic results of DH theory are shown also. As before, the difference between the two results is greatest for the larger values of the dielectric constant. At the highest value of the dielectric constant, 78, the pressure is oscillatory, although it is monotonic for the lower values. This result is familiar from theories which take the structure of the fluid into account, and one would expect this feature to remain when the structure of the solvent is included, and indeed it does. Presumably the oscillations are more pronounced at higher ionic densities, perhaps even changing sign, and this is currently under investigation.

This has direct consequences for colloidal stability. The stability of a colloid is largely determined by the forces between colloidal particles at separations of the order of a Debye length, κ^{-1}. In the system described above, the Debye length was chosen to be 10R. Thus from Fig 3.4 it can be seen that at this separation, the modification to classical theory is not very great when $\epsilon_r < 7.8$. However, at the highest dielectric constant, chosen to be equal to that fo an aqueous solution, the force predicted by the present theory is some 70% greater at this separation than that given by DH theory.

This implies that for high values of the bulk dielectric constant, liquid structure is likely to affect the conditions for colloidal stability.

The next chapter extends this formalism by treating the entropy of the fluid exactly, rather than taking the approximation used here. The formalism is then applied to the same model as in this chapter.
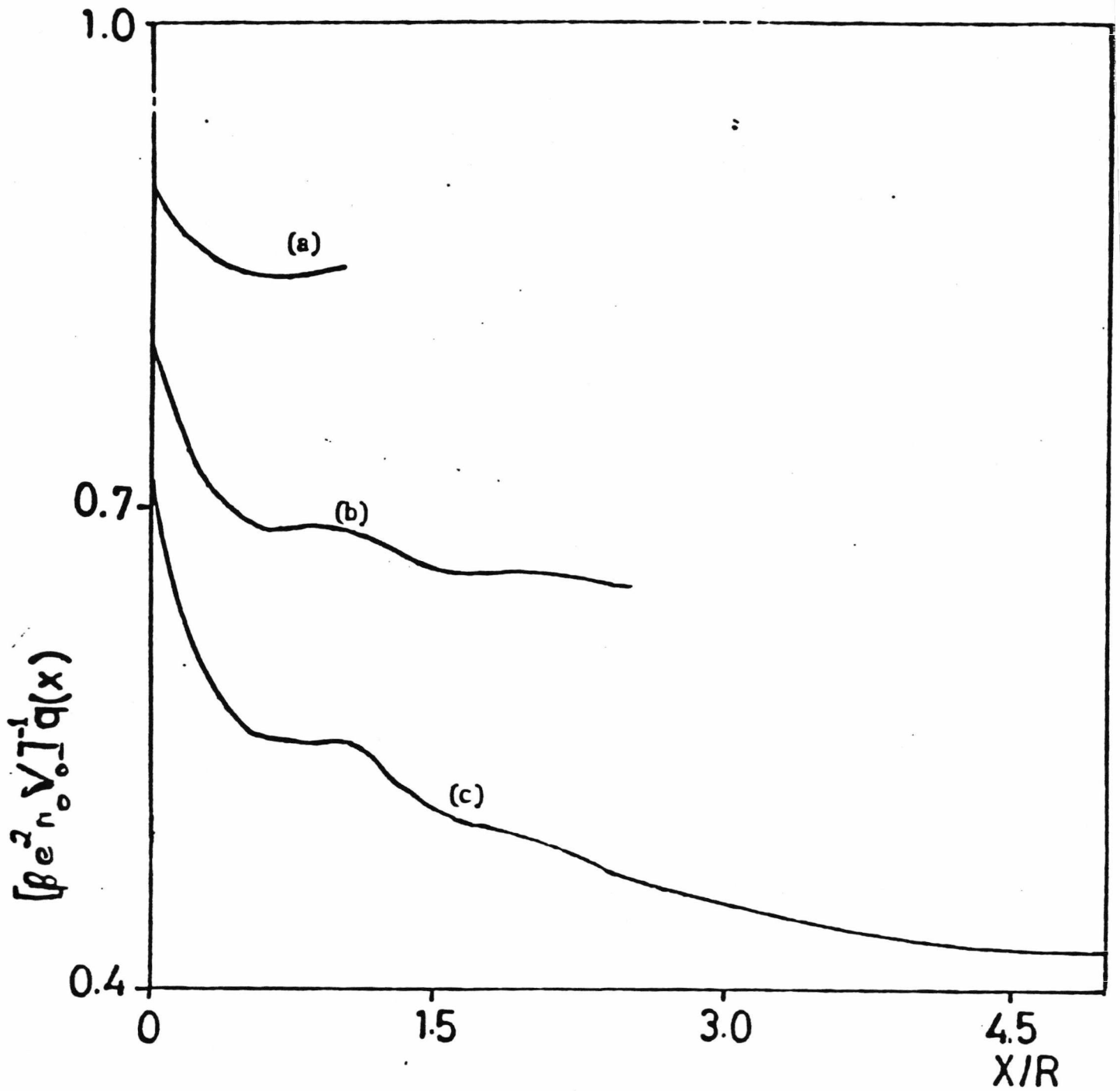
Fig 3.1(a): The charge profile $q(x)$ for various wall separations $h =$ (a) $2R$, (b) $5R$, (c) $10R$. The bulk dielectric constant ϵ_r is 78, and $\kappa R = 0.1$. The ion concentration is $0.0051M$.
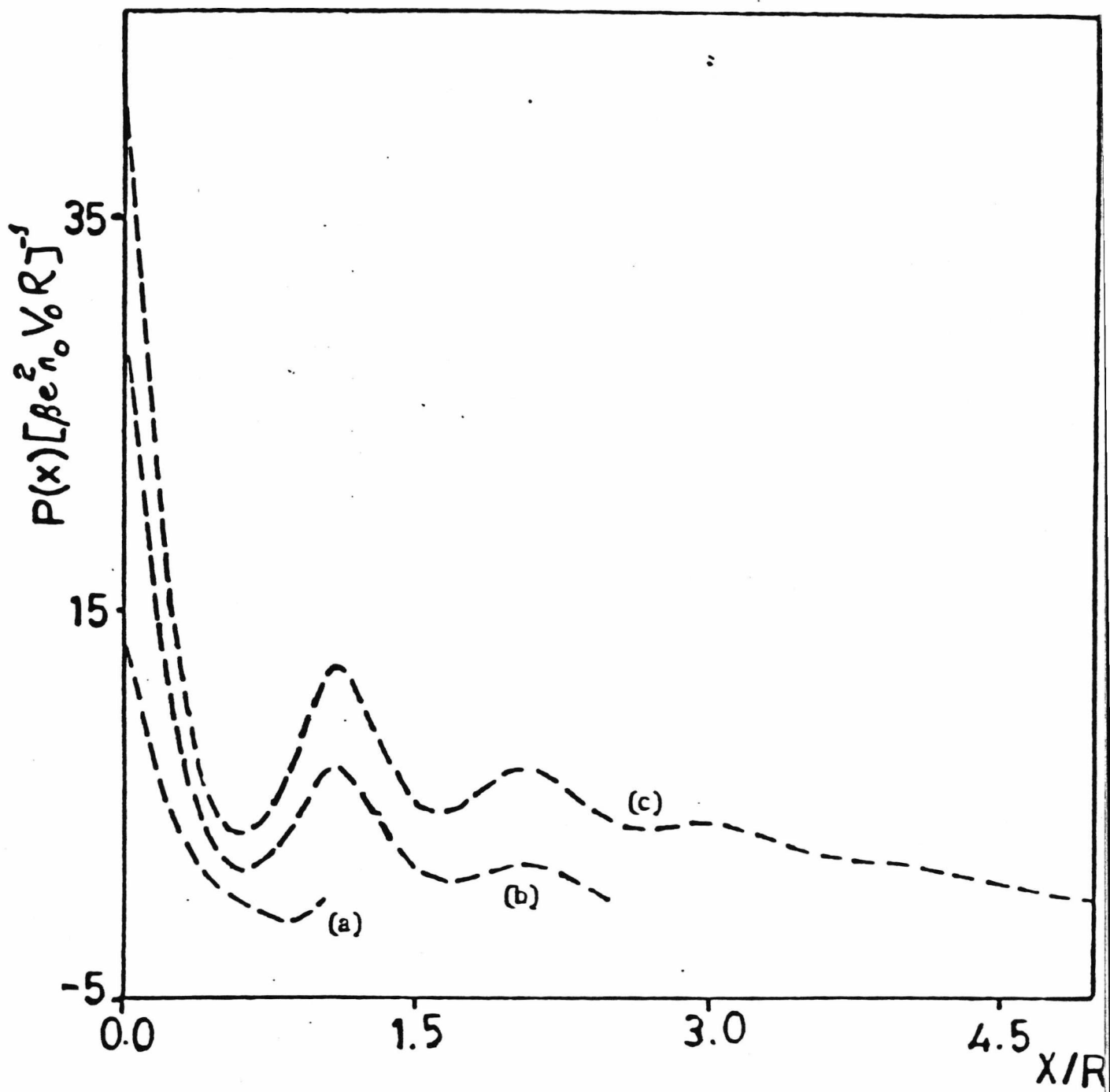
Fig 3.1(b): The polarisation profile $P(x)$; all else as for Fig 3.1(a).
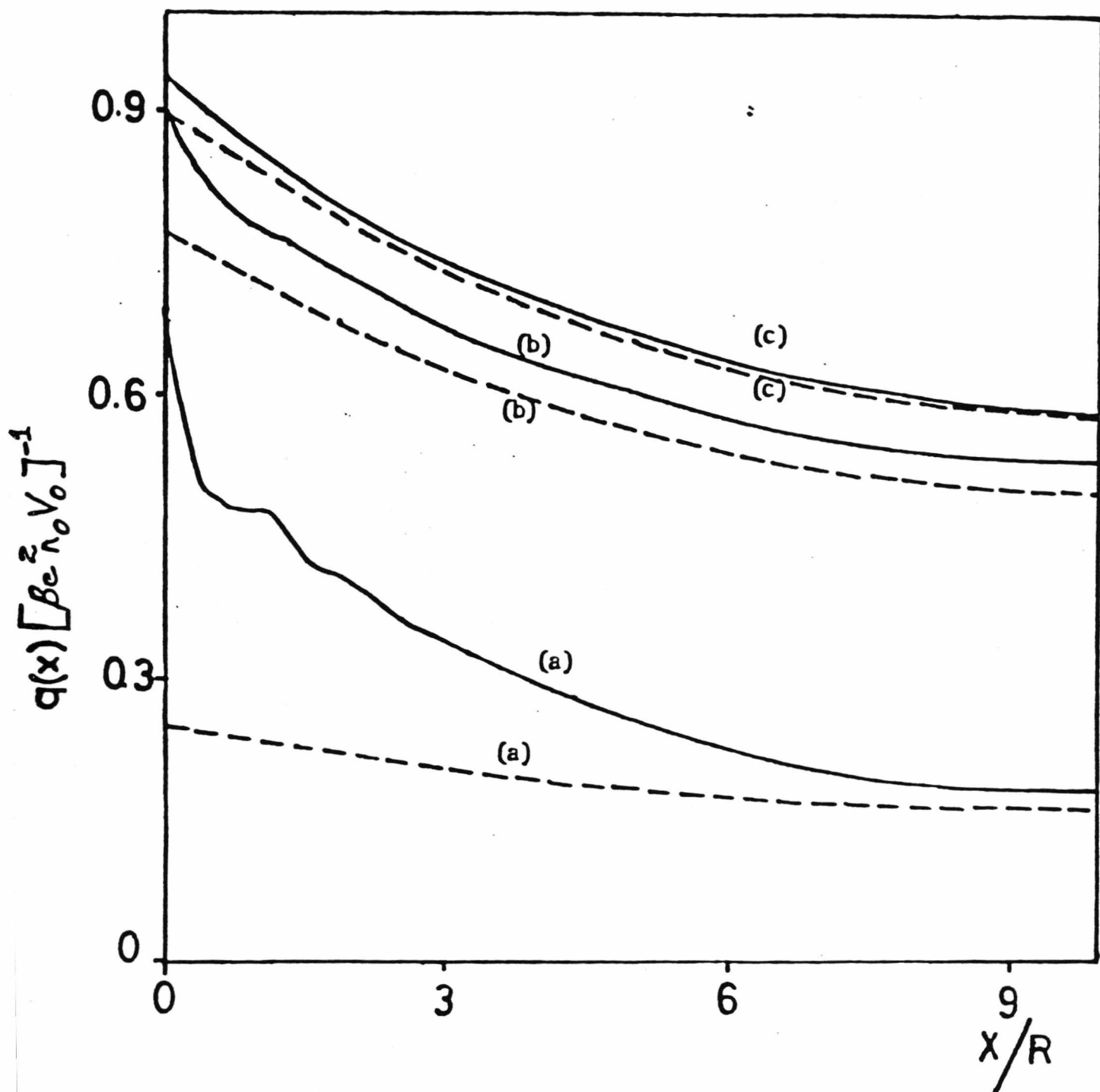
Fig 3.2: The charge profile $q(x)$ from AR (solid curve) and DH (dashed curve) theories at dielectric constants of (a) 78, (b) 7.8, (c) 3. $\kappa R = 0.1$
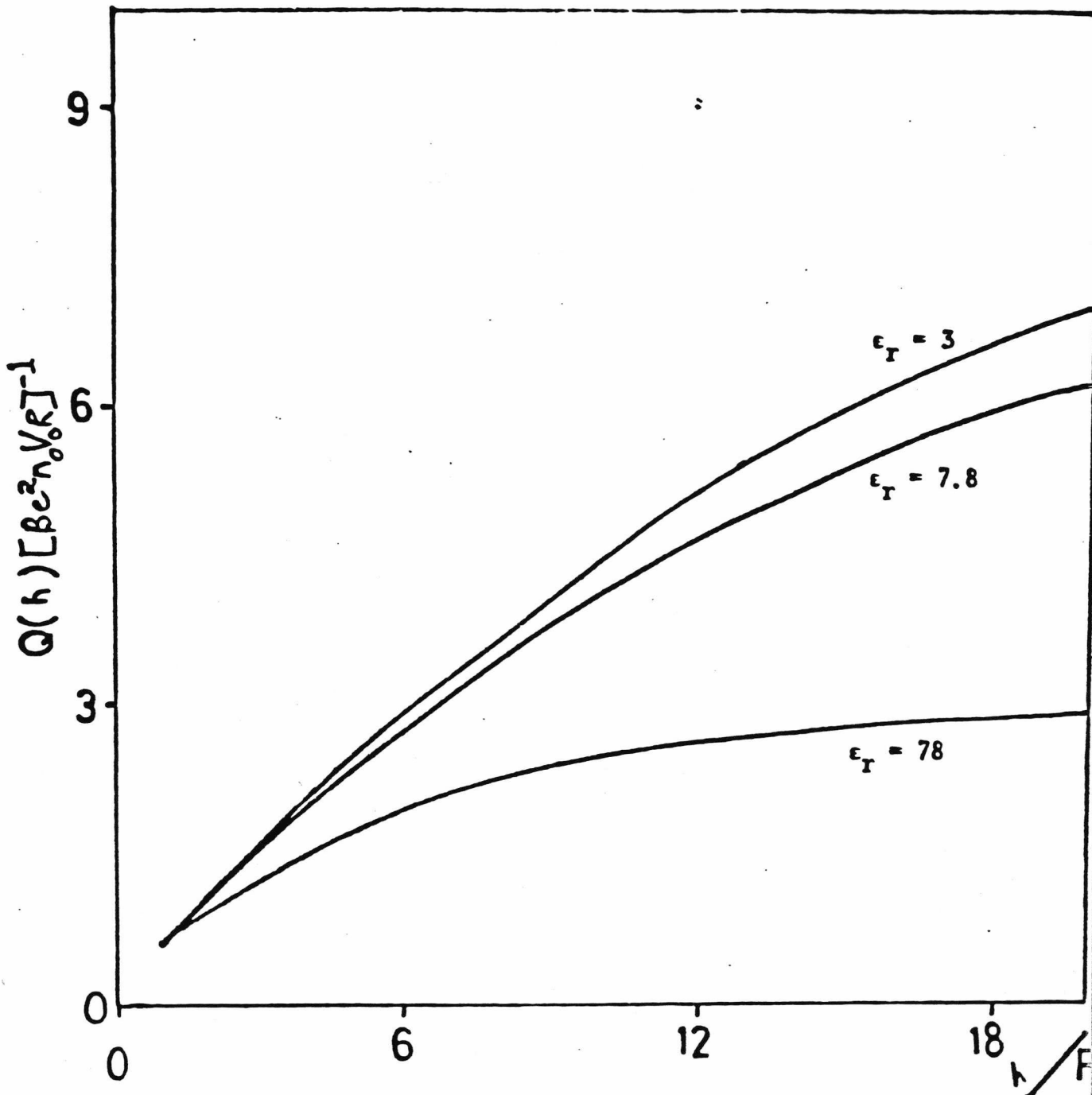
Fig 3.3: The charge on the wall $Q(h)$ as a function of wall separation, for dielectric constants $\epsilon_r = 78$, 7.8, and 3; $\kappa R = 0.1$.
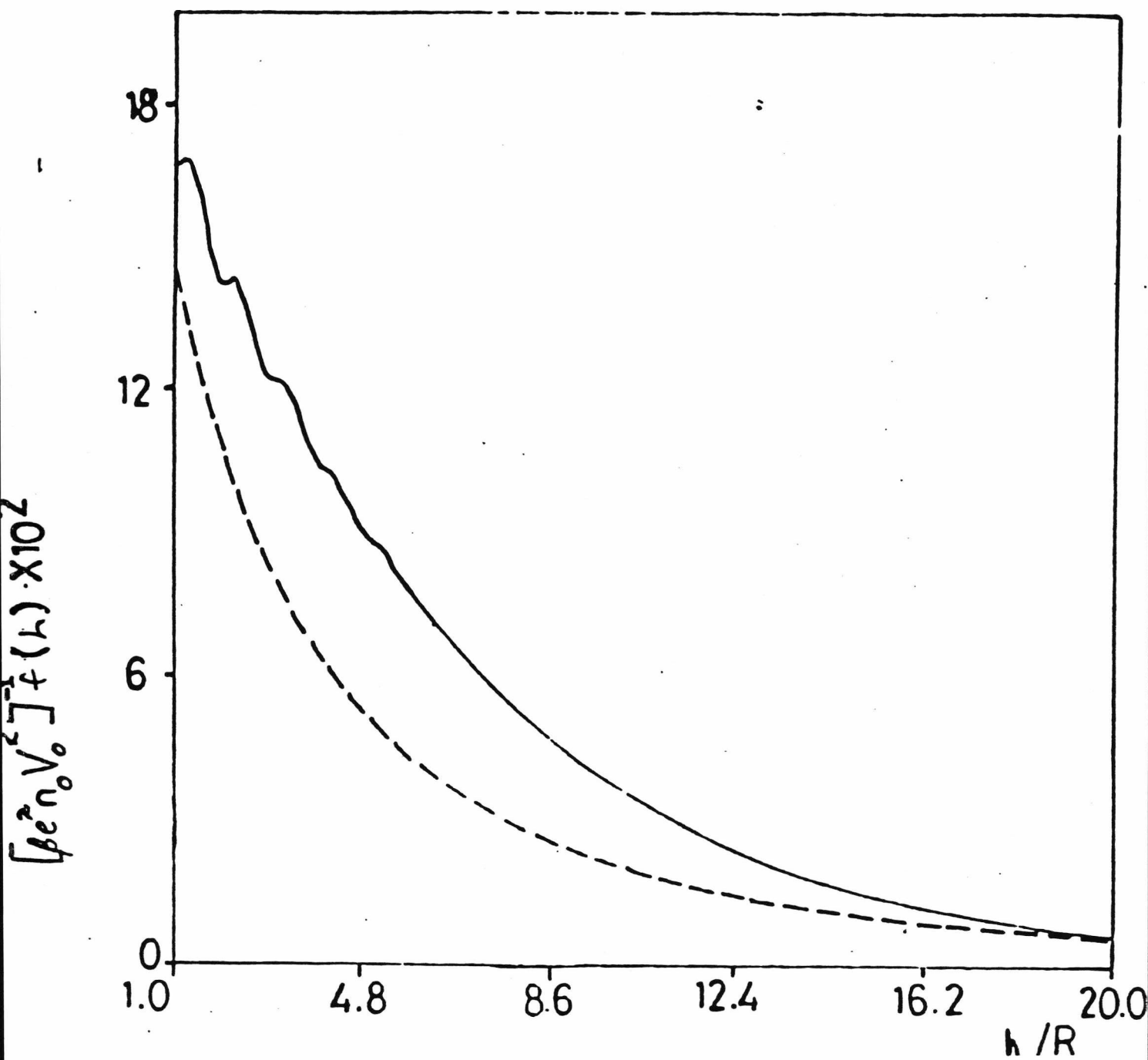
Fig 3.4(a): Comparison of pressure, f(h), from AR(solid curves)

and DH(dashed curves) theories for dielectric constants 78,

kR=0.1 (Pressure for AR theory derived from eqn. 3.34)

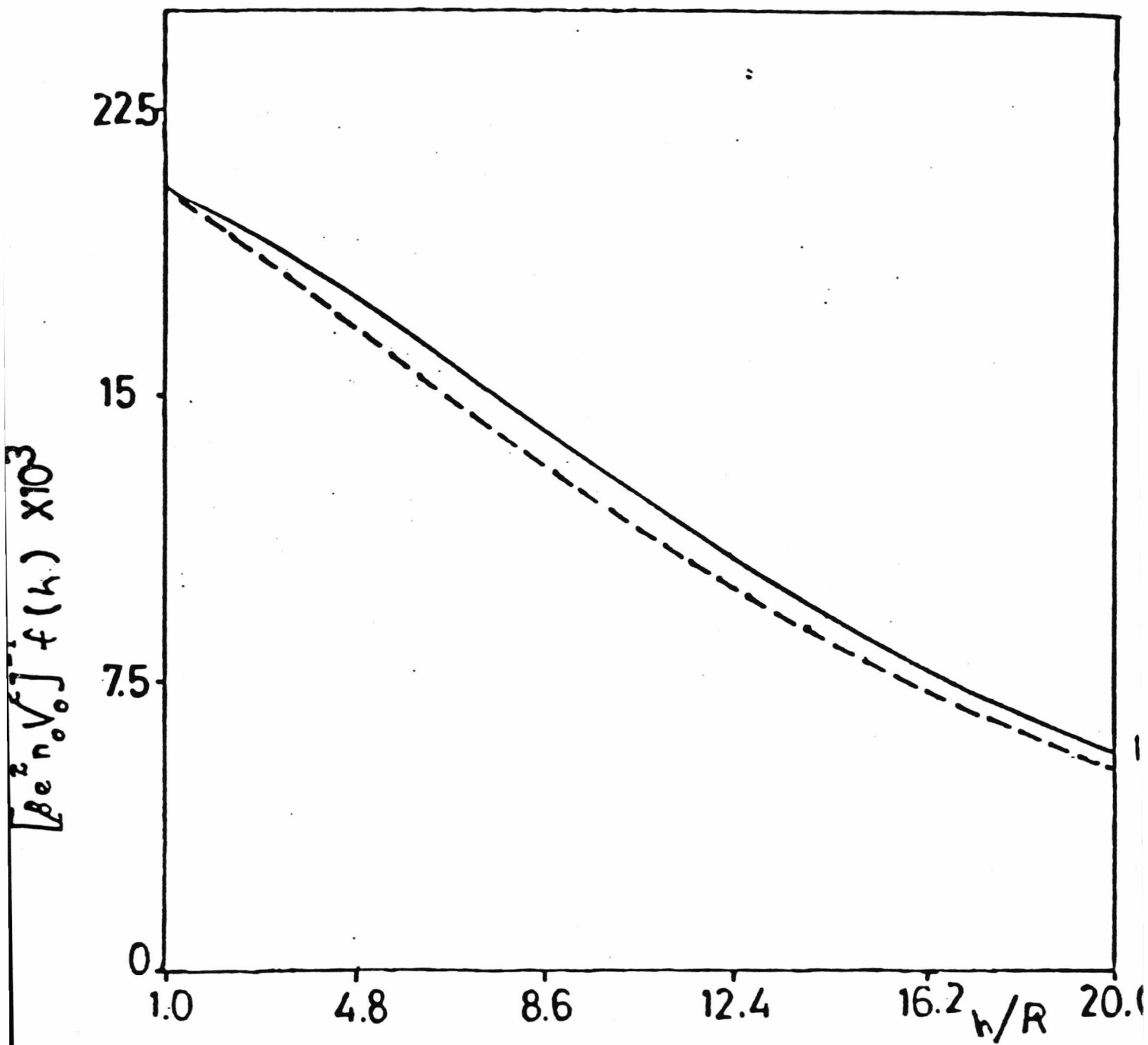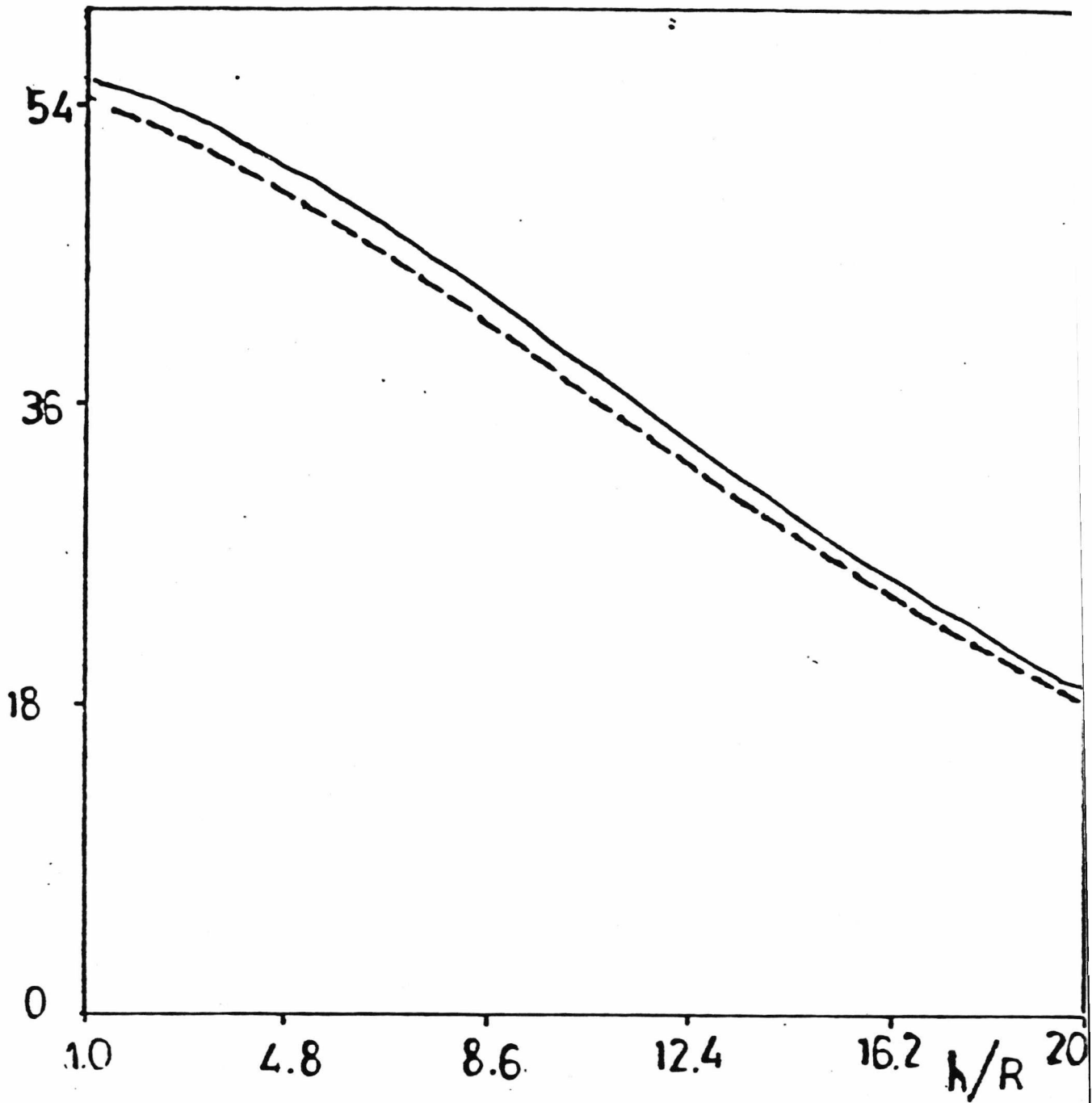Fig 3.4(b): As for Fig 3.4(a) with $\epsilon_r = 7.8$

Fig 3.4(c): As for Fig 3.4(c) with $\epsilon_r = 3$

4. A NON-LINEAR FUNCTIONAL APPROXIMATION FOR THE FREE ENERGY OF AN IONIC-DIPOLAR SYSTEM.

4.1. Introduction

The initial premise of the preceding chapter was that if the fluctuations in the density of a fluid produced by an external potential are small, then the free energy can be expressed as a quadratic functional of the fluctuations. It can be shown that this approximation is, in effect, an approximation for the entropy of the fluid. If one writes the correct form for the entropy, a logarithmic term replaces a linear one [16,17]. This is termed the non-linear theory.

This chapter applies this non-linear theory to the same model as in the previous chapter, and the results are examined. Due to the non-linearity of the theory, the equations for the equilibrium densities, although still expressible in terms of the charge and polarisation densities, are now fully coupled. As a result, 4 simultaneous non-linear integral equations must be solved rather than 2, as in the linear case. The quantities solved for are the densities of the three species and the polarisation density.

Consequently, the matrix method of solution is made harder by the increased size of the matrices required to achieve reliable results. Indeed, due to limitations on the computers capability to handle very large matrices, the results were judged not reliable enough to produce accurate values for the pressure. It must be emphasised that this is due solely to computer limitations, and not an unfortunate formulation of the problem. Given a slightly larger capacity, the problem would be rendered much more tractable.

A further obstacle is that the results must be achieved through iteration , and cannot be solved at a single stroke. This is not a serious problem, however, as the iteration converged sufficiently well.

Section 2 introduces the modification to the free energy, and the new equations for equilibrium are derived. Section 3 shows that for small fluctuations, the theory

reduces to the linear one of Chapter 3. Section 4 derives a simple formula for the pressure, and the results and discussion are presented in section 5.

4.2. Free Energy

A modified functional for the free energy of a multicomponent system is

$$
\beta\Omega = \sum_\lambda \left\{ \int dx \left[\rho_\lambda(x) - \frac{\rho_{0\lambda}}{4\pi} \right] [\beta v_\lambda(x) - 1] \right.
$$

$$
+ \int dx \rho_\lambda(x) \ln \left[\frac{4\pi\rho_\lambda(x)}{\rho_{0\lambda}} \right] \left. \right\}
$$

$$
- \frac{1}{2} \sum_{\lambda v} \int\int dx dx' \left[\rho_\lambda(x) - \frac{\rho_{0\lambda}}{4\pi} \right] c_{\lambda v}(x,x') \left[\rho_v(x') - \frac{\rho_{0v}}{4\pi} \right]
$$

$$
+ \beta\Lambda \int \delta\rho(x) \left\{ e(\rho_1(x) - \rho_2(x)) + \sigma(r) \right\} - \frac{\beta Q^2 h}{2\epsilon_0} \tag{4.1}
$$

where Ω is the free energy (or grand thermodynamic potential), $\rho_\lambda(x)$ is the number density at position r, orientation ω, $(x \equiv r, \omega)$, of species λ, $c_{\lambda v}(x,x')$ is the direct correlation function of species λ and v, $\rho_{0\lambda}$ is the number density of the fluid in the absence of inhomogeneities and is therefore a constant, $v_\lambda(x)$ is the external applied field coupling with species λ, and Λ is a Lagrange multiplier. $\sigma(r)$ is the external charge distribution, and $\beta = 1/k_B T$, k_B being Bolztmann's constant.

The first term on the right-hand side represents the coupling of the components to an external field. The second term is the entropy of the fluid and exists even for a non-interacting fluid. It is this term that was approximated by a linear term in the previous chapter. The third term represents the interaction of the fluid with itself. The fourth term is, in effect, a restatement of the electroneutrality condition *viz.* ,

$$
\int dr \left\{ e(\rho_1(r) - \rho_2(r)) + \sigma(r) \right\} = 0 \tag{4.2}
$$

and therefore does not contribute to the free energy, but it is a convenient way of including this boundary condition without having to retain a separate explicit equation. The final term represents the direct interaction of one wall with the other. [45]

The model dealt with is that of a 1:1 electrolyte with a polar solvent. These components are represented by $\lambda=1,2$ and 3 respectively. The first two components do not, therefore, depend on orientation but it is convenient in the formalism to treat them as if they do.

Now the equilibrium profile of each component minimises the free energy. Thus

$$\frac{\delta\beta\Omega}{\delta\rho_\lambda(x)}=\beta v_\lambda(x)+\ln\left(\frac{4\pi\rho_\lambda(x)}{\rho_{0\lambda}}\right)\sum_\nu\int dx' c_{\lambda\nu}(x,x')\left[\rho_\nu(x')-\frac{\rho_{0\nu}}{4\pi}\right]$$

$$+\beta e\,\Lambda=0 \tag{4.3}$$

If one now substitutes the following forms for the correlation functions, following the previous chapter, one obtains

$$\begin{aligned}
c_{ij}(\mathbf{r}^0)&=c^{HS}(\mathbf{r}^0)+z_i z_j c^c(\mathbf{r}^0)\\
c_{id}(\mathbf{r}^0,\omega)&=c^{HS}(\mathbf{r}^0)+z_i c^E(\mathbf{r}^0)E_2(\omega)\\
c_{di}(\mathbf{r}^0,\omega)&=c^{HS}(\mathbf{r}^0)-z_j c^E(\mathbf{r}^0)E_1(\omega)\\
c_{dd}(\mathbf{r}^0,\omega_1,\omega_2)&=c^{HS}(\mathbf{r}^0)+c^\Delta(\mathbf{r}^0)\Delta_{12}(\omega_1,\omega_2)+c^D(\mathbf{r}^0)D_{12}(\omega_1,\omega_2)
\end{aligned} \tag{4.4}$$

where

$$\begin{aligned}
E_\alpha&=\hat{\boldsymbol{\mu}}(\omega_\alpha)\cdot\hat{\mathbf{r}}^0, \qquad \alpha=1,2\\
\Delta_{12}&=\hat{\boldsymbol{\mu}}(\omega_1)\cdot\hat{\boldsymbol{\mu}}(\omega_2)\\
D_{12}&=\hat{\boldsymbol{\mu}}(\omega_1)\cdot(3\hat{\mathbf{r}}\hat{\mathbf{r}}-1)\cdot\hat{\boldsymbol{\mu}}(\omega_2)\\
\mathbf{r}^0&=\mathbf{r}-\mathbf{r}'
\end{aligned} \tag{4.5}$$

One may furthermore specify the external potential

$$v_\lambda(x)=\frac{e_\lambda v(r)}{4\pi} \tag{4.6}$$

where

$$e_\lambda=\begin{matrix}e\\-e\\0\end{matrix}\quad,\quad \lambda=\begin{matrix}1\\2\\3\end{matrix}$$

where e is the protonic charge.

Restricting ourselves to a fluid confined between two hard planar walls, one sees that, by symmetry, the density profiles will vary only in the co-ordinate perpendicular to the walls, say x. Thus the equilibrium equations become

$$\beta ev(x) + \ln\left(\frac{\rho_1(x)}{\rho_{01}}\right) - \int d\mathbf{x}' \left\{ \frac{c_{11}(\mathbf{x}',\mathbf{x})}{4\pi}\delta\rho_1(x') + \frac{c_{12}(\mathbf{x}',\mathbf{x})}{4\pi}\delta\rho_2(x') \right.$$
$$\left. + \frac{c_{13}(\mathbf{x}',\mathbf{x})}{4\pi}(\rho_3(x') - \rho_{03} + 4\pi\delta\rho_3(x',\omega)) \right\} + \beta e\Lambda = 0 \qquad (4.7)$$

$$-\beta ev(x) + \ln\left(\frac{\rho_2(x)}{\rho_{02}}\right) - \int d\mathbf{x}' \left\{ \frac{c_{21}(\mathbf{x}',\mathbf{x})}{4\pi}\delta\rho_1(x') + \frac{c_{22}(\mathbf{x}',\mathbf{x})}{4\pi}\delta\rho_2(x') \right.$$
$$\left. + \frac{c_{23}(\mathbf{x}',\mathbf{x})}{4\pi}(\delta\rho_3(x') + 4\pi\delta\rho_3(x',\omega')) \right\} + \beta e\Lambda = 0 \qquad (4.8)$$

$$\ln\left(\frac{\rho_3(x) + 4\pi\delta\rho_3(x,\omega)}{\rho_{03}}\right) - \int d\mathbf{x}' \left\{ \frac{c_{31}(\mathbf{x}')}{4\pi}\delta\rho_1(x') + \frac{c_{32}(\mathbf{x}')}{4\pi}\delta\rho_2(x') \right.$$
$$\left. + \frac{c_{33}(\mathbf{x}')}{4\pi}(\delta\rho_3(x') + 4\pi\delta\rho_3(x',\omega)) \right\} = 0 \qquad (4.9)$$

where the angular dependence of $\rho_3(x,\omega)$ has been expressed in the form

$$\rho_3(x,\omega) = \frac{\rho_3(x)}{4\pi} + \delta\rho_3(x,\omega) \qquad (4.10)$$

and

$$\delta\rho_i(x) = \rho_i(x) - \rho_{0i} \qquad (4.11)$$

Substituting the forms for the correlation functions from eqn (4.4), and integrating over ω' gives

$$\beta ev(x) + \ln\left(\frac{\rho_1(x)}{\rho_{01}}\right) - \int d\mathbf{r}' \left\{ \delta\rho_1(x')[c^{HS}(\mathbf{r}^0) + c^c(\mathbf{r}^0)] - \delta\rho_2(x')[c^{HS}(\mathbf{r}^0) - c^c(\mathbf{r}^0)] \right.$$
$$\left. + c^{HS}(\mathbf{r}^0)\delta\rho_3(x') + c^E(\mathbf{r}^0)\frac{\mathbf{P}(x')\cdot\hat{\mathbf{r}}^0}{\mu} \right\} - \beta e\Lambda = 0 \qquad (4.12)$$

$$-\beta ev(x) + \ln\left(\frac{\rho_2(x)}{\rho_{02}}\right) - \int d\mathbf{r}' \left\{ \delta\rho_1(x')[c^{HS}(\mathbf{r}^0) - c^c(\mathbf{r}^0)] + \delta\rho_2(x')[c^{HS}(\mathbf{r}^0) + c^c(\mathbf{r}^0)] \right.$$
$$\left. + c^{HS}(\mathbf{r}^0)\delta\rho_3(x') - c^E(\mathbf{r}^0)\frac{\mathbf{P}(x')\cdot\hat{\mathbf{r}}^0}{\mu} \right\} - \beta e\Lambda = 0 \qquad (4.13)$$

$$\ln\left(\frac{\rho_3(x)+4\pi\delta\rho_3(x,\omega)}{\rho_{03}}\right)-\int d\mathbf{r}'\left\{\delta\rho_1(x')[c^{hS}(\mathbf{r}^0)+c^E(\mathbf{r}^0)\hat{\boldsymbol{\mu}}(\omega)\cdot\hat{\mathbf{r}}^0]\right.$$

$$+\delta\rho_2(x')[c^{HS}(\mathbf{r}^0)+c^E(\mathbf{r}^0)\hat{\boldsymbol{\mu}}(\omega)\cdot\hat{\mathbf{r}}^0+c^{HS}(\mathbf{r}^0)\delta\rho_3(x')$$

$$\left.+c^\Delta(\mathbf{r}^0)\hat{\boldsymbol{\mu}}(\omega)\cdot\mathbf{P}(x')+c^D(\mathbf{r}^0)\hat{\boldsymbol{\mu}}(\omega)\cdot(3\hat{\mathbf{r}}^0\hat{\mathbf{r}}^0-1)\cdot\frac{\mathbf{P}(x')}{\mu}\right\}=0 \qquad (4.14)$$

where, by comparison with chapter 3,

$$\delta\rho_3(x,\omega)=\frac{3\boldsymbol{\mu}(\omega)\cdot\mathbf{P}(x)}{4\pi\mu^2} \qquad (4.15)$$

These may be rewritten as

$$\beta ev(x)+\ln\left(\frac{\rho_1(x)}{\rho_{01}}\right)-\int dx'\left\{\delta\rho_1(x')[C^{HS}(x^0)+C^c(x^0)]\right.$$

$$+\delta\rho_2(x')[C^{HS}(x^0)-C^c(x^0)]+C^{HS}(x^0)\delta\rho_3(x')$$

$$\left.+\frac{P(x')}{\mu}C^E(x^0)\right\}+\beta e\Lambda=0 \qquad (4.16)$$

$$-\beta ev(x)+\ln\left(\frac{\rho_2(x)}{\rho_{02}}\right)-\int dx'\left\{\delta\rho_1(x')[C^{HS}(x^0)-C^c(x^0)]\right.$$

$$+\delta\rho_2(x')[C^{HS}(x^0)+C^c(x^0)]+C^{HS}(x^0)\delta\rho_3(x')$$

$$\left.-\frac{P(x')}{\mu}C^E(x^0)\right\}-\beta e\Lambda=0 \qquad (4.17)$$

$$\ln\left(\frac{\rho_3(x)+4\pi\delta\rho_3(x,\omega)}{\rho_{03}}\right)-\int dx'\left\{\delta\rho_1(x')[C^{HS}(x^0)-C^E(x^0)\hat{\boldsymbol{\mu}}(\omega)\cdot\hat{\mathbf{r}}^0]\right.$$

$$+\delta\rho_2(x')[C^{HS}(x^0)+C^E(x^0)\hat{\boldsymbol{\mu}}\cdot\hat{\mathbf{r}}^0]+C^{HS}(x^0)\delta\rho_3(x')$$

$$\left.+C^\Delta(x^0)\hat{\boldsymbol{\mu}}(\omega)\cdot\frac{\mathbf{P}(x')}{\mu}+2C^D(x^0)\hat{\boldsymbol{\mu}}(\omega)\cdot\frac{\mathbf{P}(x')}{\mu}\right\}=0 \qquad (4.18)$$

where

$$C^{HS,C,\Delta}(x)=2\pi\int_x^\infty rc^{HS,C,\Delta}(r)dr$$

$$C^E(x)=2\pi\int_x^\infty xc^E(r)dr \qquad (4.19)$$

$$C^D(x)=2\pi\int_x^\infty\frac{1}{2}\left(\frac{3x^2}{\mathbf{r}^2}-1\right)rc^D(r)dr$$

and

$$x^0 = x - x'$$

The C's may now be identified with those obtained by Carnie and Chan.

The last equation may be split into angular-dependent and angular-independent parts, to give two separate equations. Firstly we write

$$\ln\left(\frac{\rho_3(x) + 4\pi\delta\rho_3(x,\omega)}{\rho_{03}}\right) = \ln\left(\frac{\rho_3(x)}{\rho_{03}}\left[1 + \frac{4\pi\delta\rho_3(x,\omega)}{\rho_3(x)}\right]\right)$$

$$= \ln\left(\frac{\rho_3(x)}{\rho_{03}}\right) + \ln\left(1 + \frac{4\pi\delta\rho_3(x,\omega)}{\rho_3(x)}\right) \qquad (4.20)$$

Then expanding the second logarithm to first order only, and collecting together angle-dependent and angle-independent terms separately gives the two equations

$$\ln\left(\frac{\rho_3(x)}{\rho_{03}}\right) - \int dx' \, [\delta\rho_1(x') + \delta\rho_2(x') + \delta\rho_3(x')] C^{HS}(x^0) = 0 \qquad (4.21)$$

$$\frac{3P(x)}{\rho_3(x)\mu^2} - \int dx' \left[C^+(x^0)\frac{P(x')}{\mu^2} - C^{\epsilon}(x^0)q(x')\right] = 0 \qquad (4.22)$$

where

$$C^+(x) = C^{\Delta}(x) + 2C^D(x)$$
$$q(x) = \delta\rho_1(x) - \delta\rho_2(x) \qquad (4.23)$$

Note here that unlike the linear functional discussed in the previous chapter, the density terms remain coupled to those of the charge and polarisation, as one would expect. To solve them completely one needs to solve eqns (4.16),(4.17), (4.21) and (4.22) simultaneously, a much harder task than solving the two simultaneous equations of chapter 3. The process is further complicated by the fact that the equations are no longer linear, and so an iterative solution is required.

4.3. Relation to linear theory

Now for the case of two charged plates, $(v(x)=0)$, and it can be shown that $\Lambda = V_0$, the potential on the plates. Expanding to first order in $\delta\rho_\lambda$, (having already

functionally differentiated w.r.t. $\delta\rho_\lambda(x)$ once) , we quickly obtain three further equations:

$$\beta ev(x)+\frac{\rho_1(x)}{\rho_{01}}-\int dx'\left\{\delta\rho_1(x')[C^{HS}(x^0)+C^c(x^0)]+\delta\rho_2(x')[C^{HS}(x^0)-C^c(x^0)]\right.$$
$$\left.+C^{HS}(x^0)\delta\rho_3(x')+\frac{P(x')}{\mu}C^E(x^0)\right\}+\beta e\Lambda=0 \qquad (4.24)$$

$$-\beta ev(x)+\frac{\rho_2(x)}{\rho_{02}}-\int dx'\left\{\delta\rho_1(x')[C^{HS}(x^0)-C^c(x^0)]+\delta\rho_2(x^0)+C^c(x^0)]\right.$$
$$\left.+C^{HS}(x^0)\delta\rho_3(x')+\frac{P(x')}{\mu}(x^0)\right\}-\beta e\Lambda=0 \qquad (4.25)$$

$$\frac{\delta\rho_3(x)}{\rho_{03}}+\frac{4\pi\delta\rho_3(x,\omega)}{\rho_{03}}$$
$$-\int dx'\left\{\delta\rho_1(x')[C^{HS}(x^0)-C^E(x^0)\hat{\mu}_x(\omega)]+\delta\rho_2(x')[C^{HS}(x^0)+C^E\hat{\mu}_x(\omega)]\right.$$
$$\left.+C^{HS}(x^0)\delta\rho_3(x')+C^+(x^0)\hat{\mu}_x(\omega)\frac{P(x')}{\mu}\right\}=0 \qquad (4.26)$$

where

$$\hat{\mu}_x(\omega)=\hat{\mu}(\omega)\cdot\mathbf{r}^0 \qquad (4.27)$$

Subtracting eqn (4.26) from (4.25) gives

$$\frac{\delta\rho_1(x)}{\rho_{01}}-\frac{\delta\rho_2(x)}{\rho_{02}}-2\int dx'\left\{C^c(x^0)[\delta\rho_1(x')-\delta\rho_2(x')]\right.$$
$$\left.+C^E(x^0)\frac{P(x')}{\mu}\right\}+2\beta eV_0=0 \qquad (4.28)$$

Upon dividing both sides by 2, one obtains

$$\frac{q(x)}{n_0}-\int dx'\left\{q(x')C^c(x^0)+C^E(x^0)\frac{P(x')}{\mu}\right\}+\beta eV_0=0 \qquad (4.29)$$

where

$$\rho_{01}=\rho_{02}=\frac{n_0}{2}$$

This is one of the equations of the linear theory (with $C^E(x^0)$ of opposite sign --- we shall see that this is acceptable if the sign of the polarisation is consistent in the other

54

equation involving $C^E(x^0)$, as the polarisation is antisymmetric).

If we now add eqns (4.25),(4.26) and (4.27), we get

$$\frac{\delta\rho_1(x)}{\rho_{01}}+\frac{\delta\rho_2(x)}{\rho_{02}}+\frac{\delta\rho_3(x)}{\rho_{03}}+\frac{4\pi\delta\rho_3(x,\omega)}{\rho_{03}}$$
$$-\int dx'\left\{3C^{HS}(x^0)[\delta\rho_1(x')+\delta\rho_2(x')+\delta\rho_3(x')]\right.$$
$$\left.-C^E(x^0)[\delta\rho_1(x')-\delta\rho_2(x')]\hat{\mu_x}(\omega)+C^+(x^0)\frac{P(x')}{\mu}\hat{\mu_x}(\omega)\right\}=0 \quad (4.30)$$

Separating this into its angular-dependent and angular-independent parts gives

$$\frac{\delta\rho_1(x)}{\rho_{01}}+\frac{\delta\rho_2(x)}{\rho_{02}}+\frac{\delta\rho_3(x)}{\rho_{03}}-3\int dx' C^{HS}(x^0)\delta\rho(x')=0 \quad (4.31)$$

where

$$\rho(x)=\rho_1(x)+\rho_2(x)+\rho_3(x) \quad (4.32)$$

and

$$\frac{4\pi\delta\rho_3(x,\omega)}{\rho_{03}}-\hat{\mu_x}(\omega)\int dx'\left\{C^+(x^0)\frac{P(x')}{\mu}-C^E(x^0)q(x')\right\}=0 \quad (4.33)$$

Now in the linear theory

$$\frac{\delta\rho_1}{\rho_{01}}=\frac{\delta\rho_2}{\rho_{01}}=\frac{\delta\rho_3}{\rho_{03}} \quad (4.34)$$

and it is easy to see that

$$\frac{\delta\rho_1}{\rho_{01}}=\frac{\delta\rho}{\rho_0}=\cdots \quad (4.35)$$

Therefore eqn (4.31) becomes

$$\frac{\delta\rho(x)}{\rho_0}-\int dx' C^{HS}(x^0)\delta\rho(x')=0 \quad (4.36)$$

This is the second equation of the linear theory.

Comparing the form of $\delta\rho_3(x,\omega)$ with that given in chapter 3, one can see that

$$\delta\rho_3(x,\omega)=\mu\cdot A(r) \quad (4.37)$$

where

$$A(\mathbf{r}) = \frac{3P(\mathbf{r})}{4\pi\mu^2} \tag{4.38}$$

Thus

$$\frac{4\pi\delta\rho_3(x,\omega)}{\rho_{03}} = \frac{3\boldsymbol{\mu}(\omega)\cdot\mathbf{P(r)}}{\rho_{03}\mu^2} = \frac{3P(x)\hat{\mu}_x(\omega)}{\rho_{03}\mu} \tag{4.39}$$

Dividing eqn (4.33) throughout by $\hat{\mu}_x(\omega)\mu$ gives

$$\frac{3P(x)}{\rho_{03}\mu^2} - \int dx' \left\{ C^+(x^0)\frac{P(x')}{\mu^2} - q(x')\frac{C^E(x^0)}{\mu} \right\} = 0 \tag{4.40}$$

This is the final equation of the linear theory. As can be seen, the sign of the term $C^E(x^0)$ is opposite to that of the same term in eqn (4.29). Both signs may be simultaneously reversed, the result of which is to cause the polarisation at every point to reverse direction, leaving the charge and total density unchanged. As the polarisation is antisymmetric in space, both sets of equations are acceptable, as they both describe physically possible situations.

4.4. Pressure

If the external applied potential $v(\mathbf{r})$ is zero (*i.e.* hard walls), then we can write

$$
\begin{aligned}
\beta\Omega = \int d\mathbf{x} \Bigg\{ &- \sum_{\lambda=1}^{4} (\rho_\lambda(x)\theta(h-x) - \rho_{0\lambda}) \\
&+ \theta(h-x) \left[\sum_{\lambda=1}^{3} \rho_\lambda \ln\left(\frac{4\pi\rho_\lambda(x)}{\rho_{0\lambda}}\right) + \rho_4(x)\ln\left(\frac{4\pi\rho_3(x)}{\rho_{03}}\right) + \frac{\rho_4^2(x)}{2\rho_3(x)} \right] \Bigg\} \\
&- \frac{1}{2}\sum_{\lambda,\mu=1}^{4}\int d\mathbf{x}d\mathbf{x}' \left[\rho_\lambda(\mathbf{x})\theta(h-x) - \frac{\rho_{0\lambda}}{4\pi} \right] C_{\lambda\mu}(\mathbf{x},\mathbf{x}') \left[\rho_\mu(x')\theta(h-x') - \frac{\rho_{0\mu}}{4\pi} \right] \\
&+ \beta\Lambda \left\{ \int dx \sum_\lambda e_\lambda\rho_\lambda(x)\theta(h-x) + 2Q \right\} - \frac{\beta Q^2 h}{2\epsilon_0}
\end{aligned}
\tag{4.41}
$$

where

$$\rho_3(\mathbf{x}) = \rho_3(x) + \rho_4(x), \quad \int \rho_4(\mathbf{x})d\omega = 0$$

$$C_{4\lambda}(x,x')=C_{\lambda 4}(x,x')=C_{3\lambda}(x,x') \quad \lambda=1,2,3$$
$$C_{44}(x,x')=C_{33}(x,x') \tag{4.42}$$
$$\rho_{04}=0 \ , \ e_1=-e_2=e \ , \ e_3=e_4=0$$

and h is the separation of the walls, Q the charge on one of them. The step function effectively puts limits on the integrals, as no fluid exists beyond the walls.

Now the equations for the $\rho_\lambda(x)$ are

$$\lambda=1,2 \quad \frac{\delta\Omega}{\delta\rho_\lambda(x)}=\theta(h-x)\left\{\ln\left(\frac{4\pi\rho_\lambda(x)}{\rho_{0\lambda}}\right)\right.$$

$$-\int dx' \sum_{\mu=1}^{4} C_{\lambda\mu}(x,x')\left[\rho_\mu(x')\theta(h-x')-\frac{\rho_{0\mu}}{4\pi}\right]$$

$$\left.+\beta e\Lambda \ \right\}=0 \tag{4.43}$$

$$\lambda=3 \quad \frac{\delta\Omega}{\delta\rho_\lambda(x)}=\theta(h-x)\left\{\ln\left(\frac{4\pi\rho_3(x)}{\rho_{03}}\right)+\frac{\rho_4(x)}{\rho_3(x)}-\frac{\rho_4^2}{2\rho_3^2(x)}\right.$$

$$\left.-\int dx' \sum_{\mu=1}^{4} C_{3\mu}(x,x')\left[\rho_\mu(x')\theta(h-x')-\frac{\rho_{0\mu}}{4\pi}\right] \right\}=0 \tag{4.44}$$

$$\lambda=4 \quad \frac{\delta\Omega}{\delta\rho_4}=\theta(h-x)\left\{\ln\left(\frac{4\pi\delta\rho_3(x)}{\rho_{03}}\right)+\frac{\rho_4(x)}{\rho_3(x)}\right.$$

$$\left.-\int dx' \sum_{\mu} C_{\lambda\mu}(x,x')\left[\rho_\mu(x')\theta(h-x')-\frac{\rho_{0\mu}}{4\pi}\right] \right\}=0 \tag{4.45}$$

Then the pressure is

$$\beta p=-\frac{\partial\beta\Omega}{\partial h}=\int d\omega\left\{\sum_{\lambda=1}^{4}\rho_\lambda(h,\omega)-\sum_{\lambda=1}^{3}\rho_\lambda(h,\omega)\ln\left(\frac{4\pi\rho_\lambda(h)}{\rho_{0\lambda}}\right)\right.$$

$$\left.-\rho_4(h,\omega)\left[\ln\left(\frac{4\pi\rho_3(h)}{\rho_{03}}\right)+1\right]-\frac{\rho_4^2(h,\omega)}{2\rho_3(h)}\ \right\}$$

$$+ \sum_{\lambda,\mu=1}^{4} \int d\omega \int d\mathbf{x}' \rho_\lambda(h,\omega) C_{\lambda\mu}(h,\mathbf{x}') \left(\rho_\mu(x')\theta(h-x') - \frac{\rho_{0\mu}}{4\pi} \right)$$

$$-\beta\Lambda\sum_\lambda e_\lambda \rho_\lambda(h) - \frac{\beta Q^2}{2\epsilon_0} \tag{4.46}$$

Multiplying eqns (4.43),(4.44) and (4.45) by the respective $\rho_\lambda(h,\omega)$, integrating over ω, adding them together and letting $x \to h$ gives

$$\sum_{\lambda=1}^{3} \int d\omega \rho_\lambda(h,\omega) \ln\left(\frac{4\pi\rho_\lambda(h,\omega)}{\rho_{0\lambda}} \right)$$

$$+ \sum_{\mu=1}^{4} \int d\omega d\mathbf{x}' \rho_\lambda(h,\omega) C_{\lambda\mu}(h,\omega,x') \left(\rho_\mu(x')\theta(h-x') - \frac{\rho_{0\mu}}{4\pi} \right)$$

$$\int d\omega \left\{ \rho_4(h,\omega)\ln\left(\frac{4\pi\rho_3(h)}{\rho_{03}}\right) + \rho_4(h,\omega) - \frac{\rho_4^2(h,\omega)}{\rho_3(h)} \right.$$

$$\left. + \sum_\lambda e_\lambda \beta\Lambda \int d\omega \rho_\lambda(h,\omega) \right\} = 0 \tag{4.47}$$

Thus the sum of all the terms barring the first on the right-hand side of eqn (4.46) is zero. So finally

$$\beta p = \int d\omega \sum_{\lambda=1}^{4} \rho_\lambda(h,\omega) - \frac{\beta Q^2}{2\epsilon_0} = \rho_1(h) + \rho_2(h) + \rho_3(h) - \frac{\beta Q^2}{2\epsilon_0}$$

$$= \rho(h) - \frac{\beta Q^2}{2\epsilon_0} \tag{4.48}$$

which agrees with well-known exact sum rule [59,60].

4.5. Results and Discussion

The equations for the species densities and polarisation density were solved, and the difference of the two electrolyte species fluctuations were taken, thereby giving the charge density profile. The results are displayed in Figs 4.1-4.6.

Figure 4.1 shows the charge profile for wall separations of 2 and 4 molecular diameters. The most immediately striking feature is the large increase in the wall value

compared with the equivalent case for the linear theory. This effect has also been reported for the 'primitive' model, where the dielectric medium is treated as continuous [24]. It seems purely to be an artefact of the theory. It can be shown that this non-linear density-functional formulation is equivalent to an integral equation approach, using the Ornstein-Zernike (OZ) equations for fluid mixtures, and the hyper-netted chain (HNC) closure. Now it is well-known that the HNC closure for a fluid of hard spheres produces values of the density at the wall that are very high, much higher than would be predicted from the most accurate equation of state for hard spheres, the Carnahan-Starling equation. This is true for mixtures, and presumably true when potentials other than that of hard spheres are involved, and this is therefore regarded as the cause of the abnormally high values of the charge density at the wall. As in the linear theory, the charge profile is seen to be oscillatory, contrary to macroscopic theories (e.g. DH), and is evidence for the importance of fluid structure. The maximum separation of the walls is 4 molecular diameters, since to have increased this would have resulted in a significant decrease in the accuracy of the profiles obtained. Here the mesh size was 1/8 th of a molecular diameter. The accuracy of the value of the charge density at the wall at this mesh size is believed to be no better than 10%.
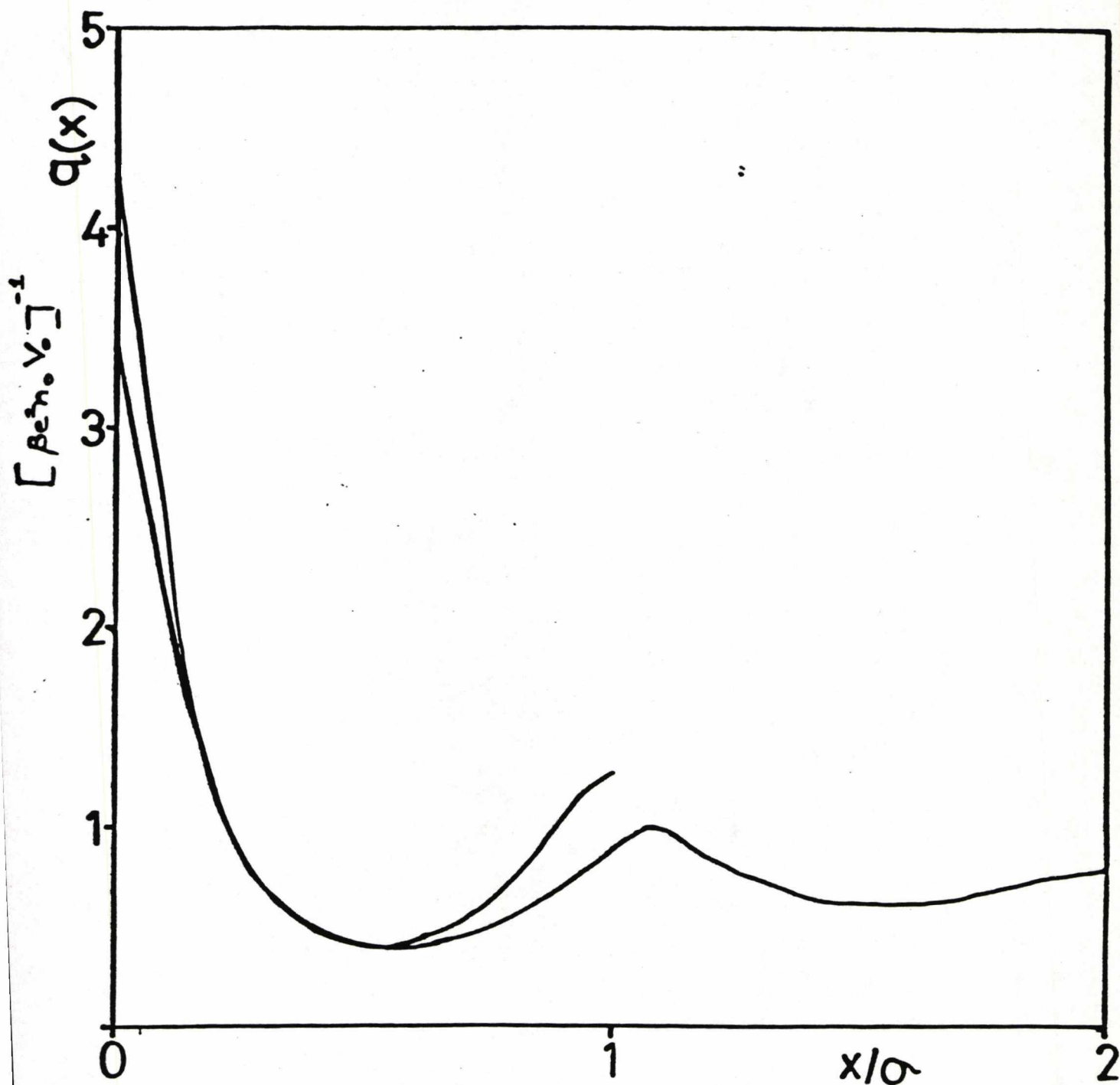
Fig 4.1: The charge profile $q(x)$ for two wall separations $2R$ and $4R$. $\epsilon_r = 78$, $\kappa R = 0.1$ and the concentration of ions is $0.0051M$. The density of the solvent is $\rho\sigma^3 = 0.6$
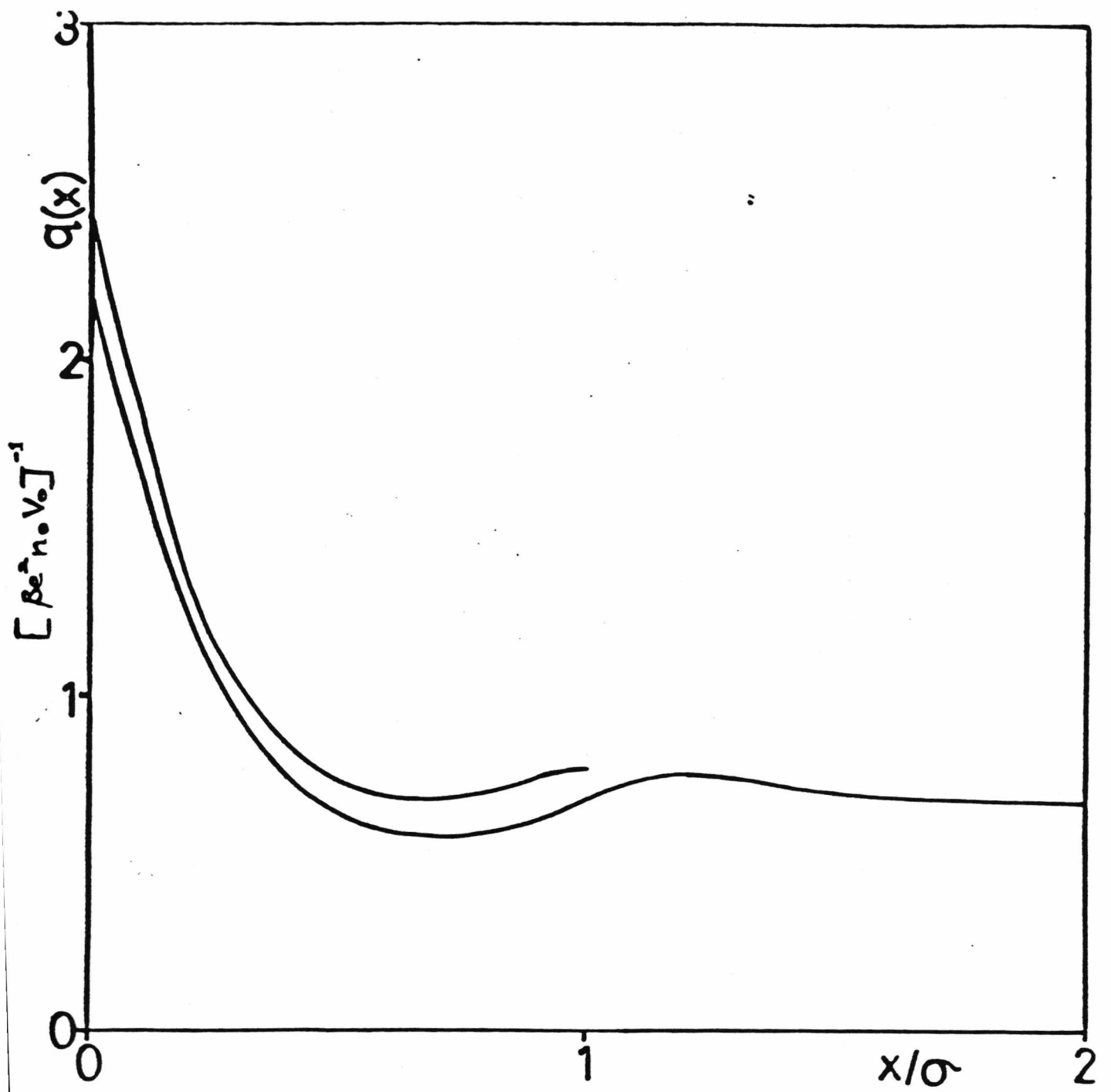
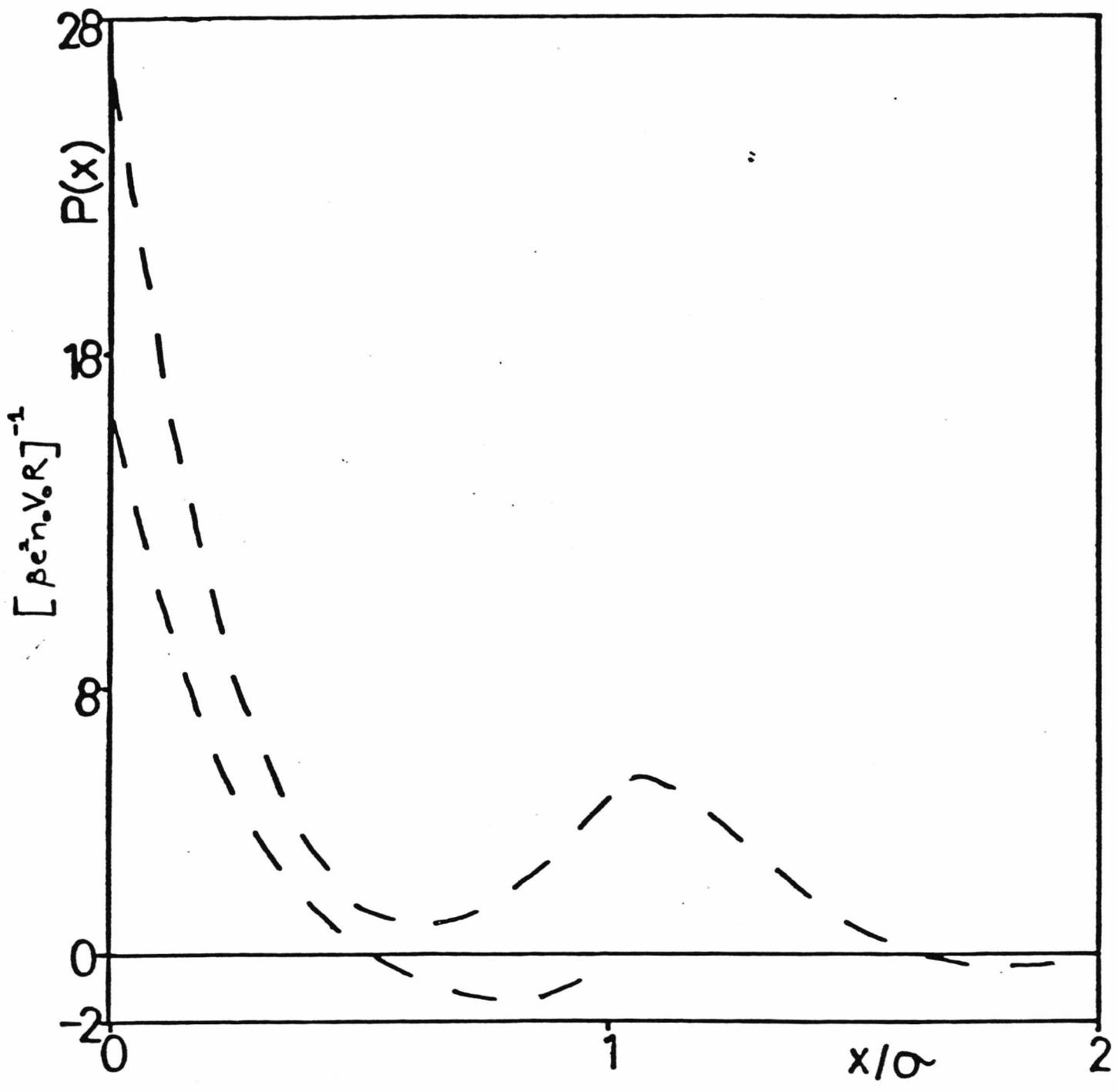Fig 4.2: As for Fig 4.1, but with $\rho\sigma^3 = 0.4$

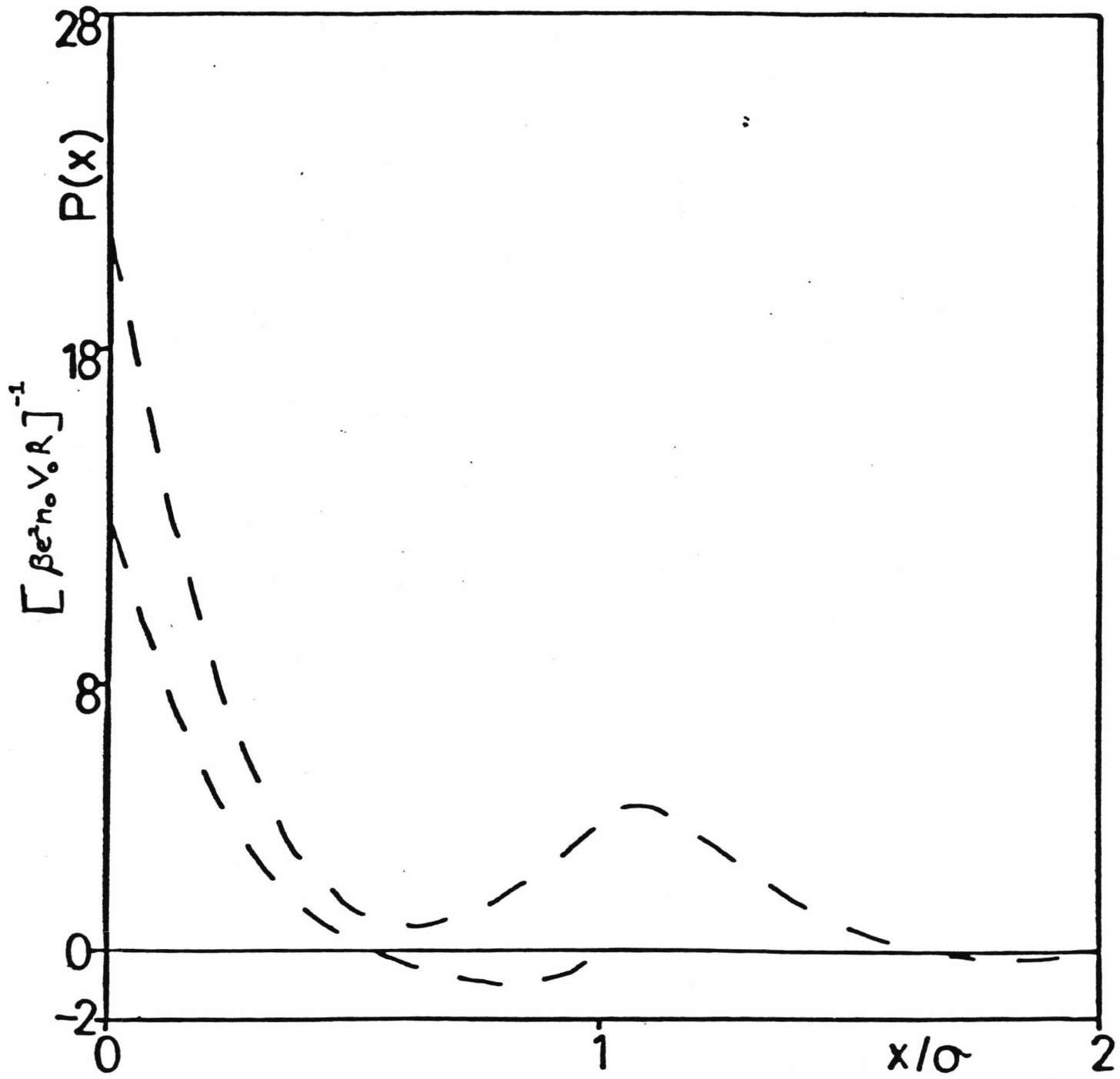Fig 4.3: The polarisation profile $P(x)$. All else as for Fig 4.1

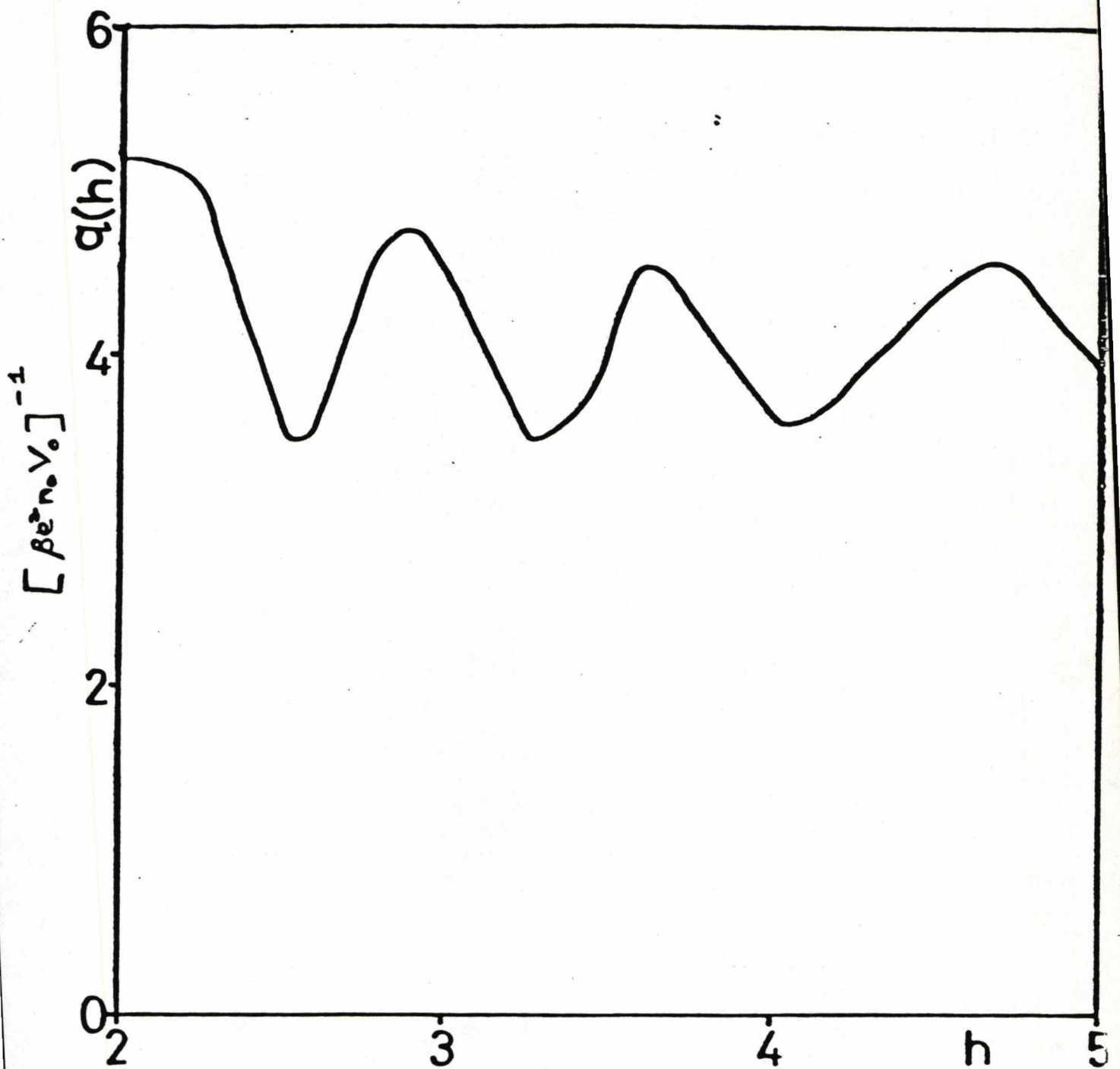Fig 4.4: As for Fig 4.3, but $\rho\sigma^3 = 0.4$

Fig 4.5: The value of the charge density at the wall $q(h)$, as a function of separation. All else as for Fig 4.1
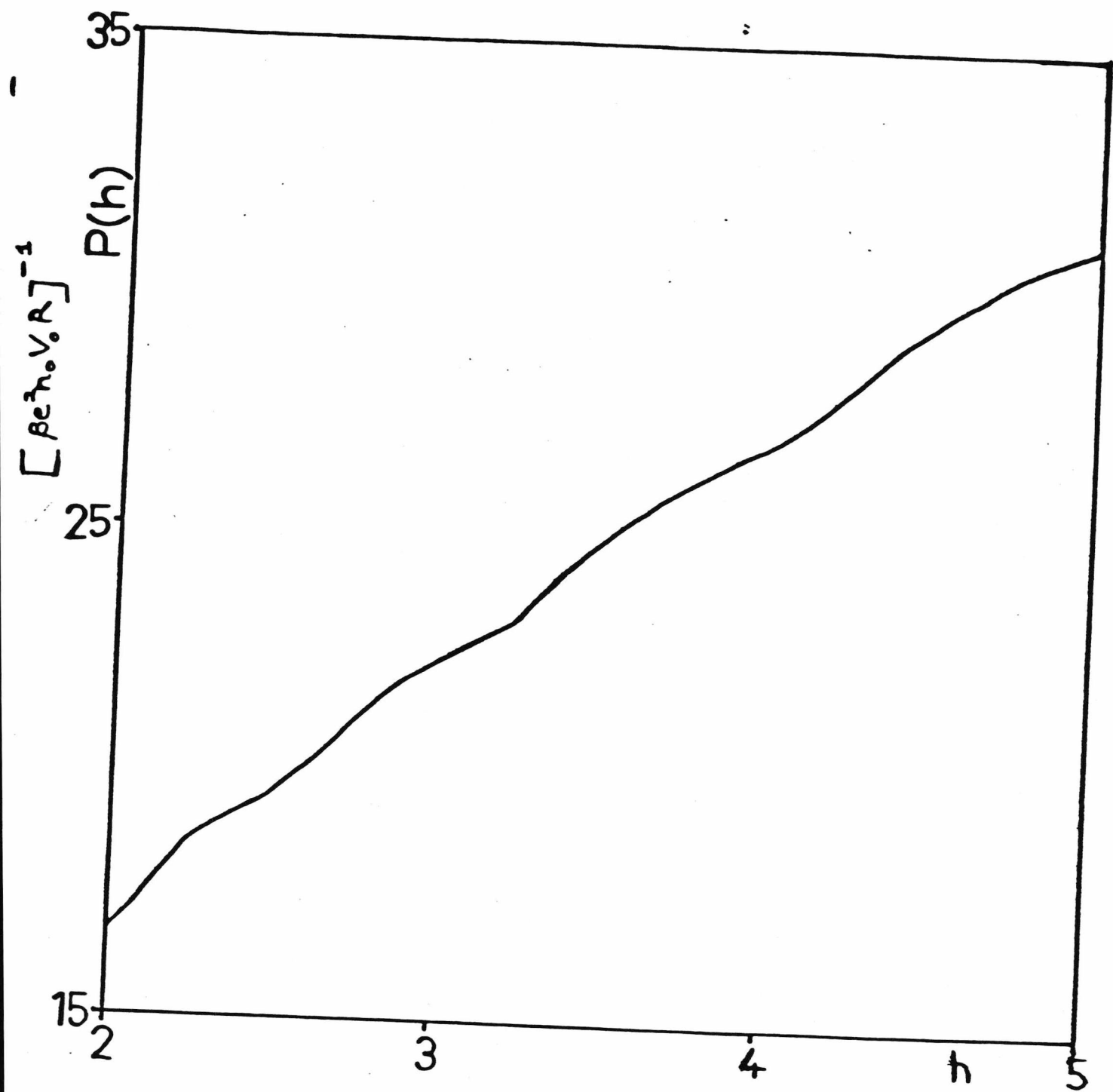
Fig 4.6: The wall polarisation density $P(h)$ versus separation. All else as for Fig 4.1

5. A GENERAL DENSITY FUNCTIONAL FOR FLUIDS

5.1. Introduction

In the previous two chapters, density functionals were used in which the interaction of the fluid with itself was represented by a term which was no greater than quadratic in the density. A generalised density-functional is introduced in this chapter, based upon a functional version of a Taylor expansion. Terms which are cubic, quartic, *etc.* are included, and these represent three-body, four-body, and higher order interactions in the liquid. It is expected that these would only be significant in very dense liquids.

This generalised functional is used to represent the free energy of a neutral hard sphere fluid confined between two planar walls. When the walls do not interact with the fluid (other than excluding the fluid from the region occupied by them), the pressure is found to be directly proportional to the value of the density at the wall. It can also be related to the inhomogeneous direct correlation function, a well-known result but derived in a new manner. It can thus be easily shown that the functional equivalent to the HNC approximation used in the last chapter will yield the wrong density at the wall.

A truncated version of the general functional is proposed which is cubic in the density. There are thus two free parameters in the functional. These are chosen so as to fulfill a constraint involving the direct correlation function, and to satisfy the density required at the wall calculated by using the Carnahan-Starling equation of state for hard spheres. In spite of the constraints, one is free to choose one of a large number of forms for the three-body interaction, and various physical choices were made.

The functional was minimised in the same way as before, and the equilibrium density profile for the fluid obtained. It was found to be in excellent agreement with

Monte Carlo simulations, even well away from the wall and at very high fluid densities. Furthermore, the solution was not very sensitive to the form of the three-body interaction.

Finally, the functional is used for a fluid with long-range Lennard-Jones interactions with hard sphere cores, and liquid-vapour coexistence is observed.

5.2. Pressure and the density functional

One can, in general, represent a function of some variable by an infinite power series in the variable. Similarly, one can represent a functional of a function by an infinite series of terms involving ever-increasing "powers" of the function. The coefficients in the first case now become functions (see Appendix A).

Thus consider a fluid of spherically symmetric particles whose free energy, $\Omega[\rho]$, is represented in this fashion, with $\rho(r)$, the particle density being the independent function. Then

$$\beta\Omega[\rho]=\int dr_1\rho(r_1)\left\{\ln[\rho(r_1)\frac{1}{\rho_1}-1\right\}+\beta\int dr_1 v(r_1)\rho(r_1)$$
$$-\sum_{n=2}^{\infty}\int dr_1\cdots dr_n K_n(r_1,\cdots,r_n)\rho(r_1)\cdots\rho(r_n) \tag{5.1}$$

where ρ_1 is related to the chemical potential μ by

$$\beta\mu=\ln\rho_1 \quad , \quad \beta=(k_B T)^{-1} \tag{5.2}$$

and $v(r)$ is an external potential. The first term on the righthand side in eqn (5.1) is the entropy of the fluid and exists for a fluid of non-interacting particles. The last term arises from the interactions of the molecules. Insofar as this describes the behaviour of a system of identical particles interacting solely through pairwise additive potentials, certain inferences can be made about the form of $K_n(r_1,\cdots,r_n)$, as it is the only term representing these interactions. Firstly, if one interchanges the positions of two or more particles, the free energy is unchanged, as they are identical. Therefore $K_n(r_1,\cdots,r_n)$ is symmetric in its arguments. Secondly, if two particles are moved in

a manner such that their separation remains unchanged, the contribution of this pair of particles to the free energy also remains unchanged. So $K_n(r_1, \cdots, r_n)$ may be expressed in terms of the differences of the co-ordinates. Note further that only $n-1$ of these differences are independent. This will be of importance later.

Now the direct correlation function, the second functional derivative of the free energy with respect to the density, is given by

$$c(r_1, r_2, \rho) = -\frac{\beta \delta^2 \Omega}{\delta \rho(r_1) \delta \rho(r_2)} + \frac{\delta(r_1 - r_2)}{\rho(r_1)}$$

$$= \sum_{n=2}^{\infty} n(n-1) \int dr_3 dr_n K(r_1, r_2, \cdots, r_n) \rho(r_3) \cdots \rho(r_n) \qquad (5.3)$$

The term in the sum with $n=2$ involves no integration and is simply $2K(r_1, r_2)$. The density dependence of the direct correlation function is now evident. One can easily see that the functions $K_n(r_1, \cdots, r_n)$ are the n-body direct correlation functions in the limit of infinite dilution, and are therefore independent of the density (just as the coefficients are independent of the variable in an ordinary power series). This, too, will be useful later.

Let us now specialise to a liquid confined between identical planar hard walls located at $x = \pm h/2$. The density will then be a function of the co-ordinate x only. We assume the external potential arises solely from the effect of the walls on the fluid. Then

$$v(r_1) = u(x_1 + h/2) + u(h/2 - x_1) \qquad (5.4)$$

where $u(x)$ is the potential at distance x from one wall.

As the system is of infinite extent, the free energy is likewise infinite. However, the free energy per unit area, a more useful quantity in this instance, is not. This can be written as

$$\beta \Omega_A[\rho] = \int_{-h/2}^{h/2} d1 \rho(1) \left[\ln\left(\frac{\rho(1)}{\rho_1}\right) - 1 \right]$$

$$+\beta \int_{-h/2}^{h/2} d1[u(x1+h/2)+u(h/2-x1)]\rho(1)$$

$$-\sum_{n=2}^{\infty} \int_{-h/2}^{h/2} d1 \cdots dnk_n(1,2,\cdots,n)\rho(1)\cdots\rho(n); \tag{5.5}$$

where the notation has been simplified so that

$$\rho(i)\equiv\rho(x_i) \ , \quad \int di \equiv \int dx_i \tag{5.6}$$

$$k_n(1,2\cdots,n)\equiv k_n(x_1,x_2,\cdots x_n)=\int dy_2 dz_2 \cdots dy_n dz_n K(\mathbf{r}_1,\mathbf{r}_2,\cdots,\mathbf{r}_n) \tag{5.7}$$

Note that for purely mathematical reasons the functions k_n are also symmetric in their arguments and depend only on the co-ordinate differences.

Following the procedure of previous chapters, the free energy is functionally differentiated and set to zero. Thus

$$\ln\left(\frac{\rho(1)}{\rho_1}\right)=-\beta[u(x_1+h/2)+u(h/2-x_1)]$$

$$+\sum_{n=2}^{\infty}n\int_{-h/2}^{h/2} d2 \cdots dnk_n(1,2,\cdots,n)\rho(2)\cdots\rho(n), \tag{5.8}$$

where the symmetry of k_n has been used to simplify the last term. The solution of this equation provides us with the equilibrium density profile.

Now for realistic wall-fluid potentials, $u(x)$ tends to zero for large x. Therefore the fluid at large distances from the walls is, in effect, in the bulk. So as $h\to\infty$, $\rho_1\to\rho_0$ almost everywhere, and as the deviations from the bulk near the wall continue to decrease in importance as the walls separate, one may write the exact equation

$$\ln\left(\frac{\rho_0}{\rho_1}\right)=\sum_{n=2}^{\infty}\int_{-\infty}^{\infty} d2 \cdots dnk_n(1,2,\cdots,n) \tag{5.9}$$

This equation relates the equilibrium density of the fluid to ρ_1 and thereby to the chemical potential μ.

A useful feature of this formalism is that one can obtain the presure directly from the free energy. It is not hard to see that

$$\beta P = -\frac{\beta \partial \Omega_A}{\partial h} \qquad (5.10)$$

Applying this equation to the form given by Eqn (5.5) and using Eqn (5.8) to eliminate various terms gives

$$\beta P = \frac{1}{2}[\rho(h/2) + \rho(-h/2)]$$
$$-\frac{\beta}{2}\int_{-h/2}^{h/2}\frac{\partial}{\partial x_1}[u(x_1 + h/2) - u(h/2 - x_1)]\rho(1) \qquad (5.11)$$

The derivatives of ρ with respect to h can be ignored because Ω is minimised w.r.t ρ. This is the well-known exact result . As the walls are identical, it is obvious, by symmetry, that the density at the two walls is the same. Equation (5.11) therefore simplifies to

$$\beta P = \rho_W - \beta\int_{-h/2}^{h/2} d1\frac{\partial}{\partial x_1}u(x_1 + h/2)\rho(1) \qquad (5.12)$$

where

$$\rho_W = \rho(-h/2) = \rho(h/2) \qquad (5.13)$$

is the density at a wall when the separation is h. This equation is further simplified when there is no wall-fluid interaction, i.e. $u(x)$ is zero.

$$\beta P = \rho_W \qquad (5.14)$$

The walls are then said to be hard walls.

Now by using a similar method to calculate the pressure for a bulk fluid (i.e. infinite wall separation), one can derive another formula for the pressure, this time in terms of the direct correlation function. This is important as it imposes a condition on the direct correlation function (assuming the pressure in the bulk fluid is known). If one can satisfy this condition by a suitable choice of direct correlation function, one guarantees the right value of the density at the wall in the limit of infinite wall separation. This alternative formula will now be derived below. One begins by making the following substitution in Eqn (5.5)

$$y_i = \frac{x_i}{h} \qquad (5.15)$$

which therefore becomes

$$\beta\Omega_A[\rho] = h\int_{-\frac{1}{2}}^{\frac{1}{2}} dy_1 \left[\ln\left(\frac{\rho(y_1 h)}{\rho_1}\right) - 1\right]$$

$$-\sum_{n=2}^{\infty} h^n \int_{-\frac{1}{2}}^{\frac{1}{2}} dy_1 \cdots dy_n k_n(hy_1, \cdots, hy_n)\rho(y_1 h)\cdots\rho(y_n h) \qquad (5.16)$$

Following the same procedure as before, to show that nothing intrinsically different is occuring, one differentiates with respect to h. As before, one can ignore the derivatives of ρ with w.r.t h, for the same reasons. So

$$\beta P = -\int_{-\frac{1}{2}}^{\frac{1}{2}} dy_1 \rho(y_1 h)\left[\ln\left(\frac{\rho(y_1 h)}{\rho_1}\right) - 1\right]$$

$$+\sum_{n=2}^{\infty} n h^{n-1} \int_{-\frac{1}{2}}^{\frac{1}{2}} dy_1 \cdots dy_n k_n(hy_1, \cdots, hy_n)\rho(y_1 h)\cdots\rho(y_n h)$$

$$+\sum_{n=2}^{\infty} n h^n \int_{-\frac{1}{2}}^{\frac{1}{2}} dy_1 \cdots dy_n \frac{y_1}{h}\frac{\partial}{\partial h} k_n(hy_1, \cdots, hy_n)\rho(hy_1)\cdots\rho(hy_n) \qquad (5.17)$$

Using Eqn (5.8) to eliminate some terms, and changing the variables back to x_i gives

$$\beta P = \frac{1}{h}\int_{-h/2}^{h/2} d1\rho(1)$$

$$+\frac{1}{h}\sum_{n=2}^{\infty} n \int_{-h/2}^{h/2} dx_1 \cdots dx_n x_1\frac{\partial}{\partial x_1} k_n(1, \cdots, n)\rho(1)\cdots\rho(n) \qquad (5.18)$$

Now we are concerned with the pressure for a fluid in the bulk. This is the limit of infinite wall separation ($h\to\infty$, and so the density tends to the bulk density ρ_0 almost everywhere. As before, the deviations near the wall become unimportant. From Eqn (5.18) it may appear that in this limit both terms on the righthand side will disappear, but this is not the case.

In both terms there exists an integral of order h, and this is therefore sufficient to make both terms non-zero. This is most easily seen in the first term, where $\rho(1)$

becomes a constant, and the size of the integral then depends purely on the limits. Now the second term involves integrations over n positions. The function k_n, however, depends only on the difference of these positions, and furthermore tends to zero if any of these differences tends to infinity. There are only $n-1$ of these. So after $n-1$ integrations the integrand is of order ρ_0^n and independent of position. Thus the final integration provides the factor of order h required. This is best shown rigourously. Hence consider the term

$$I_n = n \int_{-h/2}^{h/2} dx_1 \cdots dx_n x_1 \frac{\partial}{\partial x_1} k_n(1, \cdots, n) \rho(1) \cdots \rho(n)$$

$$= \int_{-h/2}^{h/2} dx_1 \cdots dx_n \sum_{i=1}^{n} x_i \frac{\partial}{\partial dx_i} k_n(1, \cdots, n) \rho(1) \cdots \rho(n) \tag{5.19}$$

Since k_n is a symmetric function of the difference of its arguments we can write

$$k_n(x_1, \cdots, x_n) = S_n(x_2 - x_1, \cdots, x_n - x_1) \tag{5.20}$$

where S_n is a symmetric function of its arguments. Then

$$\sum_{i=1}^{n} x_i \frac{\partial}{\partial x_i} k_n(x_1, \cdots, x_n) = \left[x_1 \frac{\partial}{\partial x_1} + \sum_{i=2}^{n} x_i \frac{\partial}{\partial x_i} \right] S_n(x_2 - x_1, ..., x_n - x_1)$$

$$= \sum_{i=2}^{n} (x_i - x_1) \frac{\partial}{\partial x_i} S_n(x_2 - x_1, \cdots, x_n - x_1) \tag{5.21}$$

and

$$I_n = \int_{-h/2}^{h/2} dx_1 \int_{-h/2-x_1}^{h/2-x_1} dz_2 \cdots dz_n \sum_{i=2}^{n} z_i \frac{\partial}{\partial z_i} S_n(z_2, \cdots, z_n) \rho(x_1)$$

$$\times \rho(x_1 + z_2) \cdots \rho(x_1 + z_n) \tag{5.22}$$

after the substitution

$$z_i = x_i - x_1, \quad (i = 2, \cdots, n) \tag{5.23}$$

The function S_n is like a one-dimensional correlation function. Therefore, as mentioned above, it must vanish if any of its arguments becomes very large. So as $h \to \infty$ in Eqn (5.22), the integrals over z_i will converge, $\rho(x_i) \to \rho_0$ once again, and

$$\lim_{h \to \infty} \frac{I_n}{h} = \rho_0^n \int_{-\infty}^{\infty} dz_2 \cdots dz_n \sum_{i=2}^{n} z_i \frac{\partial}{\partial z_i} S_n(z_2, \cdots, z_n) \tag{5.24}$$

Substituting this result back in eqn (5.18) gives

$$\beta P = \rho_0 + \sum_n \rho_0^n (n-1) \int_{-\infty}^{\infty} dz_2 \cdots dz_n z_2 \frac{\partial}{\partial z_2} S_n(z_2, \cdots, z_n) \tag{5.25}$$

It is of interest to express this in terms of the direct correlation function. This can be done in the following way. Substituting back to the variables x_i gives

$$\beta P = \rho_0 + \int dx_2 (x_2 - x_1) \frac{\partial}{\partial x_2} \sum_n \rho_0^n (n-1) \int dx_3 \cdots dx_n$$

$$\times k_n(x_1, x_2, \cdots, x_n), \tag{5.26}$$

Now the function k_n is the integral of K_n over the transverse variables y and z. As has been mentioned, K_n is the n-particle direct correlation function in the limit of infinite dilution, and therefore independent of the bulk density ρ_0. Hence k_n is also independent of ρ_0. Thus one may write eqn (5.26) as

$$\beta P = \rho_0 + \int_0^{\rho_0} d\rho \int dx_2 (x_2 - x_1) \frac{\partial}{\partial x_2} \sum_n n(n-1) \rho^{n-1}$$

$$\times \int dx_3 \cdots dx_n k_n(x_1, \cdots, x_n) \tag{5.27}$$

Using eqn (5.3, the direct correlation function for a bulk is simply

$$c(\mathbf{r}_1, \mathbf{r}_2, \rho_0) = \sum_{n=2}^{\infty} n(n-1) \rho_0^{n-2} \int d\mathbf{r}_3 \cdots d\mathbf{r}_n K_n(\mathbf{r}_1, \mathbf{r}_2, \cdots, \mathbf{r}_n) \tag{5.28}$$

Combining eqns (5.27),(5.28) and (5.7) one obtains

$$\beta P = \rho_0 + \int_0^{\rho_0} \rho \, d\rho \int d\mathbf{r}_2 (x_2 - x_1) \frac{\partial}{\partial x_2} c(\mathbf{r}_1, \mathbf{r}_2; \rho)$$

$$= \rho_0 - \int_0^{\rho_0} \rho \, d\rho \int d\mathbf{r}_2 c(\mathbf{r}_1, \mathbf{r}_2; \rho) \tag{5.29}$$

This is the usual formula for the pressure in terms of the direct correlation function. The importance of this derivation is that it establishes that the pressure (and hence the density at the wall) depends on the direct correlation function (as determined by the

form of the functional chosen). In fact, when the potential $u(x)$ is zero (hard walls), the density at the wall may be calculated directly from the two formulas for the pressures, eqns (5.14) and (5.29), without having to solve for the density profile at all. Note, however, that the latter formula is only applicable when the functions k_n are independent of ρ_0, and the free energy has the form given in eqn (5.1).

It is now evident why the hyper-netted chain (HNC) approximation fails to give the right value of the density at the wall. Here one uses the form (5.1) for the free energy, with

$$K_2(r_1,r_2)=\frac{1}{2}c(r_1,r_2;\rho_0)$$
$$K_n(r_1,\cdots,r_n)=0 \ , \ n>2. \tag{5.30}$$

The function $K_2(r_1,r_2)$, though, is now dependent on ρ_0, and thus one may proceed no further than eqn (5.26) in the calculation of the alternative form for the pressure. Thus

$$\rho_W=\beta P=\rho_0+\frac{\rho_0^2}{2}\int dr_2(x_2-x_1)\frac{\partial}{\partial x_2}c(r_1,r_2;\rho_0) \tag{5.31}$$

This is different from eqn (5.29), which gives the correct density at the wall.

Eqn (5.26) can be obtained more straightforwardly from eqns (5.1) and (5.9). In the thermodynamic limit, the fluid becomes homogeneous. Since the system dealt with is a grand canonical ensemble, the Gibbs-Duhem relation is applicable for the free energy, whence,

$$\beta PV=-\beta\Omega[\rho_0]$$
$$=-\int dr_1\rho_0\left[\ln\left(\frac{\rho_0}{\rho_1}\right)-1\right]+\sum_{n=2}^{\infty}\rho_0^n\int dr_1\cdots dr_nK_n(r_1,\cdots,r_n)$$

As mentioned earlier, K_n depends only on $n-1$ independent variables, so one of the n integrations over space may be trivially performed with an integrand of unity, simply giving the volume of the system as a result. Dividing both sides of the equation by this volume gives

$$\beta P = -\rho_0 \left[\ln \left(\frac{\rho_0}{\rho_1} \right) - 1 \right] + \sum_{n=2}^{\infty} \rho_0^n \int dr_2 \cdots dr_n K_n (r_1, \cdots, r_n)$$

Substituting for the logarithmic term from eqn (5.9) gives the desired formula for the pressure

$$\beta P = \rho_0 - \sum_{n=2}^{\infty} \rho_0^n (n-1) \int dr_2 \cdots dr_n K_n (r_1, \cdots, r_n)$$

This is the same as eqn (5.26) after one has integrated by parts. Although the required formula can be obtained in this way, it does not illustrate as directly that the density at the wall depends on the form of the density functional, and that precisely the same steps were carried out from the same starting point to obtain it in the former method, as opposed to deriving it from a different starting point in the latter.

It can be seen now that a criterion has been developed for a successful density-functional theory. In order to be successful, a minimum requirement of the theory is to reproduce the value of the density at the wall correctly. Thus the form chosen for the functional must satisfy eqn (5.26) with P being the (known) bulk pressure.

Bearing this in mind, a generalisation of the HNC density-functional is proposed in the next section which satisfies the above condition. This should therefore describe accurately the structure of a hard-sphere fluid, for which an accurate, albeit empirical, equation of state exists, from which the value of the bulk pressure appropriate to a given bulk density can be obtained.

5.3. A Hard-Sphere Fluid near a Hard Wall

The simplest generalisation of the HNC functional one can make is to introduce a third order term into the functional. Thus it becomes

$$\beta \Omega = \int \rho(1) \left[\ln \left(\frac{\rho(1)}{\rho_1} \right) - 1 \right] dr_1 + \beta \int dr_1 v(1) \rho(1)$$

$$- \int dr_1 dr_2 K(r_1, r_2) \rho(r_1) \rho(r_2)$$

$$-\int dr_1 dr_2 dr_3 L\left(r_1,r_2,r_3\right)\rho(r_1)\rho(r_2)\rho(r_3)$$

Upon functionally differentiating with respect to the density, allowing the system to tend to its homogeneous state, and dividing by the bulk density, one obtains

$$\ln\left(\frac{\rho_0}{\rho_1}\right)=-\beta v\left(1\right)+2\rho_0\int K\left(r_1,r_2\right)dr_2$$

$$+3\rho_0{}^2\int L\left(r_1,r_2,r_3\right)dr_2 dr_3 \tag{5.32}$$

thereby relating the equilibrium density to the chemical potential, μ, via ρ_1. Differentiating the free energy twice with respect to the density once more, and using the definition of the direct correlation function, eqn (5.3), gives

$$c\left(r_1,r_2;\rho\right)=2K\left(r_1,r_2\right)+6\int dr_3 L\left(r_1,r_2,r_3\right)\rho(r_3) \tag{5.33}$$

which reduces in the bulk to

$$c\left(r_1,r_2;\rho_0\right)=2K\left(r_1,r_2\right)+6\rho_0\int dr_3 L\left(r_1,r_2,r_3\right) \tag{5.34}$$

Also

$$c_3(r_1,r_2,r_3)=6L\left(r_1,r_2,r_3\right)$$

and eqn (5.26) for the pressure becomes

$$\beta P=\rho_0+\int dr_2(x_2-x_1)\frac{\partial}{\partial x_2}[\rho_0{}^2 K\left(r_1,r_2\right)$$

$$+2\rho_0{}^3\int dr_2 L\left(r_1,r_2,r_3\right)] \tag{5.35}$$

One may substitute for ρ and K by ρ_0 and $c\left(r_1,r_2;\rho_0\right)$ respectively, using eqns (5.32) and (5.34). Specialising to the case of a hard-sphere fluid between hard walls means that the density profile is a function of x only. So

$$\beta\Omega_A\left[\rho\right]-\beta\Omega_A\left[\rho_0\right]=\int_{-h/2}^{h/2}\rho(1)\ln\left(\frac{\rho(1)}{\rho_0}\right)-\int\delta\rho(1)d1$$

$$-\int d1 d2 C\left(1,2,\rho_0\right)\delta\rho(1)\delta\rho(2)$$

$$-\int d1 d2 d3 l\left(1,2,3\right)\delta\rho(1)\delta\rho(2)\delta\rho(3) \tag{5.36}$$

where

$$\delta\rho(1)=\begin{cases} \rho(1)-\rho_0 & , \quad -h/2<x<h/2 \\ -\rho_0 & , \quad \left|x\right|\geq h/2 \end{cases} \qquad (5.37)$$

$$C(1,2,\rho_0)=\int c\,(\mathbf{r}_1,\mathbf{r}_2;\rho_0)dy_2dz_2 \qquad (5.38)$$

and

$$l(1,2,3)=\int dy_2dz_2dy_3dz_3L\,(\mathbf{r}_1,\mathbf{r}_2,\mathbf{r}_3) \qquad (5.39)$$

The equilibrium density profile minimises the free energy, and is therefore the solution of the equation

$$\ln\left(\frac{\rho(1)}{\rho_0}\right)=\int d2C(1,2)\delta\rho(2)+\int d2d3l(1,2,3)\delta\rho(2)\delta\rho(3) \qquad (5.40)$$

Now the original independent parameters μ,K, and L have been replaced by ρ_0,C, and P. Choosing for C the Percus-Yevick (PY) approximation for a bulk fluid of density ρ_0, and for the pressure P the value given by the Carnahan-Starling equation of state at density ρ_0, means that μ,K, and L are given in terms of ρ_0. However, as the functional is written explicitly in terms of ρ_0,C, and L, only L need be calculated. This can be done using eqn (5.26), and substituting for K in terms of C, viz.

$$\beta P =\rho_0+ \int_{-\infty}^{\infty} dx_2(x_2-x_1)\rho_0\frac{\partial}{\partial x_2}\left[\frac{\rho_0}{2}C(1,2)-\rho_0^2\int dx_3l(x_1,x_2,x_3)\right]$$

$$=\rho_0- \int_{-\infty}^{\infty} dx_2\rho_0\left[\frac{\rho_0}{2}C(1,2)-\rho_0^2\int dx_3l(x_1,x_2,x_3)\right] \qquad (5.41)$$

Taking $c\,(\mathbf{r}_1,\mathbf{r}_2)$ equal to the PY approximation for the direct correlation function of the bulk fluid and putting l equal to zero in (5.40) yields the non-linear theory discussed by Grimson and Rickayzen [17].

Now the function $L\,(\mathbf{r}_1,\mathbf{r}_2,\mathbf{r}_3)$ must be chosen to satisfy eqn (5.41). Since this concerns the integral of the function over its two independent arguments, there is a wide latitude of choice in choosing the form of L. From the form of eqn (5.36) one would expect it to be equal to the three-particle direct correlation function of the

homogeneous fluid at density ρ_0, but this is unknown. Now it is well-known that as the arguments of an n-body direct correlation function increase, the n-body direct correlation function tends to the corresponding n-body interaction potential. For the case of simple neutral hard spheres, there are no three- or higher-body forces which might be attributed to polarisability of charge distribution on the model particles. Thus L must vanish in the in the limit of large particle separations. Similarly, one expects three-body correlations to be most important when the particles are in close proximity. A simple choice for L which has these properties is

$$L(r_1,r_2,r3)=A\,\theta(\sigma-\left|r_1-r_2\right|)\theta(\sigma-\left|r_2-r_3\right|)\theta(\sigma-\left|r_3-r_1\right|) \tag{5.42}$$

where $\theta(x)$ is the Heaviside step function,

$$\theta(x)={0 \atop 1} \quad ; \quad {x<0 \atop x>0}$$

A is a constant chosen to satisfy eqn (5.41) and σ is the diameter of a hard sphere 'molecule'.

In fact, in the one-dimensional problem only the function $l(x_1,x_2,x_3)$ occurs and it seems reasonable to approximate this directly. To see how critical the form of $l(x_1,x_2,x_3)$ was to the results, three approximations were used, two of which have two of the properties of the function obtained from eqn (5.42); they both vanish when the separation of any pair of co-ordinates exceeds σ and they are both continuous at $\left|x_i-x_j\right|=\sigma$. All of them can be written in the form

$$l(x_1,x_2,x_3)=Bf(x_1-x_2)f(x_2-x_3)f(x_3-x_1) \tag{5.43}$$

where the functions $f(x)$ are chosen to be, in case I,

$$f(x)=\left(1-\frac{\left|x\right|}{\sigma}\right)\theta(\sigma-\left|x\right|) \tag{5.44}$$

in case II,

$$f(x)=\left(1-\frac{x^2}{\sigma^2}\right)\theta(\sigma-\left|x\right|) \tag{5.45}$$

and, in case III, simply

$$f(x) = \theta(\sigma - |x|) \tag{5.46}$$

B is therefore determined by eqn (5.41), for each case, and is given in terms of ρ_0. The functional is furthermore independent of the wall-fluid potential. As already mentioned the PY approximation for $c(r_1, r_2; \rho_0)$, the bulk direct correlation function, has been used, and the Carnahan-Starling formula,

$$\frac{\beta P}{\rho_0} = \frac{1 + \eta + \eta^2 - \eta^3}{(1-\eta)^3} \qquad \eta = \frac{1}{6} \pi \rho_0 \sigma^3 \tag{5.47}$$

for the pressure.

The theory was applied to a hard-sphere fluid confined between two hard walls separated by 8 molecular diameters, as computer simulation results are available for this system, and direct comparison is therefore possible. The constant B was kept fixed, independent of h, as this is required in the derivation of eqn (5.41). Equation (5.40) was solved numerically by computer with methods described elsewhere (see Chapter 3, for example). The resulting density profiles are believed to differ from the exact solution by less than 0.5%.

The results of the calculations are displayed in Figs. 5.1-5.13 where the density profile is displayed for various values of the reduced equilibrium density $\rho_0 \sigma^3$, the one dimensionless parameter in the problem. Figs. 5.1-5.3 show the profile for $\rho_0 \sigma^3 = 0.57$, $h = 8\sigma$, obtained variously using the PY approximation (or linear theory of Grimson and Rickayzen), the HNC approximation (or non-linear theory of Grimson and Rickayzen), and the three approximations of this theory. It is evident that the PY and HNC approximations do not give the right value of the density at the wall, as has been demonstrated earlier. Since B has been chosen to give the bulk pressure, it naturally gives the right value of the density at the wall as the separation tends to infinity. It was found that in all three cases the density at the wall at 8σ differed by no more than 0.5% from the density at the wall at infinite separation. So the density

profile is similar to that found near a single wall (the limit of infinite wall separation). Considering that the only constraint on the form of L is that it is chosen to give the right value of the wall density, the fit to the simulation results of Snook and Henderson [25] is extremely good. Although not very apparent at this density, there exists a cusp in the profile for case III. This is a well-known feature of profiles obtained by using a discontinuous direct correlation function, as was the case here. At this low density, all three approximations give similar results, all of which are superior to those obtained from the PY and HNC approximations.

Figures 5.4 and 5.5 show similar results for the next density at which Snook and Henderson performed their simulation, namely $\rho\sigma^3 = .755$. The increased density emphasises the inaccuracy of the PY and HNC approximations, and the cusp in III is now more evident. It can be seen that the first approximation, however, still gives very good results.

The trend continues as the bulk density is increased, and this is displayed in Figs 5.6-5.10. Here the reduced bulk density $\rho\sigma^3$ is 0.81. The same features as before are now exaggerated even more. Note that the results of cases I and II are not very different, indicating that the form of $l(1,2,3)$ is not too important, providing that the constraints imposed upon it are fulfilled. However, case II does fit the peak, located at about a molecular diameter from the wall, slightly better, but the improvement is not significant.

In Fig 5.10, the HNC and PY approximations, along with the best approximation of this theory, case II, are plotted out to a distance of 4 molecular diameters from the wall. Not surprisingly, beyond about 2 molecular diameters, the results are not very different; in fact, the perturbations from the equilibrium density there are not very great, (of the order of a few per cent), and the spatial oscillations of the three approximations occur virtually in phase. Each peak is located at about an integral number of molecular diameters from the wall, the usual result.

Finally, the results for the (somewhat unrealistic) reduced liquid density of 0.91 are shown in Figs 5.11-5.13. Here the cusp in case III is very prominent, and the HNC value of the density at the wall differs from the correct value by a factor of about 2. Yet the failure of the PY approximation is more complete, as it results in negative densities at various distances from the wall, a feature shared by the generalised mean spherical approximation (GMSA) [26]. Once again, case II gives slightly better results than case I.

The constant B was found to be negative. In the nature of the mean spherical approximation, one can identify the 3-body direct correlation function as the algebraic opposite of an effective three-body potential. This makes the three-body potential a positive quantity, and therefore repulsive. This serves to reduce particle correlations, as witnessed by the lower heights of the peaks in cases I and II compared with the peaks due to the HNC approximation.

It is a measure of the amount by which the the wall pressure given by the HNC approximation differs from the bulk pressure. The dimensionless constant $B\sigma^4$ depends strongly on the density and in case I it varies from -58.5 to -184.6 while in case II it varies from -27.4 to -86.4 as $\rho_0\sigma^3$ varies from 0.57 to 0.91.

5.4. Attractive forces, and the wetting of a Hard Wall by Vapour

This formalism may now be applied to a mixture containing attractive long-range forces. Henderson [27] and others [28] have shown that for a functional to represent the behaviour of a either a liquid or a vapour in the bulk, depending on the conditions, the functional must be at least cubic in the density. Presumably this applies to inhomogeneous fluids too, and as the functional used in this chapter is indeed cubic in the density, it was considered interesting to find out if the same functional could produce liquid or vapour behaviour, or even liquid-vapour coexistence, depending on the conditions.

A Lennard-Jones-type potential of the form

$$V(r)=-\epsilon \qquad\qquad r<2^{1/6}\sigma$$

$$=4\epsilon\left[\left(\frac{\sigma}{r}\right)^{12}-\left(\frac{\sigma}{r}\right)^{6}\right] \quad r>2^{1/6}\sigma \qquad\qquad (5.48)$$

was chosen for the long-range attractive forces. A hard sphere core potential was maintained.

The direct correlation function of the fluid was calculated using the random phase approximation (RPA). So

$$c(r)=c_{HS}(r)-\beta V(r) \qquad\qquad (5.49)$$

This choice of approximation scheme was useful in that the correction to the free energy of the system is simply the addition of an extra term, *viz.*

$$\beta\Omega[\rho]=\beta\Omega_{HS}[\rho]+\frac{\beta}{2}\int\rho(r)V(r-r')\rho(r')drdr' \qquad\qquad (5.50)$$

This equation is easily minimised to give

$$\beta\frac{\delta\Omega_{HS}[\rho]}{\delta\rho(r)}+\beta\int\rho(r')V(r-r')dr'=0 \qquad\qquad (5.51)$$

This equation was solved in the same manner as before.

Now for a homogeneous fluid, the pressure is given by

$$P=P_{HS}+\frac{\rho_0^2}{2}\int V(r)dr \qquad\qquad (5.52)$$

At the critical point,

$$\frac{\partial P}{\partial\rho_0}=0$$

and

$$\frac{\partial^2 P}{\partial\rho_0^2}=0 \qquad\qquad (5.53)$$

So from eqns (5.53) and using the Carnahan-Starling formula for the pressure due to the hard spheres, one arrives at the following values for the critical temperature, T_c,

and the critical packing fraction, η_c

$$\frac{\epsilon}{kT_c}=.963 \quad , \quad \eta_c=.129 \tag{5.54}$$

The value of the reduced temperature was therefore chosen as

$$T^* =\frac{kT}{\epsilon}=.82 \tag{5.54}$$

At this temperature, the density of coexisting liquid was in the region of $\rho_0\sigma^3=.76$, and the corresponding density of coexisting vapour was found to be about $\rho_0\sigma^3=.019$.

The results for different bulk densities are shown in Fig 5.14. As can be seen, as the density approaches that of coexistence, the value of the density at the wall decreases dramatically. It tends to the density of the vapour. Thus one can see that a thin layer of vapour is built up at the wall.
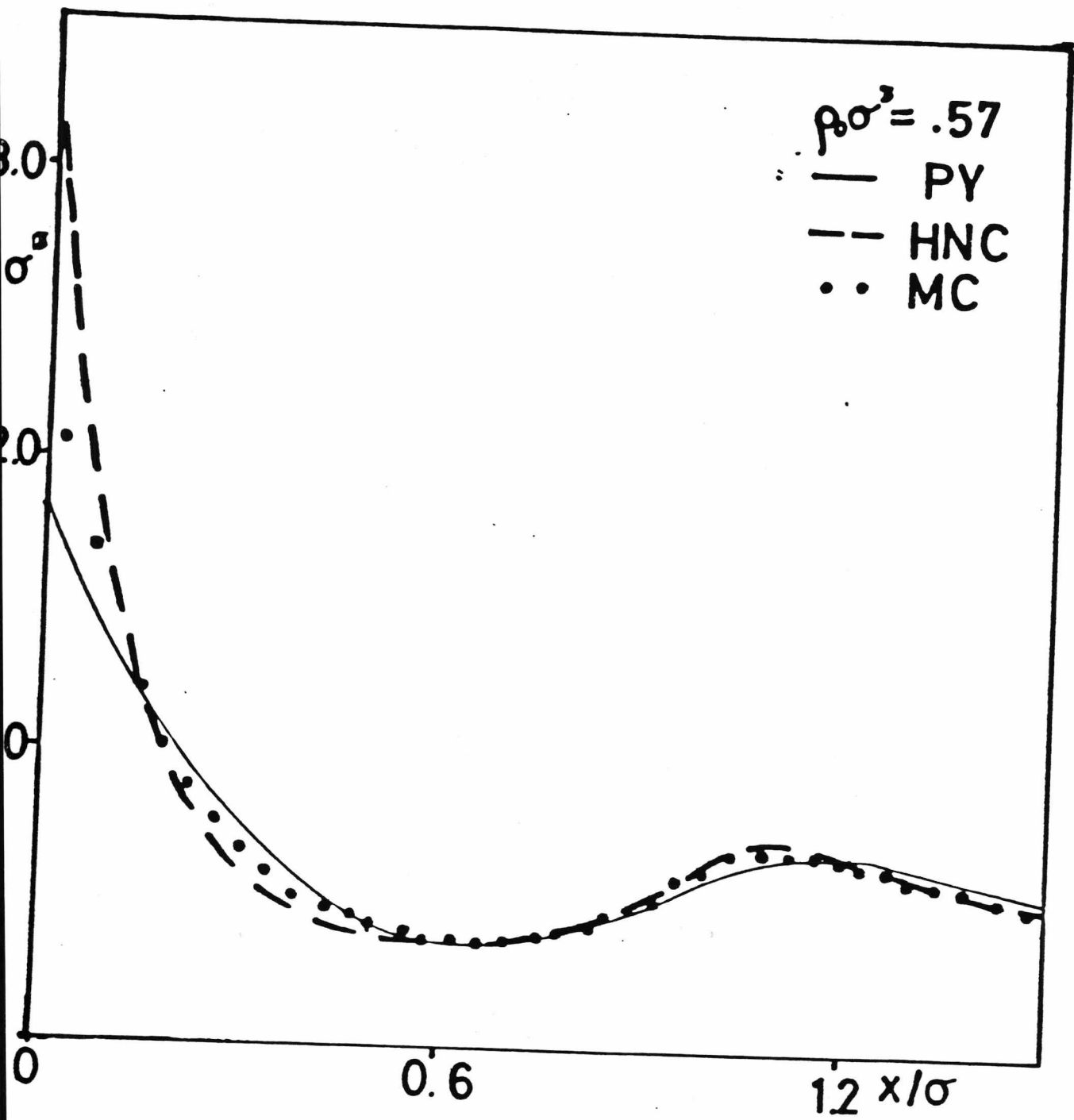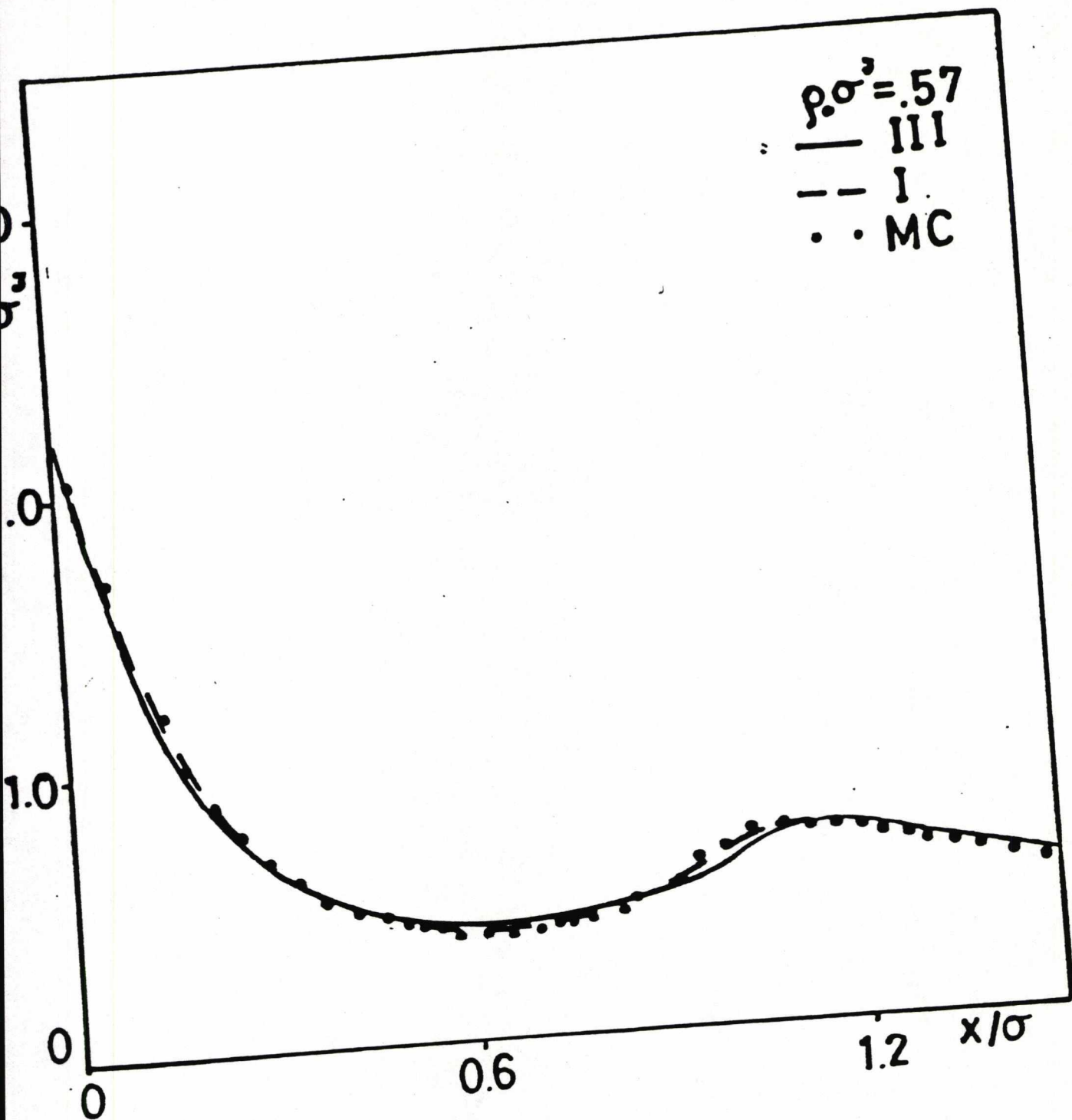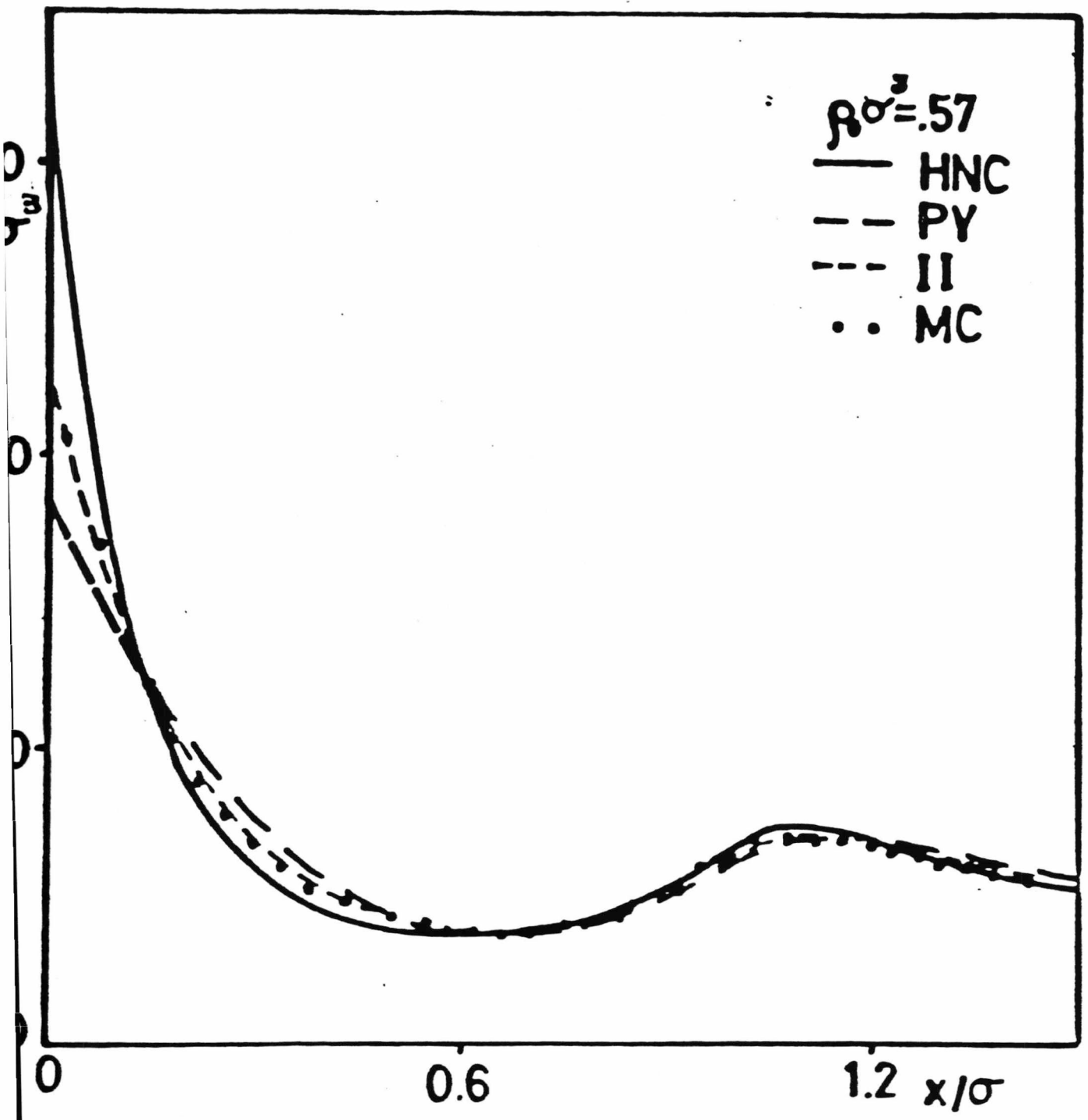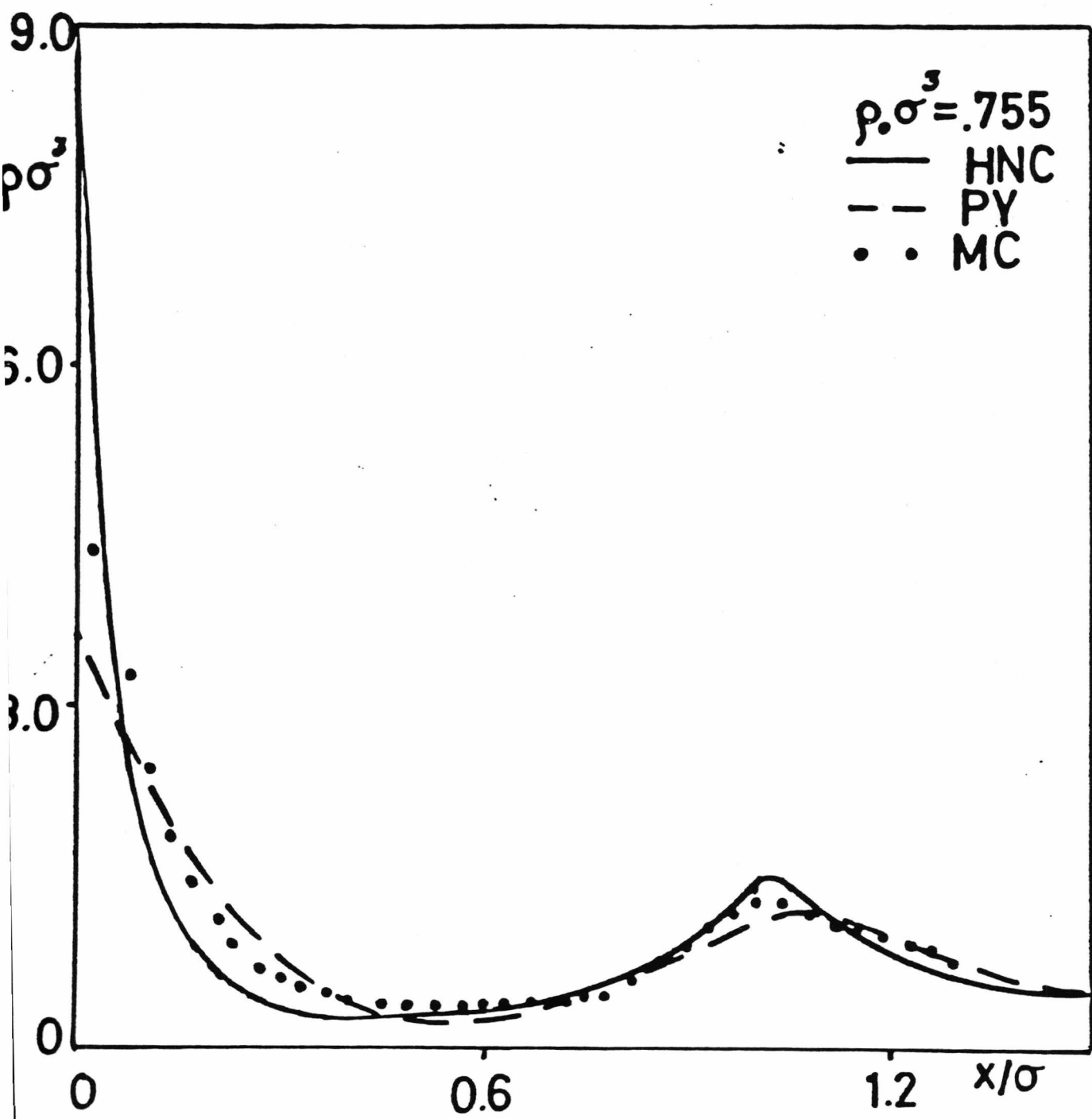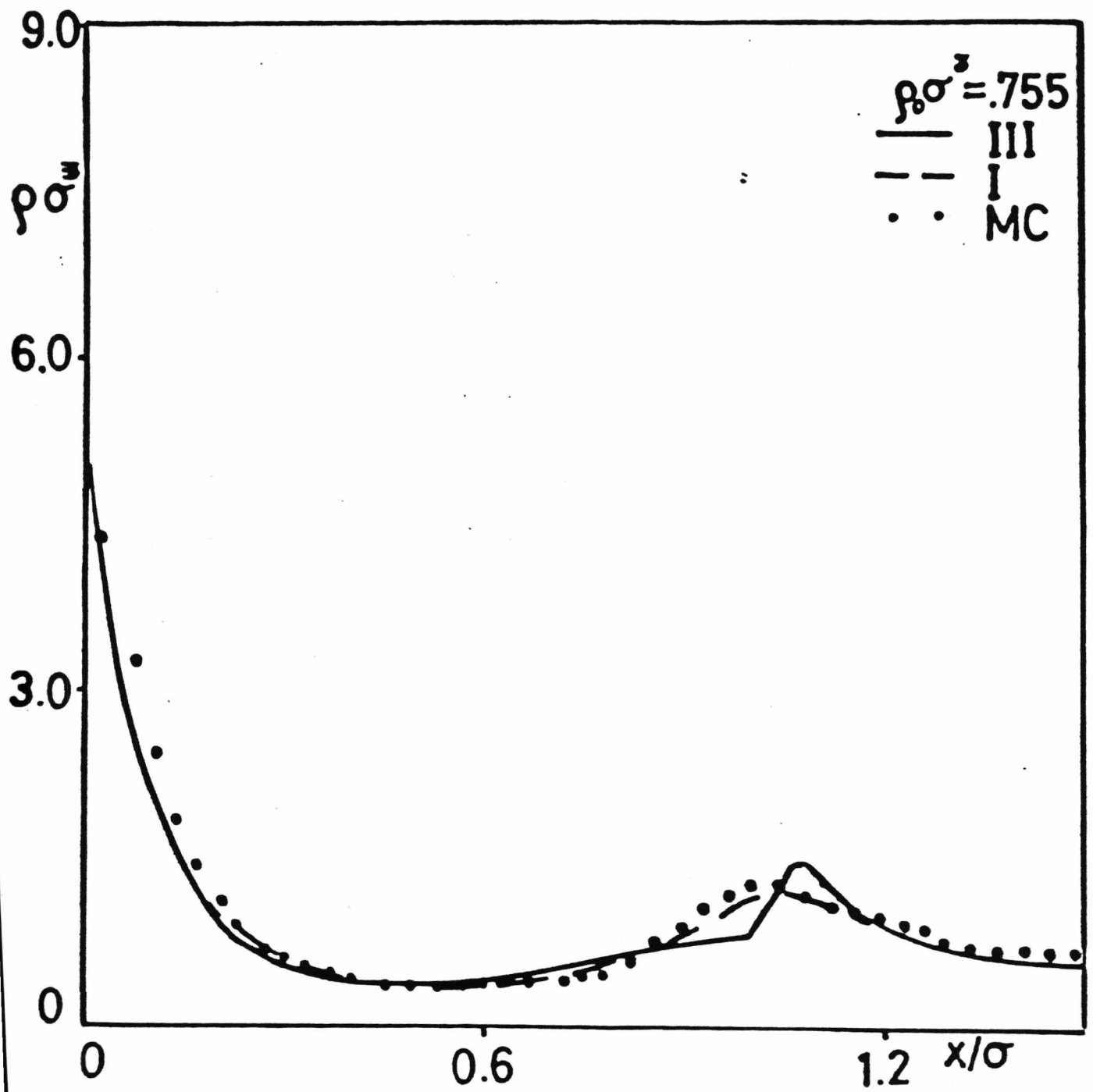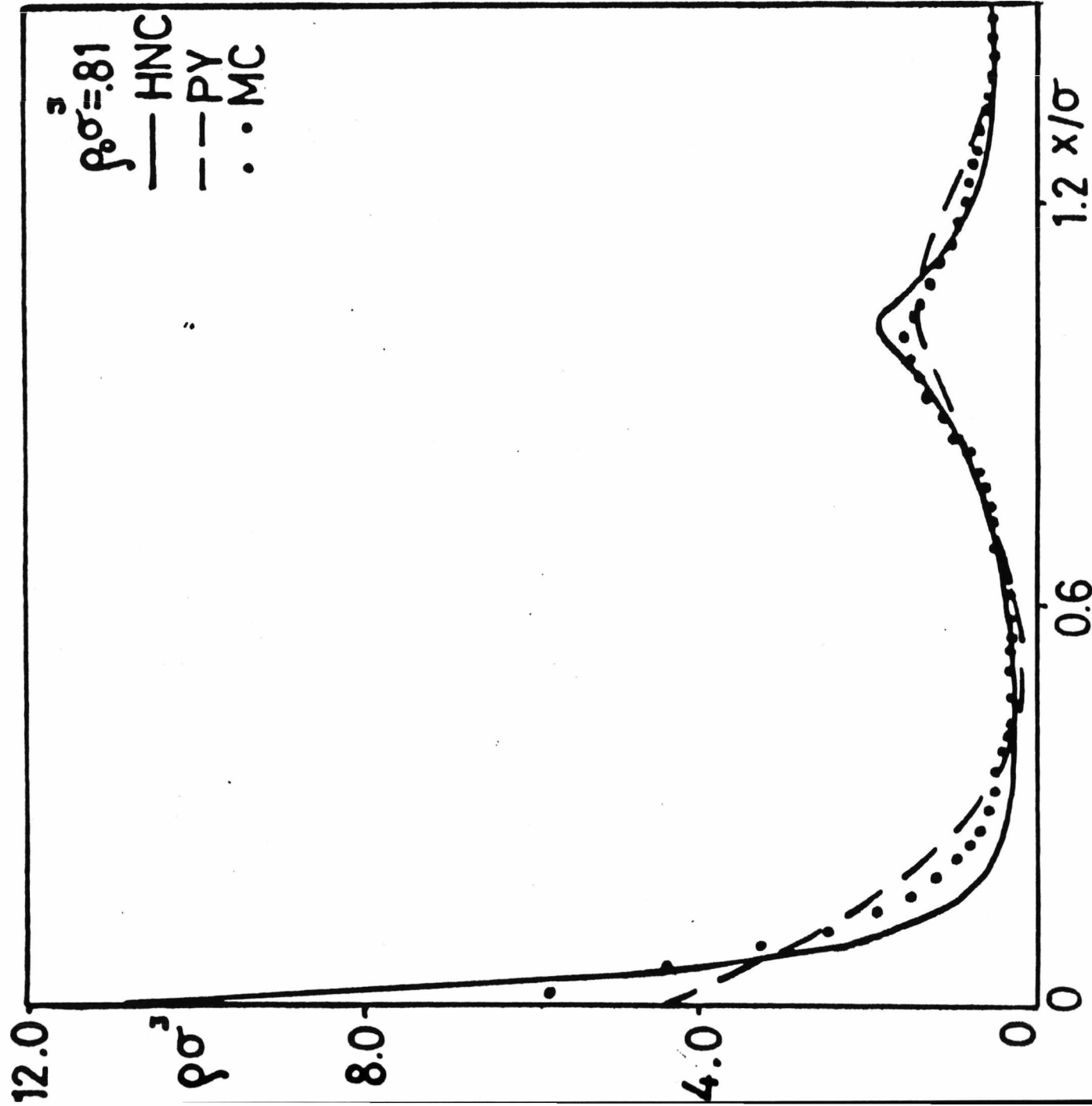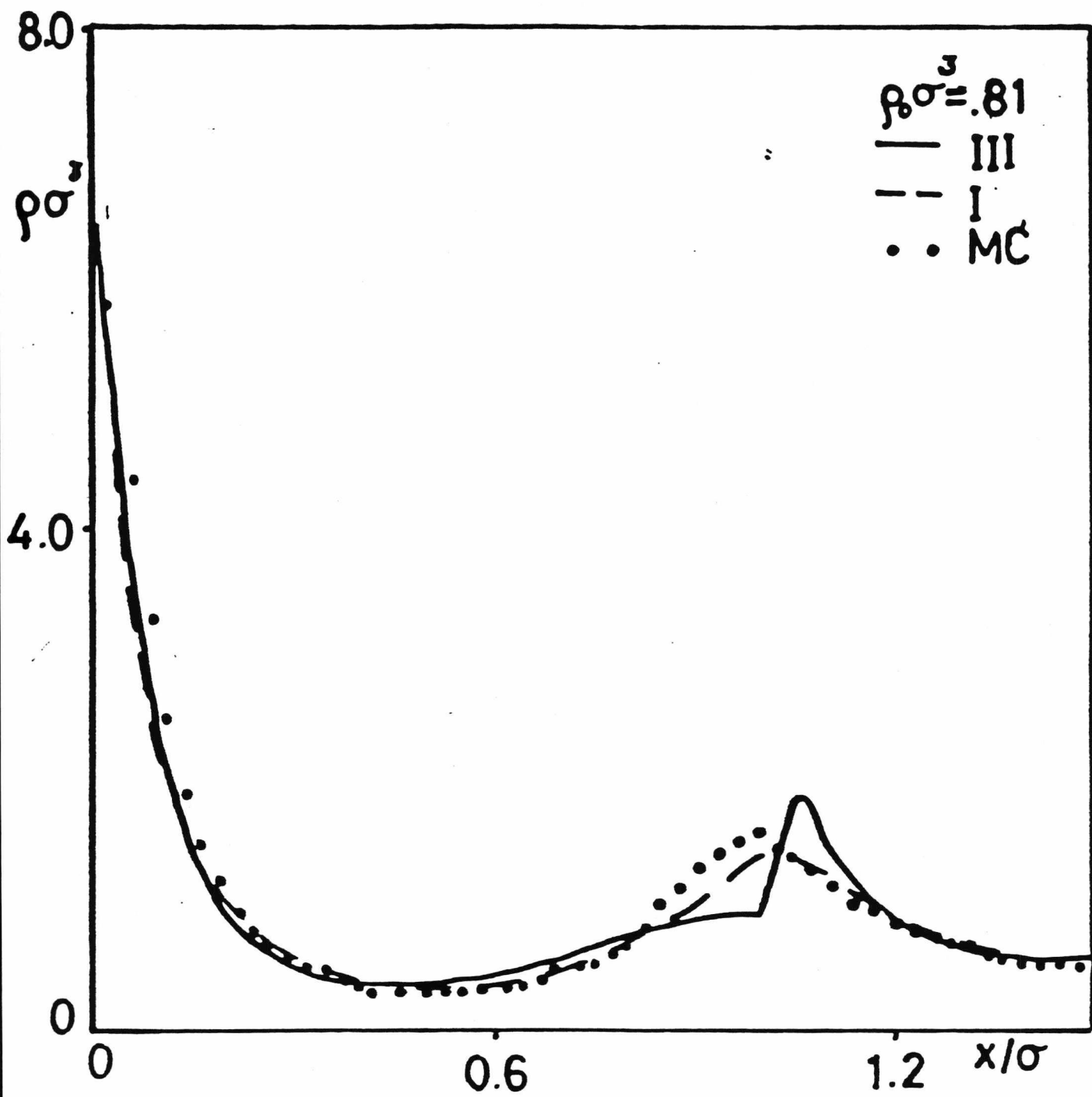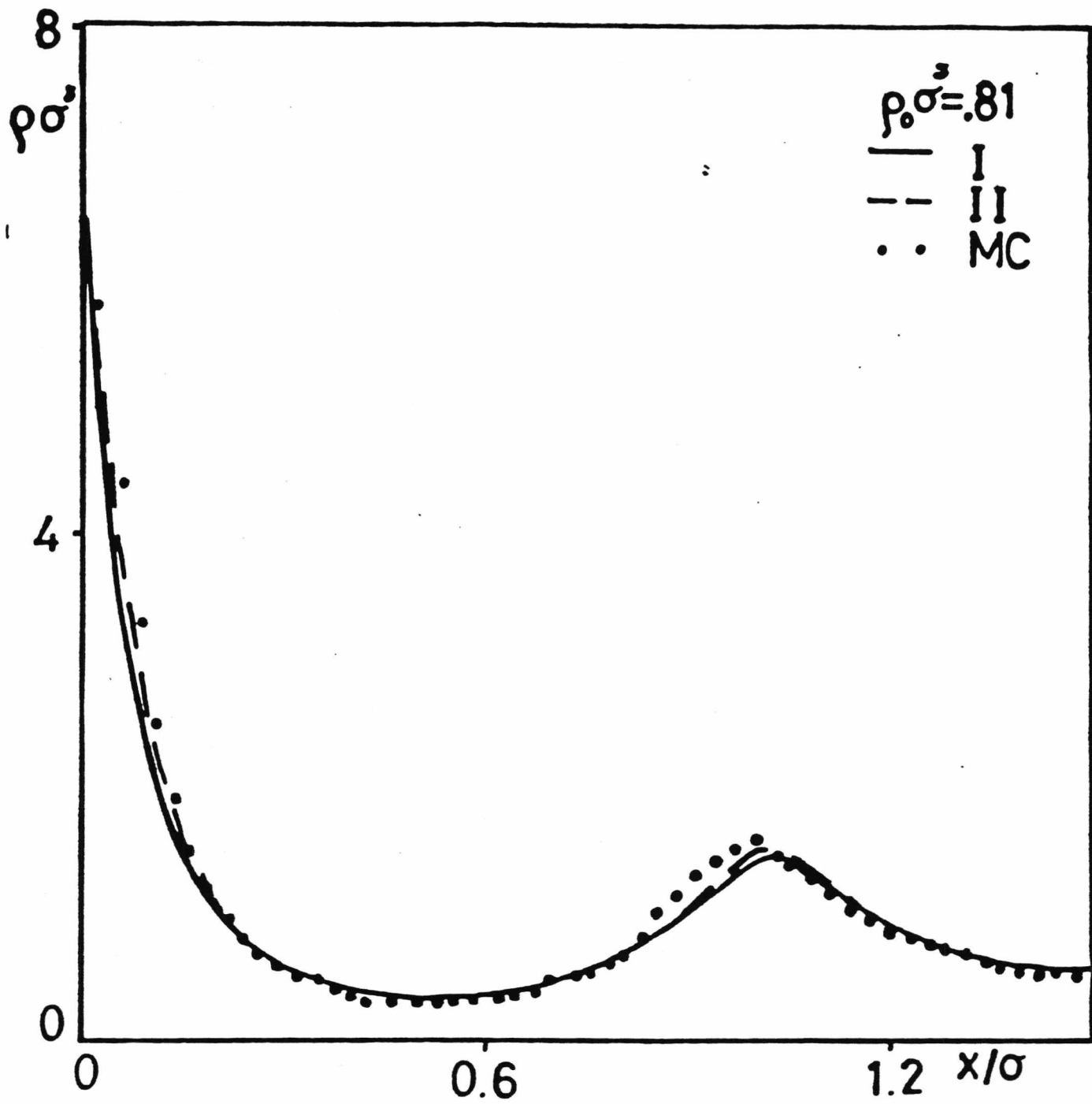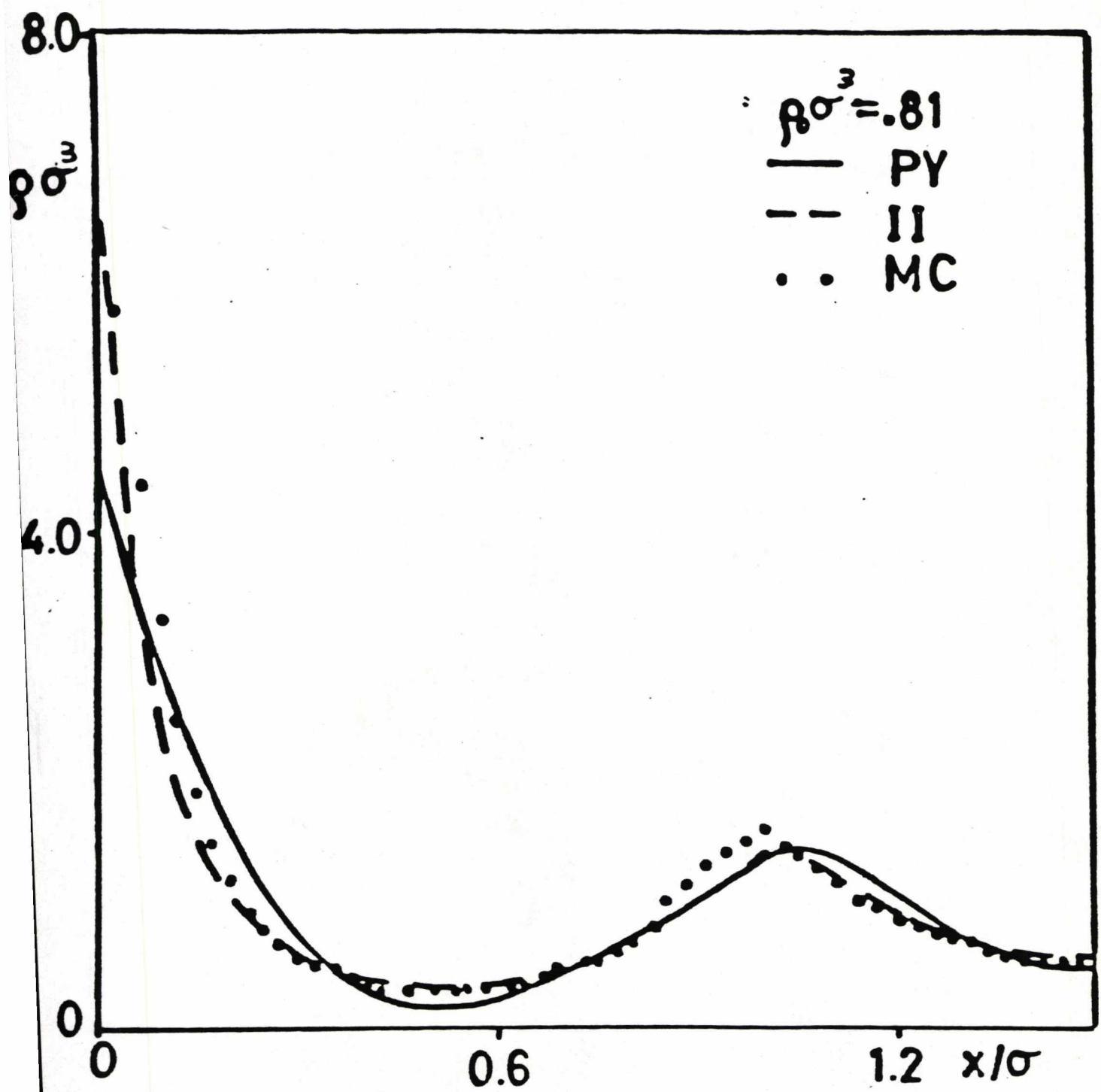
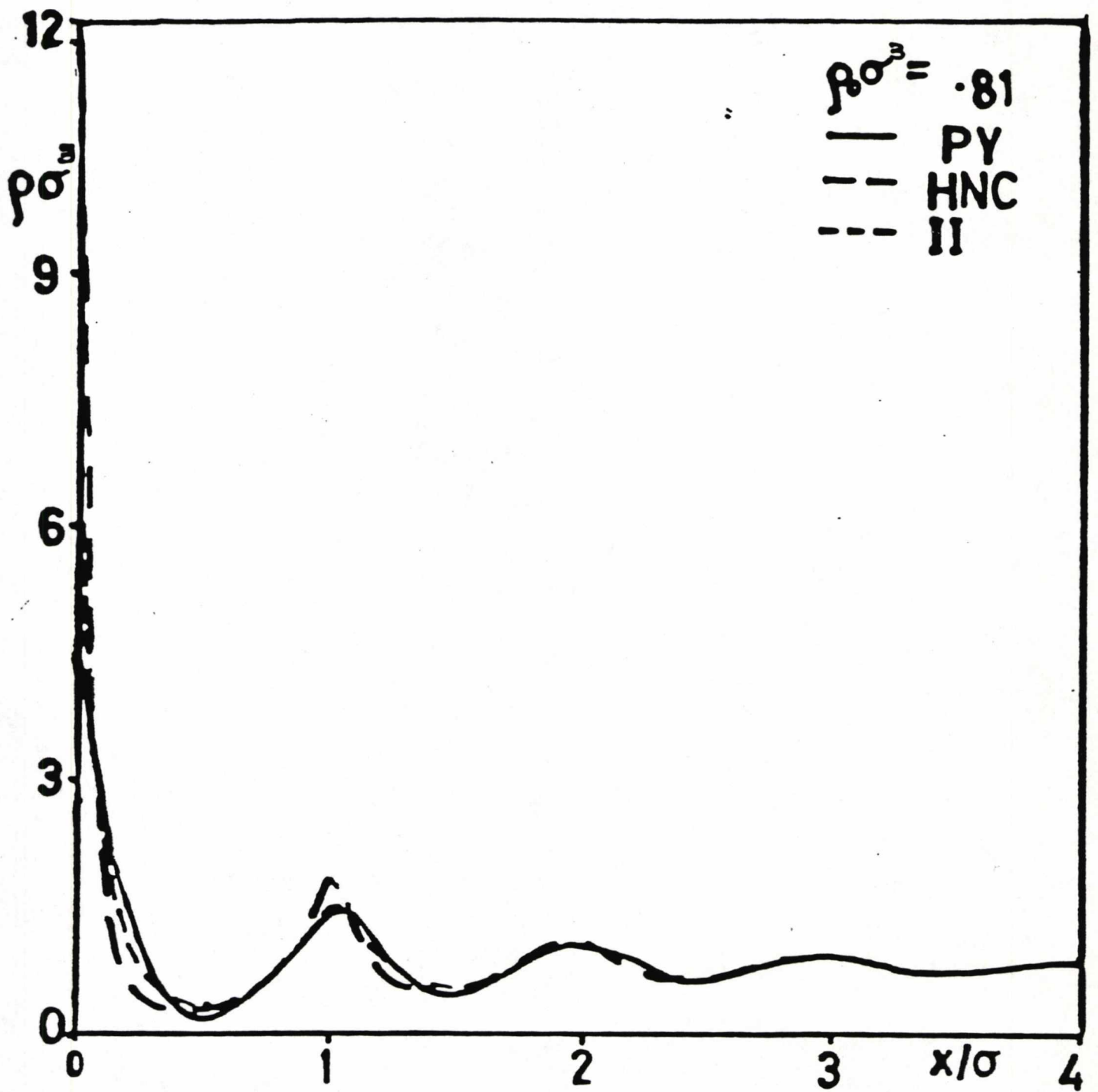Fig 5.1

Fig 5.2

Fig 5.3

Fig 5.4

Fig 5.5

Fig 5.6

Fig 5.7
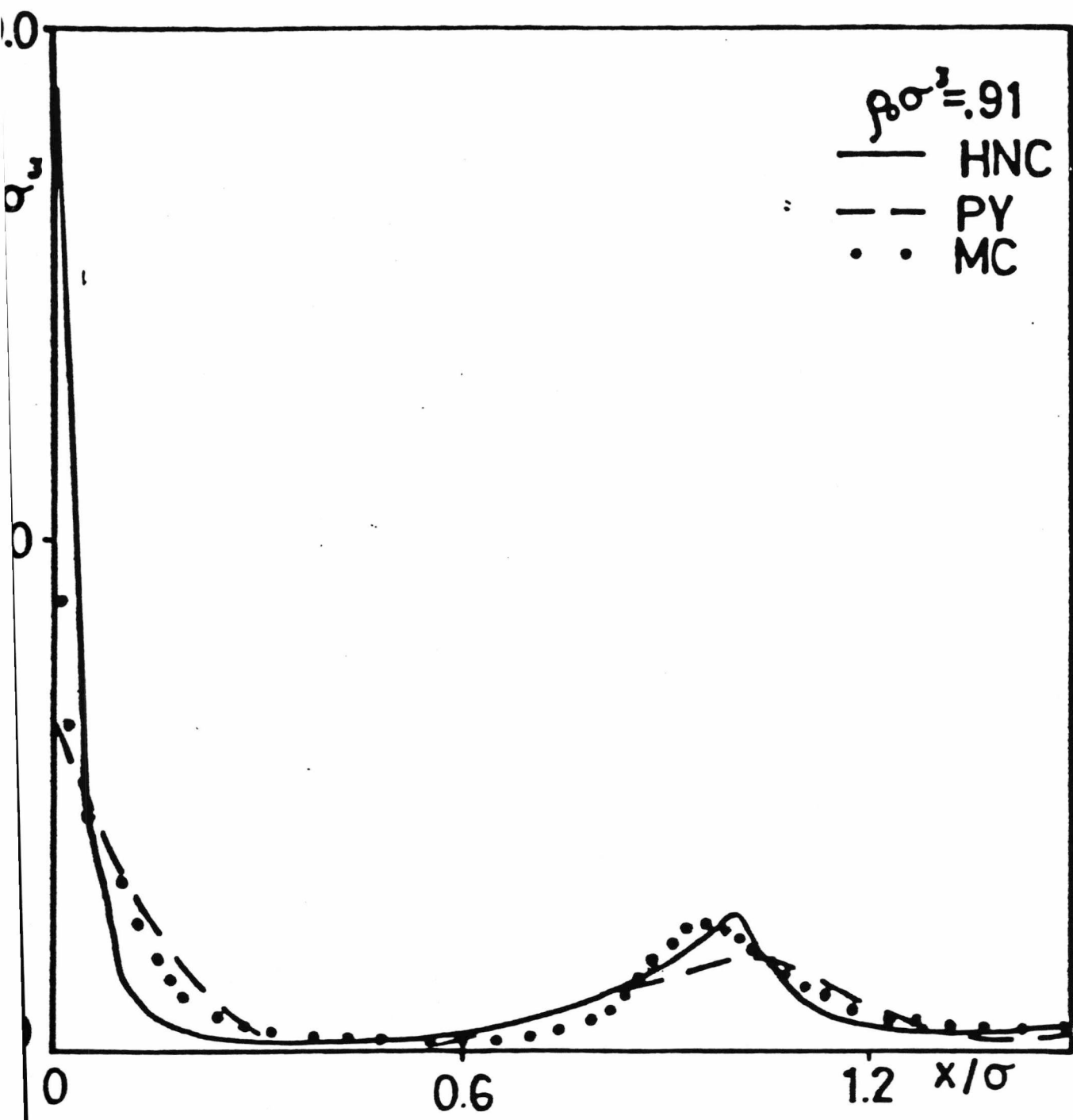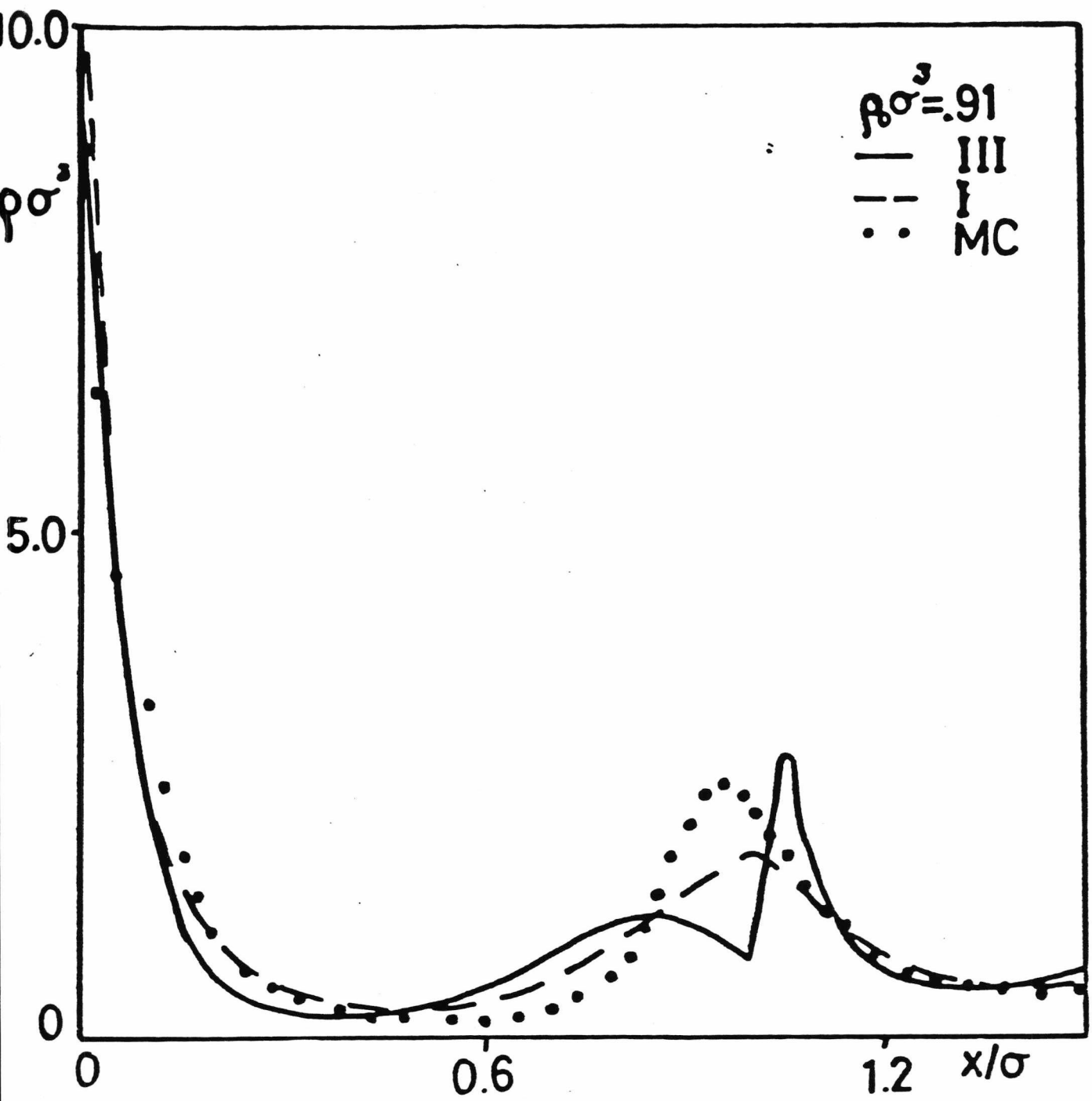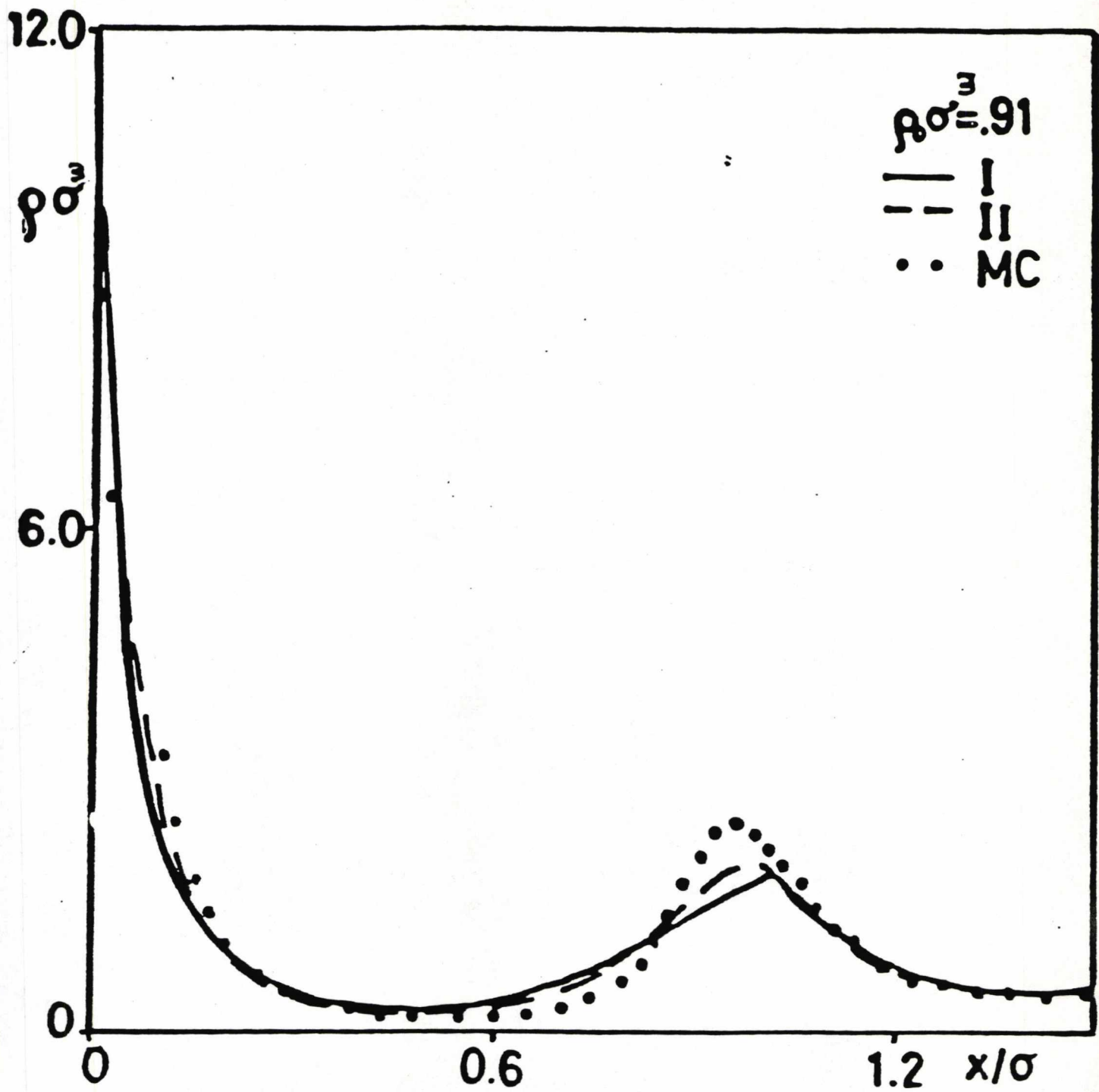
Fig 5.8

Fig 5.9

Fig 5.10

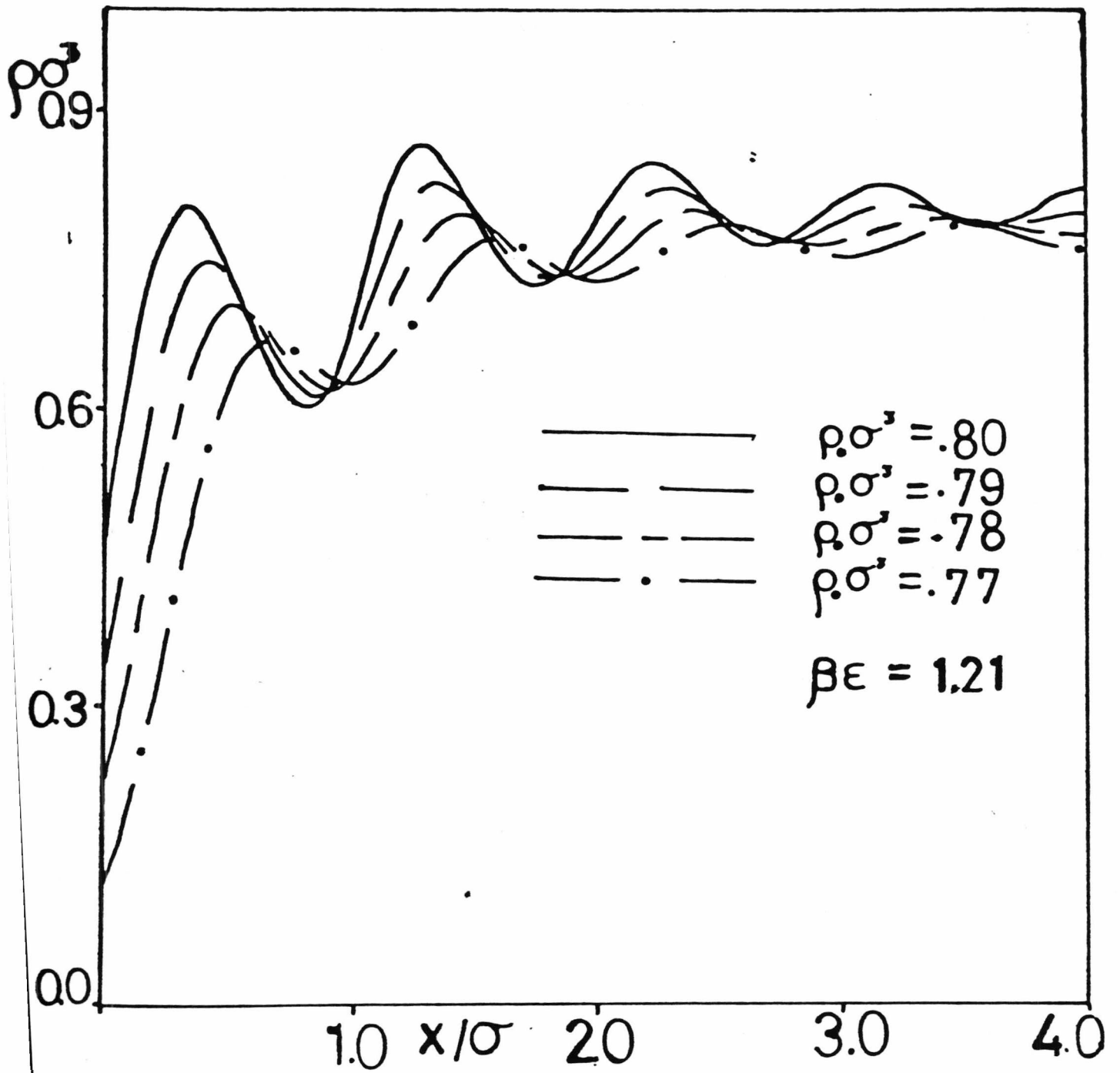Fig 5.11

Fig 5.12

Fig 5.13

Fig 5.14

6. SHOULDERED HARD SPHERE MODEL FOR CHARGED COLLOIDAL DISPERSIONS

6.1. Introduction

The work up until now has dealt with the structure of liquids near a wall from a fundamental starting point, the free energy. Information regarding the distribution of the fluid follows directly from this approach. It is possible however, to obtain such information in an indirect way, via the structure factor. This is related to the fourier transform of the radial distribution function, (similar to the density profile for a homogeneous fluid), and is of importance as it can be measured directly by scattering experiments.

The rest of this thesis deals with this aspect of fluid structure, and the structure factor according to several theories, as applied to specific models, is found and compared with experiment.

This chapter introduces a perturbation theory in which a real fluid is modelled by a reference potential, and the difference between the structure factor calculated from the reference potential and the structure factor measured by experiment is used to calculate a correction to the reference potential. The reference potential chosen is a shouldered hard sphere potential. The structure factor for a fluid with softer cores is also calculated, but not used in the perturbation theory, as it does not fit the experimental data any better than the potential already used.

6.2. Theory and Results

Light and neutron scattering studies of the static structure factor $S(q)$ for aqueous dispersions of charged colloidal particles bear a strong resemblance to similar studies of simple liquids. This has led authors to try to interpret experimentally determined structure factors with models that are familiar from theories of simple liquids. In particular, the well-known hard sphere fluid and one-component plasma (OCP) have

been used with varying degrees of success. For all of the models used, the free parameters of the interaction potential between the particles are chosen to ensure that the principal peak in $S(q)$ for the model fluid matches that of the dispersion. But it has been found that the second peak in $S(q)$ for the hard sphere fluid is located at too small a wavevector to model the experimental data after the principal peak has been fitted (see, for example, Fig. 6.1). The OCP is considerably better than the hard sphere fluid at locating the positions of the peaks of $S(q)$ in agreement with experiment, but significantly underestimates the magnitude of the second peak in $S(q)$. Perhaps the most successful model to date in terms of fitting experimental data for charged dispersions has been the rescaled mean spherical approximation (RMSA) of Hansen and Hayter.

This model involves a rescaling procedure to extend the range of applicability of a fluid of particles interacting through a hard sphere plus long-ranged repulsive Yukawa potential in the MSA. This model is as successful as the OCP in locating the position of the peaks in $S(q)$, but is noticeably better in reproducing the magnitude of the second peak. The major deficiency of the RMSA is its inability to reproduce accurately the trough between the principal and second peaks in $S(q)$ with regard to the position of the minimum and asymmetry of the trough.

As an example of the asymmetry of the trough in $S(q)$ Fig 6.1 shows the structure factor for an aqueous dispersion of polystyrene spheres of nominal density $\rho = 2.53 \times 10^{12} cm^{-3}$ obtained by Grüner and Lehmann[29] in a light scattering experiment. The asymmetry of the trough in $S(q)$ is not unique to colloidal dispersions, a similar phenomenon arises in some liquid metals which exhibit a shoulder on the high angle side of the principal peak of $S(q)$. Silbert and Young[30] have shown that this feature is consistent with a fluid whose pair potential has the form of a shouldered hard sphere,

$$\phi_{SHS}(r) = \begin{cases} \infty & r < d \\ \epsilon & d < r < \lambda d \\ 0 & r > \lambda d \end{cases} \tag{6.1}$$

with suitable choices for the constants d, ϵ and λ. While the study of Silbert and Young was performed using an approximate analytic theory, the results have been confirmed by Monte Carlo simulations due to Levesque and Weis[31] and an exact study of a one-dimensional analogue due to Kincaid and Stell.[32]

Here the method of Silbert and Young is followed in using a simple analytic approximation for the structure factor of this shouldered hard sphere fluid based on the random phase approximation (RPA). This formalism has been described elsewhere[33] and consists of writing the direct correlation function of the shouldered hard sphere fluid $c_{SHS}(r)$ as the sum of the direct correlation function for a fluid of hard spheres of diameter d, $c_{HS}(r)$, and a perturbation potential arising from the shoulder in $\phi_{SHS}(r)$. The structure factor for the shouldered hard sphere fluid is then given by

$$S_{SHS}(q)=(1-c_{SHS}(q))^{-1} \tag{6.2}$$

where the Fourier transform of $c_{SHS}(r)$ is given by

$$c_{SHS}(q)=\int d\mathbf{r}\, 4\pi r^2 \frac{\sin qr}{qr}[c_{HS}(r)-\beta\epsilon\theta(\lambda d -r)] \tag{6.3}$$

When the analytic form of $c_{HS}(r)$ from the Percus-Yevick approximation is used, the integral in eqn (6.3) is straightforward. Although the RPA formalism has its limitations at high momentum transfers, previous work suggests that it should be adequate for the present study.

For a system of particles of packing fraction $\eta=\dfrac{\pi}{6\rho d^3}$, the shouldered hard sphere fluid represents a model with four adjustable parameters ($\eta, d, \epsilon, \lambda$) and it is difficult to be sure that a unique solution has been found in a search to obtain the combination of parameters to satisfy the observed data. But Fig 6.1 shows the the structure factor for a shouldered hard sphere fluid with $\eta=0.27$, $d=5.2\times10^{-5}cm$, $\beta\epsilon=0.28$ and $\lambda=2.1$ in relation to the experimental data of Grüner and Lehmann for an aqueous dispersion of polystyrene spheres of nominal density $\rho=2.53\times10^{12}cm^{-3}$. It is reasonable to treat η as a variational parameter, since doubt exists as to the correct value of the density. For

comparative purposes Fig 6.1 also shows the best fit to experiment that can be obtained with a hard sphere fluid by varying the the two parameters η and d (η=0.34 and d=5.6×10^{-5}cm). It can be seen that the shouldered hard sphere model is significantly superior to the hard sphere model in modelling the observed data. Indeed the shouldered hard sphere fluid is very successful in its ability to locate and model the second peak in $S(q)$ in addition to the reproduction of the asymmetry of the trough between the first and second peaks of $S(q)$. Further note that the shoulders on the low and high angle sides of the principal peak in $S(q)$ for the shouldered hard sphere model mimic corresponding features in the experimental data. Thus the shouldered hard sphere fluid represents a useful model system for interpreting experimental data that will complement the RMSA of Hansen and Hayter which also contains four free parameters.

The primary aim of this study is to produce a model system that can represent the experimentally observed structure factor at high momentum transfers accurately enough to perform perturbation treatments on the available small angle scattering data. Given the success of the shouldered hard sphere fluid above, one may use this model as a reference system in a RPA calculation of the interaction potential from the observed $S(q)$. In this treatment the effective interparticle pair potential $\phi(r)$ for the colloid is given by

$$\phi(r)=\phi_{SHS}(r)+\frac{k_B T}{(2\pi)^3 \rho_0}\int dq\, 4\pi q^2 \frac{\sin qr}{qr}\left[\frac{1}{S(q)}-\frac{1}{S_{SHS}(q)}\right] \qquad (6.4)$$

This technique has been seen to be semi-quantitatively accurate when applied to simple liquids and liquid metals and the results of a calculation based on the shouldered hard sphere fluid and experimental data shown in Fig 6.1 are given in Fig 6.2.

The effective pair potential shown in Fig 6.2 displays a cusp at the hard core and a discontinuity at larger particle separations due to the form of the shouldered hard sphere potential. Thus we may expect the calculated $\phi(r)$ to be only an approximation

to the effective pair potential. But it is interesting to note that the oscillatory nature of the calculated pair potential is consistent with a similar study of high density dispersions. As noted in the analysis of the result in ref 39, the shallow primary minimum in $\phi(r)$ differs qualitatively from the form given by DLVO theory. The deficiencies of DLVO theory in predicting the structure of concentrated dispersions of charged particles are evident from the work of Hansen and Hayter[34]. They use a fluid of particles interacting via a hard core plus repulsive Yukawa pair potential that is equivalent to a DLVO theory in the absence of van der Waals interactions, which are thought to be negligible in these systems, and fail to accurately reproduce the large wavevector form of $S(q)$. The failure of the Hansen and Hayter model in the small angle scattering regime is far more serious and questions the long-range form of the DLVO pair potential. However, the status of DLVO theory from these scattering measurements may appear to be artificially bad for two reasons. Firstly the simple DLVO pair potential is derived in the dilute dispersion limit and is not strictly valid for the concentrated systems studied in the light and neutron scattering experiments. Secondly, the samples used in the experiments are known to be polydisperse to a small extent and it can be shown that the polydispersity of the sample around some representative monodisperse system may be regarded at the level of the RPA as an additional contribution to the effective pair potential. Thus a study of the polydispersity of the samples used in the experiment is essential if structure factor measurements are to provide information on colloid interaction potentials.

It must be emphasised that the model presented for the large wavevector form of the structure factor is by no means unique, but given the simplicity of the shouldered hard sphere model it may provide a guide for the interpretation of experimental data. Much more work is required on the possible degree of polydispersity of the polystyrene sphere system used in the experiments if the physical origin of the shoulder in the interaction potential is to be attributed to either an intrinsic softness of the core in the

pair potential, polydispersity of the hard cores or some other effect.

6.3. Soft Core reference potential

A second potential was also used as a reference potential in order to find a good fit to the data. This was the so-called "soft core" potential. The form of the potential is not given explicitly, but rather its effect on the radial distribution function of a pure hard fluid is specified. From this the correction to the structure factor may be calculated. This has been done by Hoshino [35].

Thus the following terms are added to the hard-sphere radial distribution function (rdf)

$$\Delta g_1(r) = \begin{cases} A \exp[\delta(r/\sigma) - 1] & r < \sigma \\ -B \exp[-\epsilon(r/\sigma) - 1] & r > \sigma \end{cases} \tag{6.5}$$

where $A, B, \delta,$ and ϵ are dimensionless positive parameters. These are chosen so as to fulfil the following conditions;

(i) continuity of $g(r)$ at $r = \sigma$

(ii) continuity of $\dfrac{dg(r)}{dr}$ at $r = \sigma$

(iii) conservation of the normalisation of the rdf

$$4\pi\rho \int \Delta g_1(r) r^2 dr = 0 \tag{6.6}$$

Thus there is only one free parameter in the model. Using a pure hard sphere fluid to give the rdf which will be "softened", the conditions (6.6) become

$$A + B = \alpha + \beta + \gamma$$
$$A\delta - B\epsilon = \beta + 3\gamma$$
$$A(1/\delta - 2/\delta^2 + 2/\delta^3) = B(1/\epsilon + 2/\epsilon^2 + 2/\epsilon^3) \tag{6.7}$$

where

$$\alpha = \frac{(1+2\eta)^2}{(1-\eta)^4}$$
$$\beta = \frac{-6\eta(1+\eta/2)^2}{(1-\eta)^4}$$

$$\gamma = \frac{\eta}{2}\alpha \tag{6.8}$$

and $\eta \equiv \frac{\pi\rho\sigma^3}{6}$, the packing fraction.

Then the structure factor is given by

$$S(k) - 1 = 4\pi\rho \int (g(r) - 1)\frac{\sin kr}{kr} r^2 dr \tag{6.9}$$

The equations (6.7) were solved by computer for various values of the density, and A was chosen to be the free parameter. Figures 6.3-6.5 show the best fit to the data of Grüner and Lehmann obtained at three different densities. As has already been mentioned with regards to the shouldered hard sphere potential, it is valid to treat the packing fraction as a variable parameter, as doubt exists concerning the correct value to choose. As can be seen from the graphs, the resulting curves all fit the data fairly well, but not significantly better than each other or the shouldered hard-sphere potential. It was therefore not deemed worthwhile to use this potential in the perturbation theory.
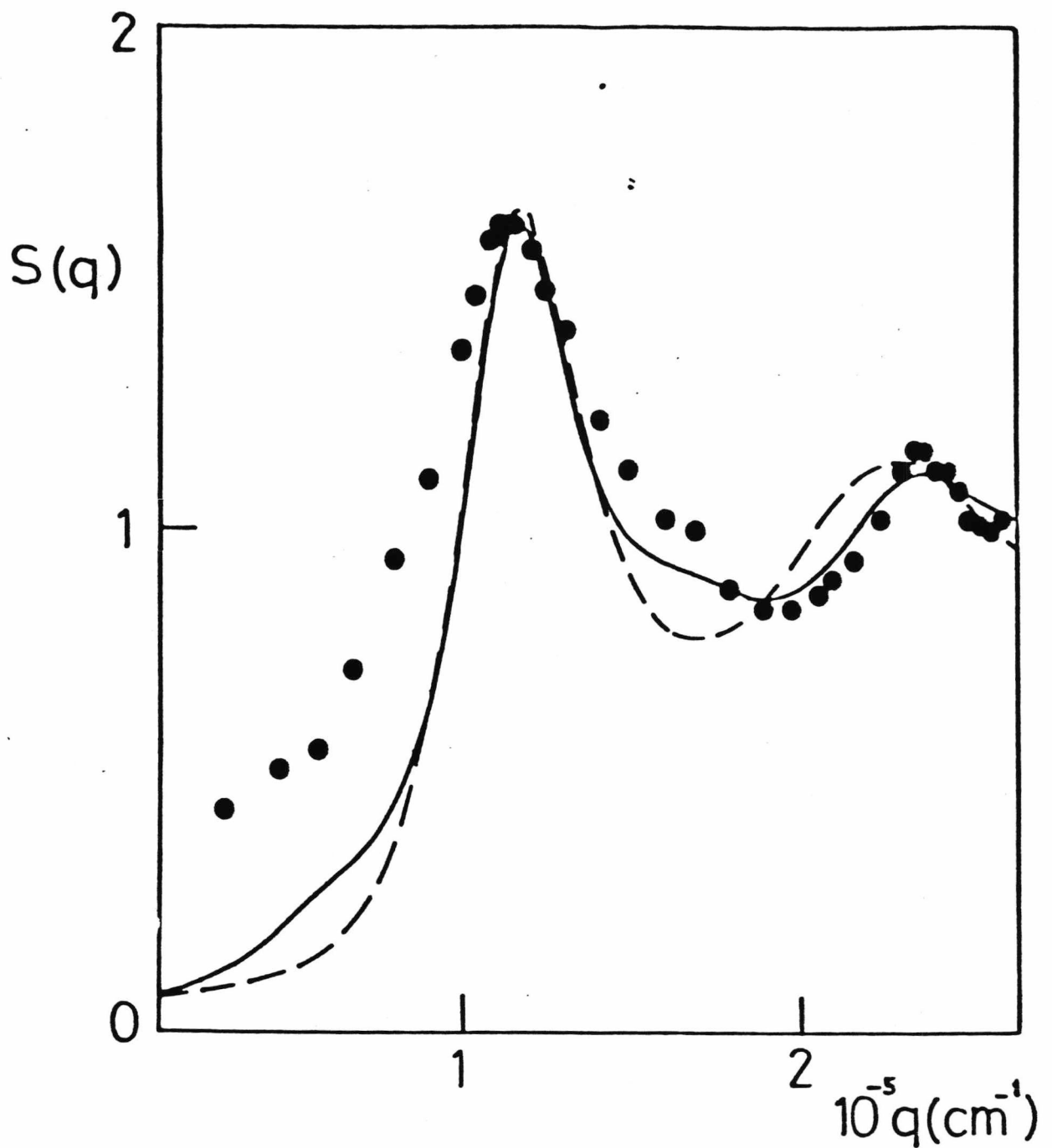
Fig 6.1: The structure factor for an aqueous dispersion of polystyrene hard spheres given by the shouldered hard sphere model (solid curve) and the pure hard sphere model (dashed curve). The points represent the experimental data of Grüner and Lehmann. For relevant parameters see text.
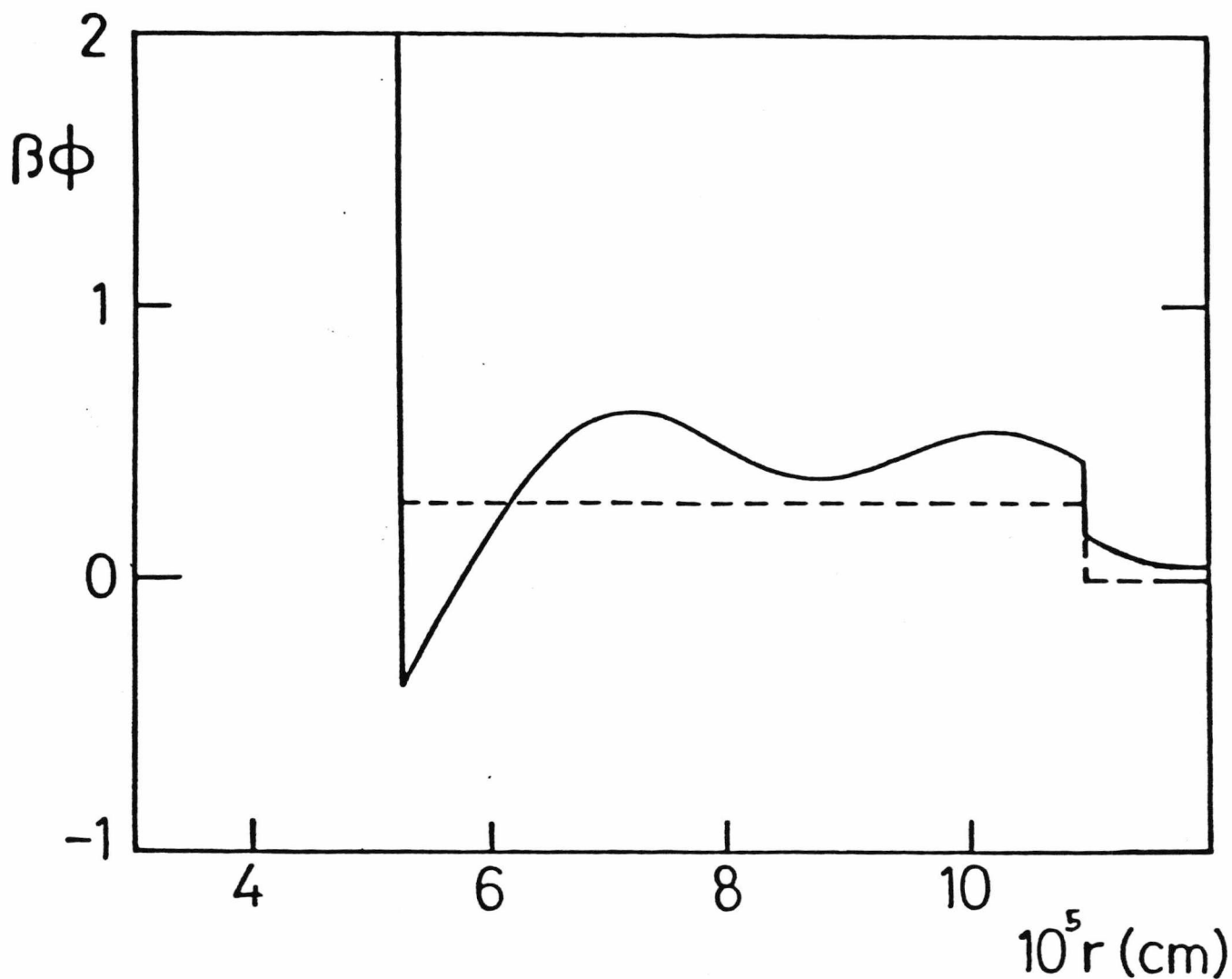
Fig 6.2: Effective interparticle pair potential for an aqueous dispersion of polystyrene spheres with structure factor depicted in Fig 6.1. The dashed line shows the reference shouldered hard sphere potential used to obtain the structure factor in Fig 6.1

Fig 6.3: Structure factor for soft core potential with $A = 1.83$, $B = 2.21$, $\delta = 8.71$, $\epsilon = 15.13$, and $\eta = .45$. The dots are the experimental data of Grüner and Lehmann.

Fig 6.4: As for Fig 6.3, but with $\eta = .4$, $A = 1.58$, $B = 1.75$, $\delta = 11.30$, and $\epsilon = 16.84$

Fig 6.5: As for Fig 6.3, but with $\eta = .35$, $A = 1.38$, $B = 1.40$, $\delta = 49.16$, and $\epsilon = 53.95$

7. CONCLUSION
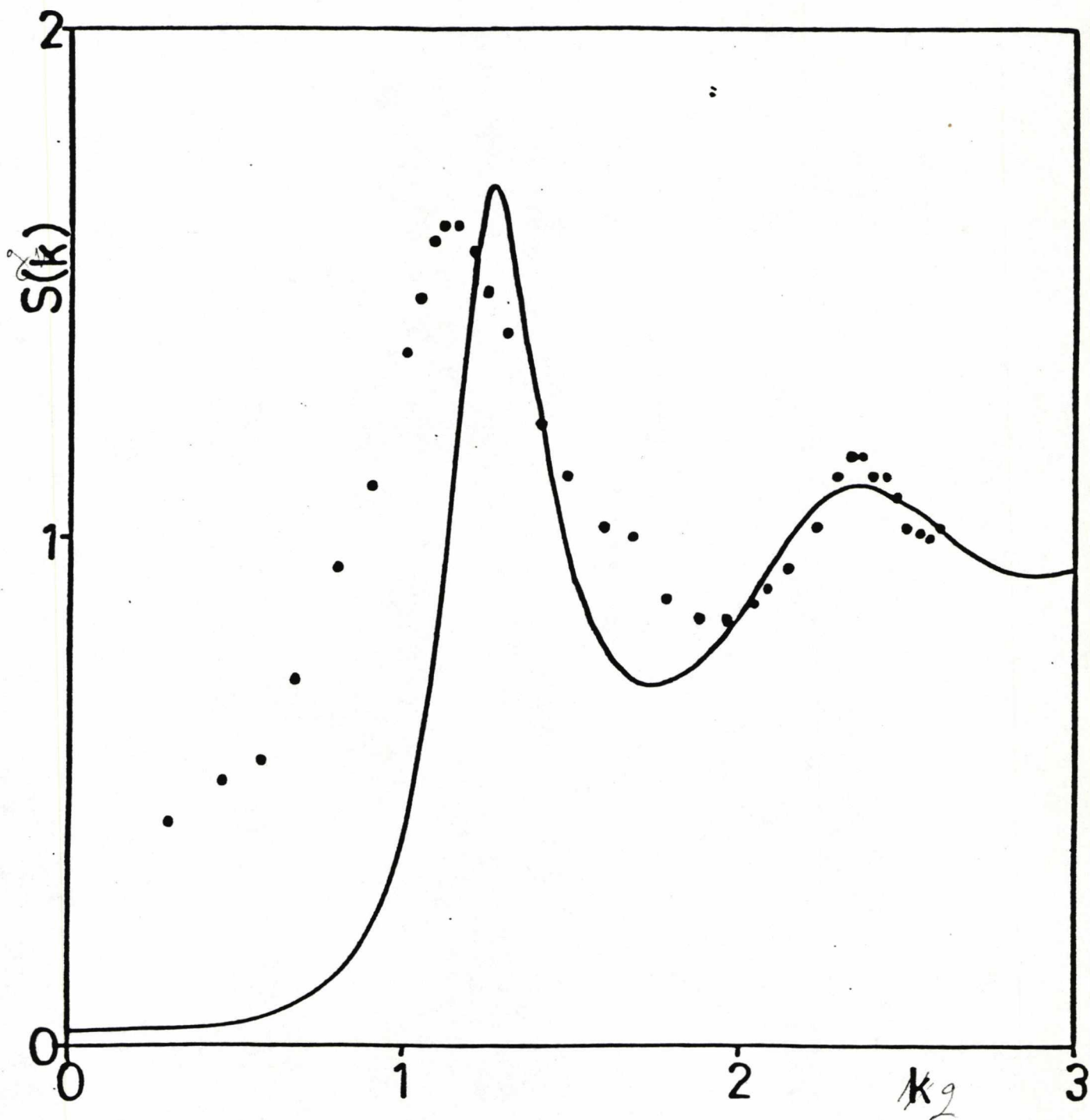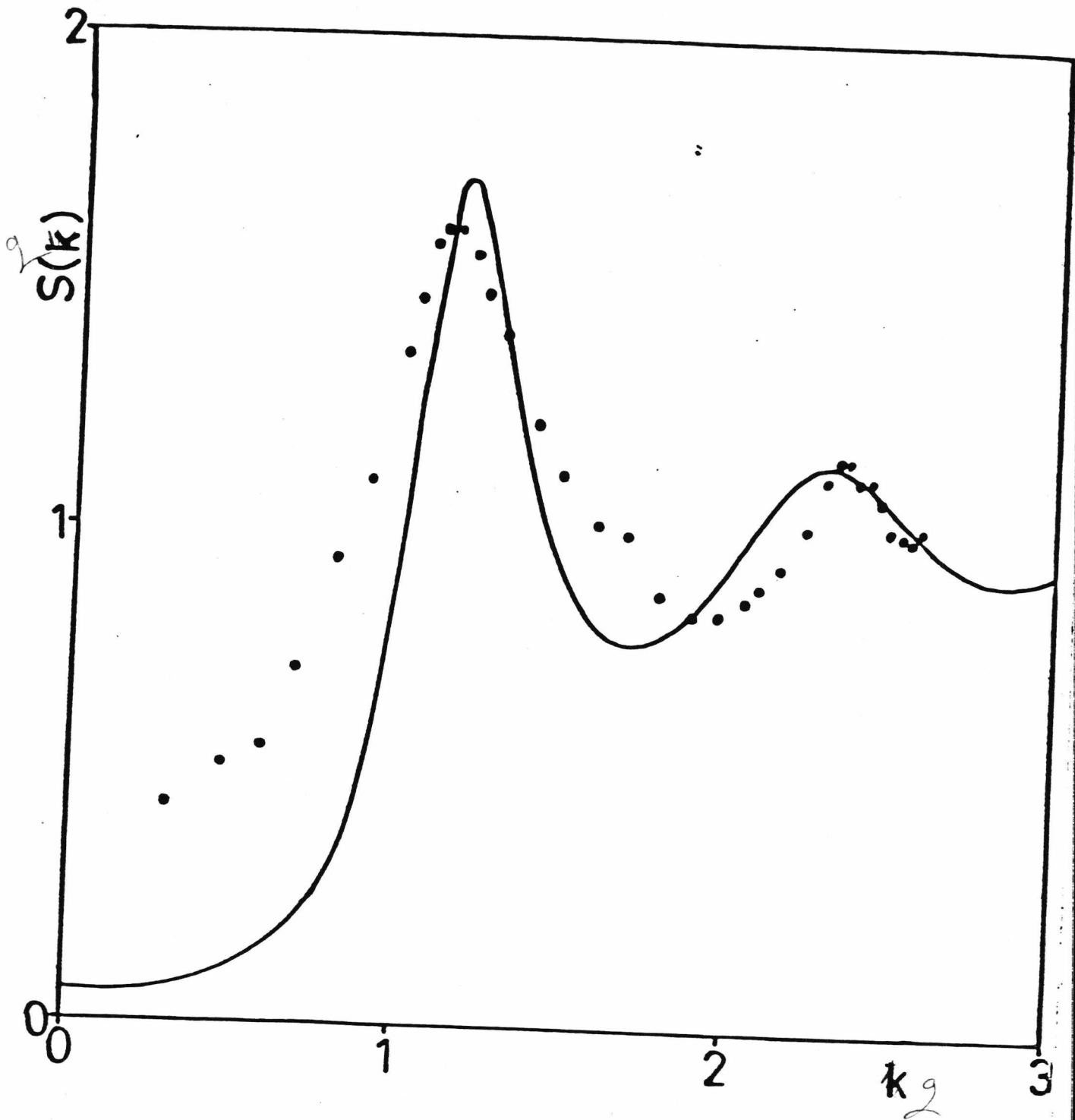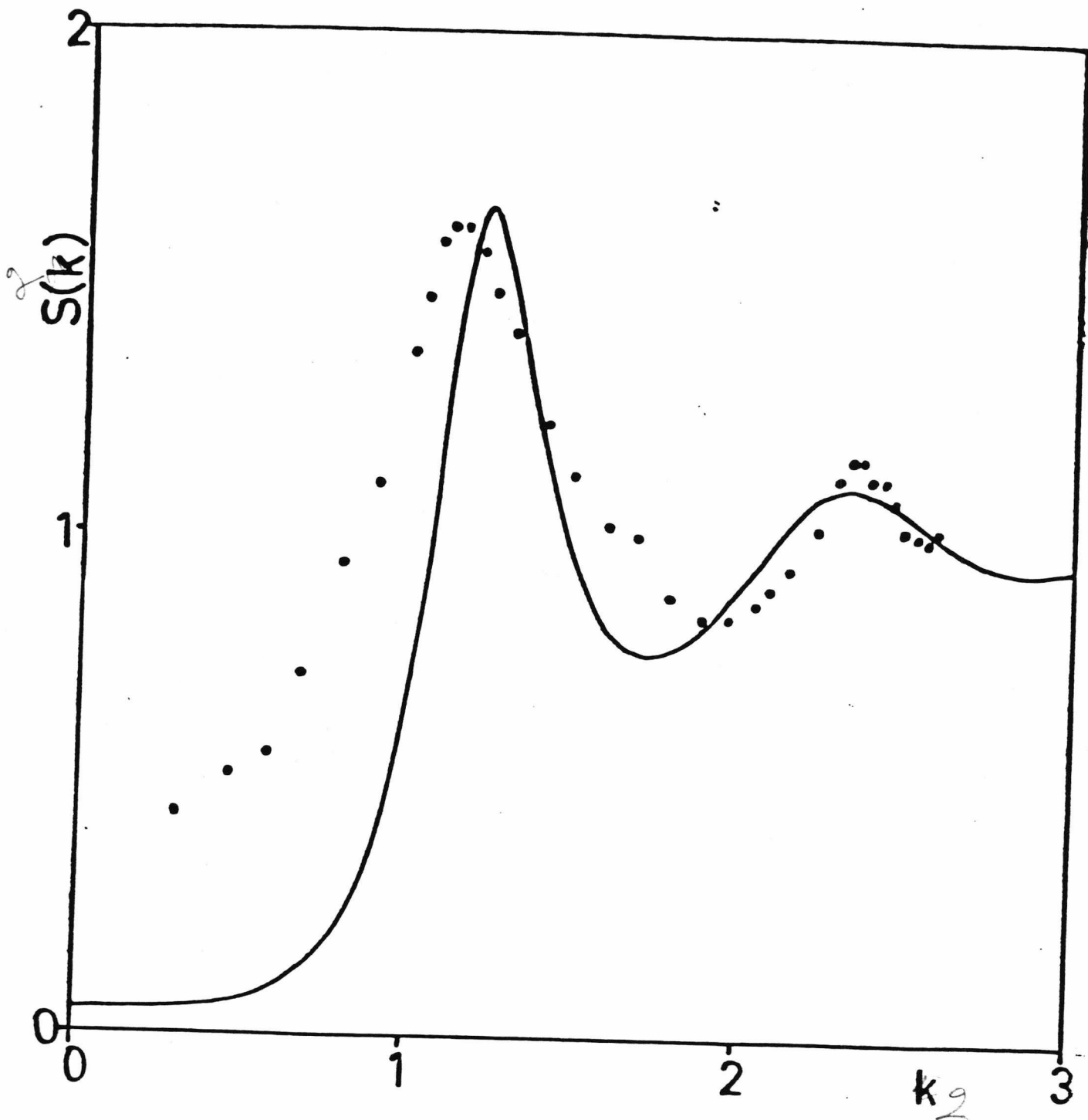
This thesis has mostly concerned itself with the structure of a fluid near a hard wall. The formalism of Grimson and Rickayzen has been extended and applied to the case of a fluid comprised of hard spheres with embedded point dipoles or ions confined between two hard walls. The model was treated using two separate approximations (the linear and non-linear theories of chapters 3 and 4 respectively) and the results obtained for the polarisation and charge profiles, as well as the pressure as a function of wall separation, were compared and contrasted. The most striking difference in the non-linear theory is the large increase in the value of the charge density at the wall. Similar results have been reported by Grimson[24] for the simpler case of a pure hard sphere electrolyte, where the polarisation due to the discrete solvent particles has been approximated by a continuous background with a bulk dielectric constant. The pressure could not be directly compared, however, as the results in the non-linear case were not regarded as being sufficiently accurate to be reliable, for reasons explained in chapter 4.

Both of the results derived here differ qualitatively and quantitatively from earlier macroscopic theories (Debye-Hückel, Gouy-Chapman) in having oscillatory profiles for charge, polarisation and pressure, as opposed to monotonically decaying ones. This would appear to have grave consequences for DLVO theory, whose prediction of a single minimum in the intercolloidal potential, arising from the choice of Debye-Hückel theory for the repulsive electrical double-layer component, is challenged. However, as the deviations of the pressure from monotonicity are greatest at relatively small separations (< 3 molecular diameters), the value of DLVO theory is not undermined in describing dilute systems, or heavily salted systems in which the repulsive potential is of short range anyway. It would seem, though, that DLVO theory is not to be used in describing coagulation, or, rather, to be used with caution.

The results also appear to be in agreement with the calculations of other workers

near a single wall, this case being the limit of infinite separation of two walls.

The advantage of a treatment using two walls is that one can obtain an intercolloidal potential directly instead of inferring one from experimental data, or assuming one with several adjustable parameters. Thus one should be able to predict the behaviour of a system to some degree, a feature which is not available otherwise.

To date no direct measurement of the force between colloid particles has been made, to the best knowledge of the author, and so the predictions remain untested. It would be desirable for an experiment to do this to be carried out, to test the assumptions present in the theory, and the power of the density-functional method.

A generalised density functional was introduced in chap 5, and some well-known results were derived from it which had not been done this way before, namely that the pressure at the wall was directly proportional to the density of the fluid at the wall for systems with no wall-particle interaction (hard walls). A model system of hard spheres confined between two hard infinite planar walls was treated using an approximation to the generalised functional in which some attempt to take three-body interactions into account was made. The results were found to be in excellent agreement with Monte Carlo simulations, particularly when one considers the simplicity of the approximations made. The density profile was seen to be fairly insensitive to the form of the term representing the three-body interaction, a useful feature.

The form of the functional, being cubic in the density, was capable of describing liquid-vapour coexistence, and this was demonstrated by applying the functional to a system of hard spheres interacting with a truncated Lennard-Jones potential, with the direct correlation function given by the RPA. Choosing appropriate values for the density and reduced temperature gave similar results to those obtained by Tarazona and Evans[28], namely the wetting of a wall by vapour.

The functional is evidently useful, and attempts to apply it to a system representing an argon fluid bounded by solid carbon dioxide walls are currently being

made.

The structure of bulk fluids has also been investigated. This has not been done by studying the pair distribution function (or density profile) directly, but rather by examining the related fourier transform, the structure factor, as measured by experiment and calculated theoretically. The purpose of the studies was to obtain an intercolloidal potential by approximating the experimental structure factor by a close-fitting theoretical one derived from a known interparticle reference potential, and then using a perturbation approach to derive a correction to the reference potential from the difference of the the two structure factors.

When one uses this technique to analyse a system of charged polystyrene balls, using as a reference potential a hard sphere potential with an added hard shoulder, one finds, perhaps not surprisingly, that the calculated potential contains a deep primary minimum, as well as a shallower secondary one. The depth of the minimum is about two orders of magnitude greater than the corresponding minimum predicted solely on the basis of van der Waals forces. Now it may be argued that this large attractive correction to the reference potential is an artificial effect due to the fact that the effects of polydispersity were not included in the treatment. Certainly there was some degree of polydispersity present in the sol. However it seems that although this is true, it may not be deleterious to the theory--- one may, in fact, represent the polydisperse system as a monodisperse one interacting with a suitable potential of mean force. The accuracy of this representation remains to be established. Certainly, it can reproduce the observed structure factor, but does it allow calculation of thermodynamic or structural quantities which are close to those in the real system? This aspect of the theory needs further investigation.

The data was also modelled using a "soft" core as a reference potential. The resulting fit to the data was not deemed sufficiently good to merit its use in the perturbation theory, but the results are included for the sake of completion.

Now the logical extension of the present formalism as applied to a system of ions and dipoles in Chapters 3 and 4 is to apply it to a fluid comprised of ions, dipoles and quadrupoles. This work is currently being carried out, although at present no progress beyond calculating the bulk direct correlation functions has been made.

Two further avenues of research already mentioned are

(i) the application of the improved functional of Chapter 5 to other systems,

(ii) the investigation of the accuracy of representing a polydisperse system as a monodisperse system interacting through a suitable potential of mean force.

A further refinement to the perturbation theory for the derivation of the interparticle potential has also been considered, though not yet implemented. This involves using the derived potential as the new input for a reference potential, and calculating the new structure factor from this. This is to say one would use a different approximation to the RPA (the PY or HNC approximations, for example) to derive the direct correlation function from the new potential, and hence the new reference structure factor. One would continue iterating in this fashion until convergence (hopefully) was achieved, thus justifying the use of the RPA approximation (exact in the limit of small perturbations), and becoming self-consistent. The resulting interparticle potential would be the correct one, within the limitations of the approximation chosen for the derivation of the direct correlation function from the potential. The RPA will introduce no error, as it essentially correct at convergence.

In summary, the structure of a fluid both in the bulk and near a wall has been studied using the method of the density-functional, and perturbation theories. The results subsequently derived for the pressure between two hard walls cast doubt on the validity of DLVO theory, or rather, on its range of applicability. An improved functional, taking three-body forces into account, has been introduced, and its successful application to a hard sphere system demonstrated. Finally, a simpler representation of polydispersity has been (somewhat tentatively) put forward. Its

ability to accurately represent the polydisperse system beyond the reproduction of its structure factor is not yet established.

It is evident that, based upon the work which has already been done, there are many exciting possibilities yet to be explored.

REFERENCES

(1) R.H.Ottewill and J.N.Shaw, Discuss. Far. Soc., **42** 143 (1966)

(2) B.A.Matthews and C.T.Rhodes, J. Pharm. Sci., **57** 557 (1968)

(3) R.M.Joseph-Petit, F.Dumont and A.Watillon, J. Coll. and Int. Sci., **43** 649 (1973)

(4) K.Norrish, Discuss. Far. Soc. **18** 120 (1954)

(5) R.G.Horn, E.Perez and R.K.Tandon, J. Coll. and Int. Sci. **78** 260 (1980)

(6) J.N.Israelachvili and R.G.Horn, Chem. Phys. Lett. **71** 192 (1980)

(7) J.N.Israelachvili, R.K.Tandon and L.R.White, J. Coll. and Int. Sci. **78** 430 (1980)

(8) R.G.Horn, J.N.Israelachvili and E.Perez, J. Phys.(Orsay,Fr.) **42** 39 (1981)

(9) J.N.Israelachvili and G.Adams, JCS Far. Trans. I **74** 975 (1978)

(10) R.J.Baxter, J. Chem. Phys. **52** 4559 (1970)

(11) J.Lyklema, P.C.Sholten and K.J.Mysels, J.Phys.Chem. **69** 116 (1965)

(12) A.Scheludko, B.Rodoev, T.Kolarov Trans. Far. Soc. **64** 2213 (1968)

(13) H.Sonntag and J.Netzel, Z. Phys. Chem. (Leipzig) **250** 330 (1972)

(14) ' The Theory of Simple Liquids ' J.-P.Hansen and I.Macdonald Academic Press, London, (1976)

(15) Cahn and Hilliard, J. Chem. Phys., **28** 258 (1958)

(16) W.F.Saam and C.Ebner, Phys. Rev. A **15** 2566 (1977)

(17) M.J.Grimson and G.Rickayzen, Mol. Phys. **42** 767 (1981)

(18) S.L.Carnie and D.Y.C.Chan, J. Chem. Phys., **73** 2949 (1980)

(19) L.Blum and D.Henderson, J. Chem. Phys. **74** 1902 (1981)

(20) D.Henderson and L.Blum, Far. Symp. Chem. Soc. **16** 151 (1982)

(21) M.J.Grimson, G.Rickayzen and P.Richmond, Mol. Phys. **39** 61 (1980)

(22) M.J.Grimson and G.Rickayzen, Mol. Phys. **44** 817 (1981); **45** 221 (1982)

(23) D.Y.C.Chan, D.J.Mitchell and B.W.Ninham J. Chem. Phys. **70** 2946 (1979)

(24) M.J.Grimson, private communication

(25) I.K.Snook and D.Henderson J. Chem. Phys. **68** 2134 (1978)

(26) E.Waisman, D.Henderson and J.L.Lebowitz, Mol. Phys. **32** 1373 (1976)

(27) J.Henderson, in press

(28) P.Tarazona and R.Evans, in press

(29) F.Grüner and W.Lehmann, J. Phys. A **13** 2155 (1980)

(30) M.Silbert and W.H.Young, Phys. Lett. A **58** 469 (1976)

(31) D.Levesque and J.J.Weis, Phys. Lett. A **60** 473 (1977)

(32) J.M.Kincaid and G.Stell, Phys Lett A **65** 131 (1978)

(33) M.J.Grimson, JCS Far. Trans. II **79** 817 (1983)

(34) J.-P. Hansen and J.B.Hayter, Mol. Phys. **46** 651 (1982)

(35) K.Hoshino, J. Phys. C Solid State Physics, **13** 3097 (1980)

(36) G.Rickayzen, private commnuication

(37) L.Blum, Molec. Phys. **30** 1529 (1975)

(38) I.Hiroike, Molec. Phys. **33** 1195 (1977)

(39) A.T.Augousti and M.J.Grimson, Phys. and Chem. of Liquids, **14** 53 (1984)

(40) S.L.Carnie and D.Y.C.Chan, J. Chem. Phys. **74** 1293 (1981)

(erratum --- J. Chem. Phys. **78** 3348 (1983))

(41) L.Blum and D.Henderson, J.Chem.Phys. **74** 1902 (1981)

(42) D.Henderson, L.Blum and J.L.Lebowitz J.Electroanal. Chem. **102** 315 (1979)

(43) R.Parsons, Electrochim.Acta **21** 681 (1976)

(44) C.A.Barlow,Jnr. in Phys.Chem.:An advanced Treatise,9A H.Eyring and

D.Henderson Eds., Academic Press NY (1970)

(45) W.R.Fawcett, Isr.J.Chem. **18** 3 (1979)

(46) S.Trasatti in Modern Aspects of Electrochemistry, **13** J.O'M.Bockris and B.E.Conway, Eds. Plenum NY (1979)

(47) F.H.Stillinger, Adv. Chem. Phys. **31** 1 (1975)

(48) G.C.Lie, E.Clementi, and M.Yoshine, J.Chem.Phys. **64** 2314 (1976)

(49) W.L.Jorgensen, J.Chem.Phys. **77** 4156 (1982)

(50) S.A.Adelman and J.M.Deutch, J.Chem.Phys. **60** 3935 (1974)

(51) L.Blum, J.Chem.Phys. **61** 2129 (1974)

(52) D.Levesque,J.J.Weis and G.N.Patey, J.Chem.Phys. **72** 1887 (1980)

(53) S.L.Carnie and D.Y.C.Chan, Adv. Coll. Int. Sci. **16** 81 (1982)

(54) G.N.Patey, D.Levesque and J.J.Weis, Mol.Phys. **38** 219 (1979)

(55) S.L.Carnie and G.N.Patey, Mol.Phys. **47** 1129 (1982)

(56) G.P.Morriss and P.T.Cummings, Mol.Phys. **45** 1099 (1982)

(57) F.Hirata, P.J.Rossky and B.M.Pettit, J.Chem.Phys. **78** 4153 (1983)

(58) G.N.Patey and S.L.Carnie, J.Chem.Phys. **78** 5183 (1983)

(59) L.Blum, C.Gruber, D.Henderson, J.L.Lebowitz and P.A.Martin, J.Chem.Phys. **78** 3195 (1983)

(60) L.Blum, C.Gruber, J.L.Lebowitz and P.A.Martin, Phys.Rev.Lett. **48** 1769 (1982)

(61) S.L.Carnie and G.Torrie, Adv. Chem. Phys. **56** 145 (1984)

APPENDIX A

FUNCTIONAL TECHNIQUES

Functions of several variables

One may begin by considering functions of several variables, and then extending the formalism to deal with a continuous infinity of variables. $f(x_1,x_2, \cdots ,x_n)$ exists if to every value $(x1,x_2, \cdots ,x_n)$ in a set one can assign a unique value of f.

Under well defined conditions one can define partial derivatives $\frac{\partial f}{\partial x_i}$ (i=1, 2, ... , n) such that (to first order in Δx_i)

$$\Delta f = f(x_1+\Delta x_1,x_2+\Delta x_2, \cdots ,x_n +\Delta x_n)-f(x_1,x_2, \cdots ,x_n)$$
$$= \sum_{i=1}^{n} \frac{\partial f}{\partial x_i}\Delta x_i \tag{A.1}$$

Alternatively

$$G(\epsilon)=f(x_i +\epsilon\Delta x_i)$$

With this new definition, we may write

$$\frac{dG(\epsilon)}{d\epsilon}=\sum_{i=1}^{n} \frac{\partial f}{\partial x_i}\Delta x_i \tag{A.2}$$

The second definition is more exact.

For second order derivatives:

$$\delta^2 f = \frac{1}{2} \sum_{i,j=1}^{n} \frac{\partial^2 f}{\partial x_i \partial x_j}\Delta x_i \Delta x_j$$

or

$$\frac{d^2 G(\epsilon)}{d\epsilon^2}=2\times\frac{1}{2} \sum_{i,j=1}^{n} \frac{\partial^2 f}{\partial x_i \partial x_j}\Delta x_i \Delta x_j \tag{A.3}$$

Under appropriate conditions, one can expand a function in terms of its first and higher order derivatives in a Taylor expansion,

$$f(x_i +\Delta x_i)=f(x_i)+ \sum_{r=1}^{\infty} \frac{1}{r!} \sum_{r_i=1}^{n} \frac{\partial^r f}{\partial x_{r_1} \cdots \partial x_{r_n}}\Delta x_{r_1} \cdots \Delta x_{r_n}$$

Integration

$$I = \int f(x_1, x_2, \cdots, x_n) dx_1 \cdots dx_n$$

can be defined. In liquid theory, examples are :

Energy;

$$E = \sum_{i=1}^{n} \left\{ \frac{\phi_i^2}{2m} + V(x_1, x_2, \cdots, x_n) \right\} \equiv E(\phi_i, x_i)$$

Partition function;

$$Z = C \int \Pi dp_i \, dx_i \exp(-\beta E(\phi_i, x_i))$$

Functionals

One can extend the previous definition to the case where the " function " depends on a continuous infinity of variables *i.e* on a function.

$F[\phi(x)]$ is a functional of the function $\phi(x)$, (defined in the range $a \leq x \leq b$, if to every function $\phi(x)$, we ascribe a unique value of F.

Examples:

(i)

$$F[\phi] = 1 \quad \text{if} \quad \phi(x) \geq 0 \quad \text{everywhere}$$
$$= 0 \quad \text{otherwise}$$

(ii)

$$F[\phi] = \int_a^b \phi(x) dx$$

(iii)

$$F[\phi] = \int \left[A \left(\frac{d\phi}{dx} \right)^2 + B \phi^2(x) \right] dx$$

(iv)

$$F[\phi] = \phi(a) \quad \text{as a special case}$$

Functional Derivatives

Consider small changes in the functional $F[\phi]$ resulting from small changes in $\phi(x)$.

To first order in $\Delta\phi$, when ϕ changes from ϕ to $\phi+\Delta\phi(x)$, we have

$$\Delta F = \int_a^b A(x)\Delta\phi(x)dx \tag{A.4}$$

(A.4) is the analogue of continuous analogue of (A.1). It is usual to write

$$A(x) = \frac{\delta F}{\delta\phi(x)}$$

This is a function of x, and a functional of $\phi(x)$.

Alternative definition

Define

$$\Phi(\epsilon) = F[\phi(x)+\epsilon X(x)]$$

where X and ϕ are given. Then

$$\left(\frac{d\phi}{d\epsilon}\right)_{\epsilon=0} = \int \frac{\delta F}{\delta\phi(x)}X(x)dx \tag{A.5}$$

Examples:

(ii)

$$F = \int_a^b \phi(x)dx \quad , \quad \Delta F = \int_a^b \Delta\phi(x)dx$$

and

$$\frac{\delta F}{\delta\phi(x)} = 1$$

(iii)

$$F = \int_a^b \left[A\left(\frac{d\phi}{dx}\right)^2 + B\phi^2(x)\right]dx$$

$$\Delta F = 2\int_a^b \left[-A\left(\frac{d^2\phi}{dx^2}\right) + B\phi(x)\right]\Delta\phi(x)dx$$

$$\frac{\delta F}{\delta\phi(x)}=2\left[-A\left(\frac{d^2\phi}{dx^2}\right)+B\,\phi(x)\right]$$

(iv)

$$F=\int\int\phi(x)K(x,x')\phi(x')dxdx'$$

$$\Delta F=\int\int\Delta\phi(x)K(x,x')\phi(x')dxdx'+\int\int\phi(x)K(x,x')\Delta\phi(x')dxdx'$$

$$=\int\int\Delta\phi(x)K(x,x')\phi(x')dxdx'+\int\int\phi(x')K(x,x')\Delta\phi(x)dxdx'$$

Therefore

$$\frac{\delta F}{\delta\phi(x)}=\int[K(x',x)+K(x,x')]\phi(x')dx'$$

Note that this is a function of x and a functional of $\phi(x)$.

(v)

$$F(x)=f(\phi(x))$$

(e.g) $\exp(-\phi(x)))$

$$\Delta F(x)=\frac{\partial F}{\partial\phi(x)}\Delta\phi(x)$$

$$\Delta F(x)=\frac{\partial F}{\partial\phi(y)}\Delta\phi(y)$$

$$=\int\frac{\partial F}{\partial\phi(x)}\delta(x-y)\Delta\phi(x)dx$$

Therefore

$$\frac{\delta F}{\delta\phi(x)}=\delta(x-y)\frac{\partial F}{\partial\phi(x)}$$

Higher Derivatives

Let

$$\Phi(\epsilon)=F[\phi+\epsilon X]$$

$$\frac{d^2\Phi(\epsilon)}{d\epsilon^2}\bigg|_{\epsilon=0}=\int\frac{\delta^2 F}{\delta\phi(x)\delta\phi(x')}X(x)X(x')dxdx' \tag{A.6}$$

where $\dfrac{\delta^2 F}{\delta\phi(x)\delta\phi(x')}$ is symmetric in x and x'.

For higher derivatives

$$\Phi(\epsilon)=F[\phi(x)+\epsilon X(x)]$$

$$\frac{d^n\Phi}{d\epsilon^n}\bigg|_{\epsilon=0}=\int\cdots\int\frac{\delta^n F}{\delta\phi(x_1)\cdots\delta\phi(x_n)}X(x_1)\cdots X(xn)dx_1\cdots dx_n \quad (A.7)$$

This defines $\dfrac{\delta^n F}{\delta\phi(x_1)\cdots\delta\phi(x_n)}$ provided that it is symmetric in $x_1, x_2, \cdots, x_n$.

E.g.

(i)

$$F=\int\phi(x)K(x,x')\phi(x')dxdx'$$

$$\Phi(\epsilon)=\int[\phi(x)+\epsilon X(x)]K(x,x')[\phi(x')+\epsilon X(x')]dxdx'$$

$$\frac{d^2 F}{\delta\phi(x)\delta\phi(x')}=K(x,x')+K(x',x)$$

(ii)

$$F=\int f(\phi(x))$$

$$\Phi(\epsilon)=\int f(\phi(x)+\epsilon X(x))dx$$

$$\frac{d^2\Phi}{d\epsilon^2}\bigg|_{\epsilon=0}=\frac{d^2 f(\phi(x))}{d\phi^2}X^2(x)dx$$

$$=\int\frac{d^2 f(\phi(x))}{d\phi^2}\delta(x-x')X(x)X(x')dxdx'$$

$$\frac{\delta^2 F}{\delta\phi(x)\delta\phi(x')}=\frac{d^2 f(\phi(x))}{d\phi^2}\delta(x-x')$$

Taylor Series

$$F[\phi+\epsilon X(x)]=\Phi(\epsilon)$$

provided that Φ can be expanded in a Taylor series in ϵ.

$$\Phi(\epsilon)=\Phi(0)+\sum_{n=1}^{\infty}\frac{1}{n!}\left(\frac{d^n\Phi}{d\epsilon^n}\right)_{\epsilon=0}\epsilon^n$$

Therefore

$$F[\phi+\epsilon X]=F[\phi]$$

$$+\sum_{n=1}^{\infty}\frac{1}{n!}\epsilon^n\int\frac{\delta^n F}{\delta\phi(x_1)\cdots\delta\phi(x_n)}\Delta\phi(x_1)\cdots\Delta\phi(x_n)dx_1\cdots dx_n \quad (A.8)$$

provided that the righthand side exists.

All of the above theory is valid if ϕ is a function of several variables e.g. $\phi=\phi(r)$.

Then the Taylor series is

$$F[\phi+\Delta\phi]=F[\phi]$$
$$+\sum_{n=1}^{\infty}\frac{1}{n!}\int\frac{\delta^n F}{\delta\phi(r_1)\cdots\delta\phi(r_n)}\Delta\phi(r_1)\cdots\Delta\phi(r_n)dr_1\cdots dr_n \quad (A.9)$$

A similar idea is used as the basis of Chapter 5

APPENDIX B

Relationship of linear ion-dipole theory to Debye-Hückel theory

It will now be shown that when the diameter, R, of the ions and dipoles tends to zero, the equations derived in chapter 3 become those of Debye-Hückel theory. In this limit we have

$$C^c(x)=\frac{\beta e^2}{2\epsilon_0}\left|x\right|, \qquad C^E(x)=\frac{\beta e\mu}{2\epsilon_0}\mathrm{sign}x$$
$$C^+(x)= ^\Delta(x)+2C^\Delta(x)=\tilde{C}(0)\delta(x) \tag{B.1}$$

where

$$\tilde{X}(0)=\int\limits_{-\infty}^{\infty} C^+(x)dx \tag{B.2}$$

and the limit is taken in such a way that $\tilde{X}(0)$ remains finite. These functions have the properties

$$\frac{\delta^2 C^c(x)}{dx^2}=\frac{\beta e^2}{\epsilon_0}\delta(x), \qquad \frac{dC^E(x)}{dx}=\frac{\beta e\mu}{\epsilon_0}\delta(x). \tag{B.3}$$

Hence, if these functions are substituted into eqns (3.22) and (3.23) and the equations differentiated with respect to x, the former twice and the latter once, one obtains

$$\frac{1}{\beta n_0}\frac{d^2 q}{dx^2}-\frac{e^2 q}{\epsilon_0}+\frac{e}{\epsilon_0}\frac{dP}{dx}-\frac{e\sigma}{\epsilon_0}=0 \tag{B.4}$$

$$\frac{3}{\rho_{03}\mu^2}\frac{dP}{dx}-\frac{\tilde{C}^+(0)}{\mu^2}\frac{dP}{dx}-\frac{\beta e}{\epsilon_0}q=0 \tag{B.5}$$

where σ is the external charge density such as that on the walls.

The polarisation can now be eliminated between eqns (B.4) and (B.5) to yield

$$\frac{1}{\beta n_0}\frac{d^2 q}{dx^2}-\frac{e^2 q}{\epsilon_0\epsilon_r}-\frac{e\sigma}{\epsilon_0}=0 \tag{B.6}$$

where

$$\frac{1}{\epsilon_r}=1-\frac{\beta\rho_{03}\mu^2/3\epsilon_0}{1-\frac{1}{3}\rho_{03}\tilde{C}^+(0)} \tag{B.7}$$

Eqn (B.6) is the Debye-Hückel equation for ions in a medium of dielectric constant ϵ_r. The latter can be expressed in the more conventional notation using

$$1-\frac{1}{3}\rho_{03}\tilde{c}^+(0)=q_+=(1+4x_i)^2(1-2x_i)^{-4} \tag{B.8}$$

where x_i satisfies

$$q_+-q_-=\frac{\beta\rho_{03}\mu^2}{3\epsilon_0}, \qquad q_-=(1-2x_i)^2(1+x_i)^{-4} \tag{B.9}$$

Then

$$\epsilon_r=\frac{q_+}{q_-} \tag{B.10}$$

This is the dielectric constant of the bulk dipolar liquid as given in the MSA.

APPENDIX C

Equivalence of Eqns (3.26) and (3.34)

From eqn (3.34) we have that

$$p(h)=-\frac{1}{2}V_0\left\{q(h)+\int_0^h dx\frac{\partial q(x)}{\partial h}\right\}$$

(C.1)

Now the equations for q and   can be written

$$Yq(x)-\int_0^h K(x-x')q(x')dx+V=0$$

(C.2)

where

$$Y=\frac{1}{\beta}\begin{bmatrix}1/\rho_1 & 0\\ 0 & 1/\rho_2\end{bmatrix}\quad K(x-x')=\frac{1}{\beta}\begin{bmatrix}\left(C^t(x-x')-\frac{(h+R)}{4\epsilon_0}\right)-C^E(x-x')\\ C^\epsilon(x-x') \qquad C^c(x-x')\end{bmatrix}$$

$$q(x)=\begin{bmatrix}q(x)\\ P(x)/\mu\end{bmatrix},\quad V=\begin{bmatrix}V_0\\ 0\end{bmatrix}$$

(C.3)

Hence

$$Yq(h)-\int_0^h K(h-x')q(x')dx'+V=0$$

(C.4)

If we differentiate eqn (C.2) w.r.t. h, (V constant)

$$Y\frac{\partial q}{\partial h}-\int_0^h K(x-x')\frac{\partial q(x')}{\partial h}+\int_0^h dx'\frac{q(x')}{4\epsilon_0 V_0}V-K(x-h)q(h)=0$$

(C.5)

Take the transpose and use $K^{tr}(x-x')=K(x'-x)$. Then

$$\frac{\partial q^{tr}(x)}{\partial h}Y-\int_0^h\frac{\partial q^{tr}(x')}{\partial h}K(x'-x)dx'+V^{tr}\int_0^h\frac{q(x')dx'}{4\epsilon_0 V_0}-q^{tr}(h)K(h-x)=0$$

(C.6)

Multiply by $q(x)$ on the right and integrate over x. Then

$$\int_0^h dx\frac{\partial q^{tr}(x)}{\partial h}Yq(x)-\int_0^h dx\int_0^h dx'\frac{\partial q^{tr}(x)}{\partial h}K(x'-x)q(x)+\frac{Q^2}{\epsilon_0}$$

$$=\mathbf{q}^{tr}(h)\int_0^h \mathbf{K}(h-x)\mathbf{q}(x)dx \tag{C.7}$$

This can be rewritten

$$\int_0^h dx \frac{\partial \mathbf{q}^{tr}(x)}{\partial h}\left\{\mathbf{Yq}(x)-\int_0^h dx'\,\mathbf{K}(x-x')\mathbf{q}(x')\right\}+\frac{Q^2}{\epsilon_0}=\mathbf{q}^{tr}(h)\int_0^h \mathbf{K}(h-x)\mathbf{q}(x)dx \tag{C.8}$$

Now use eqn (C.4) for the curly bracket to obtain

$$\mathbf{q}^{tr}(h)\int_0^h \mathbf{K}(h-x)\mathbf{q}(x)dx =-\int_0^h dx\frac{\partial \mathbf{q}^{tr}(x)\mathbf{Y}}{\partial h}+\frac{Q^2}{\epsilon_0} \tag{C.9}$$

Substituting for the integral from eqn (C.4) gives

$$\mathbf{q}^{tr}(h)[\mathbf{Yq}(h)+\mathbf{V}]=-\int_0^h dx\frac{\partial \mathbf{q}^{tr}}{\partial h}\mathbf{V}+\frac{Q^2}{\epsilon_0} \tag{C.10}$$

Therefore

$$-\left[\mathbf{q}^{tr}(h)+\int_0^h dx\frac{\partial \mathbf{q}^{tr}(x)}{\partial h}\right]\mathbf{V}=\mathbf{q}^{tr}(h)\mathbf{Yq}(h)-\frac{q^2}{\epsilon_0} \tag{C.11}$$

Using the elements of the matrices, this becomes

$$-\left[q(h)+\int_0^h dx\frac{\partial q(x)}{\partial h}\right]V_0=\frac{q^2(h)}{\beta\rho_1}+\frac{\mathcal{P}^2(h)}{\beta\rho_2\mu^2}-\frac{q^2}{\epsilon_0} \tag{C.12}$$

Thus, from eqn (C.1)

$$p(h)=\frac{q^2(h)}{2\beta\rho_1}+\frac{\mathcal{P}^2(h)}{2\beta\rho_2\mu^2}-\frac{Q^2(h)}{\epsilon_0} \tag{C.13}$$

where

$$\rho_1=n_0,\qquad \rho_2=\rho_{03}/3 \tag{C.14}$$